Title

Induction, Specification and Differentiation of Neural Crest Cells in Xenopus and Danio rerio

Permalink

https://escholarship.org/uc/item/9kx8p8hx

Author

Monica, Stefanie Dolores

Publication Date

2016

Peer reviewed|Thesis/dissertation

Induction, Specification and Differentiation of Neural Crest Cells in *Xenopus* and *Danio rerio*

By

Stefanie Dolores Monica

A dissertation submitted in partial satisfaction of the

requirements for the degree of

Doctor of Philosophy

in

Molecular and Cell Biology

in the

Graduate Division

of the

University of California, Berkeley

Committee in charge:
Professor Richard M. Harland, Chair
Professor David A. Weisblat
Professor Craig Miller
Professor Xiaohua Gong

Spring 2016

Abstract

Induction, Specification and Differentiation of Neural Crest Cells in *Xenopus* and *Danio rerio*

by

Stefanie Dolores Monica

Doctor of Philosophy in Molecular and Cell Biology

University of California, Berkeley

Professor Richard Harland, Chair

The neural crest (NC) is a vertebrate-specific population of multipotent cells, often referred to as the fourth germ layer because of its unique ability to migrate to all parts of the body and contribute to a variety of tissues. Positional information allows neural crest cells to determine their location relative to each other and in complex 3D environments, and to respond accordingly. A central question in developmental biology is how these positional cues are imparted to cells, and how the cells interpret them for the appropriate response. The work in this thesis sets out to determine 1) how Wnt and BMP gradients define cells as neural crest, 2) how the position along the AP axis determines neural crest fate and 3) how abolishing one positional cue results in a craniofacial phenotype.

Precise control of BMP and Wnt signaling in both space and time is necessary for proper neural crest induction. While the Wnt signaling pathway has been extensively studied, it is not clear how the cells interpret and respond to the Wnt signals. Knowing the importance of these pathways in setting up the embryo axes, I wanted to further our understanding of the precise way these pathways initiate the neural crest program. An important first step toward determining how the intersection of the Wnt and BMP signaling pathways set up the neural crest cell program in space and time was to develop a method to rapidly and uniformly manipulate the signaling pathways in *Xenopu laevis* embryos. I was able to validate that small molecules can replace the use of mRNA injections in order to manipulate signaling pathways.

The next chapter of my thesis determines how neural crest cells are specified at different axial levels. The derivatives and migratory paths of neural crest cells in the cranial and non-cranial regions are very distinct, so the gene regulatory networks are likely to differ as well. Previous work has focused on the cranial neural crest cells, and therefore, regulation of the non-cranial neural crest program remains poorly understood. By taking advantage of transgenic zebrafish lines, I show that a neural crest cell's position along the AP axis during early development determines its fate.

In the final chapter of this thesis, I examine how abolishing one cue (Wnt signaling) affects patterning of neural crest-derived cells without affecting earlier aspects of neural crest formation, such as proliferation and differentiation. Analysis of the craniofacial structures in mutants for

1

multiple components of non-canonical Wnt signaling provides evidence that each component is required for proper formation in different axes.

Table of Contents

List of Figures

Acknowledgments

Contributions

Chapter 1: Introduction

1.1 NEURAL CREST

Induction is a process by which a tissue releases a signal that causes the responding tissue to change its direction of differentiation (Gurdon, 1987). One example of embryonic induction is the induction of the neural crest. During gastrulation, expression of different transcription factors in the neural plate and the non-neural ectoderm, as well as the underlying paraxial mesoderm, overlap in the intermediate ectodermal domain referred to as the neural border zone (Saint-Jeannet and Moody, 2014). This neural border zone will give rise to the neural crest (NC), a vertebrate-specific population of multipotent cells often referred to as the fourth germ layer because of its widespread contribution to the formation of many tissues (Hall, 2000) (Figure 1.1 A). The developmental flexibility of the neural crest allowed multiple evolutionary innovations. (Green et al., 2015).

The formation of the neural crest is a long process that begins during gastrulation and extends into late organogenesis. The formation of neural crest is a two-step process in which Wnt and bone morphogenetic (BMP) signaling each play distinct roles (Steventon et al., 2009). The first step occurs during gastrulation at the border of the neural plate and non-neural ectoderm, where Wnt and/or fibroblast growth factor (FGF) activation and BMP inhibition via BMP antagonists induces neural crest formation. Neural crest only forms with moderate BMP inhibition, while higher levels of BMP inhibition are required for neural tissue induction (Marchant et al., 1998). The second step, which occurs during neurulation, maintains the neural crest cell population and requires activation of both Wnt and BMP signaling (Steventon et al., 2009). In addition to Wnt and BMP signaling, several other signaling cascades are involved in neural crest induction including FGF, retinoic acid and Notch signaling.

After the formation of neural crest, the cells undergo epithelial-to-mesenchymal transitions (EMT) during which they lose cell-cell adhesions, and cytoskeletal rearrangements and morphological changes that allow them to delaminate from the neuroepithelial cells and migrate throughout the body to contribute to different tissues (Bronner-Fraser, 1993; Dupin et al., 2006; Knecht and Bronner-Fraser, 2002). The process of EMT involves two steps: delamination and cell dispersion, during which premigratory neural crest cells are separated into individual cells. The delamination process is mediated by transcriptional regulation of cadherins, while changes in cytoskeletal organization are necessary for cell dispersion.

After delamination, neural crest cells enter migratory streams, which will eventually lead them to their target destination. During migration, the neural crest cells (NCCs) integrate extrinsic signals from the neural tube and the microenvironement encountered with intrinsic guidance cues until they settle into their distinct territories and differentiate (Sauka-Spengler and Bronner-Fraser, 2008). The migratory route and derivatives of the neural crest cells are thought to roughly depend on the axial position of the cells in the embryo. Based on their anteroposterior positioning in the embryo, neural crest cells can be divided into two main groups: cranial and non-cranial (Figure 1.1 B), and the non-cranial group can be further subdivided into: vagal,

sacral, cardiac, and trunk. Cranial neural crest cells follow a dorsolateral pathway and contribute to the craniofacial skeleton (Minoux and Rijli, 2010). Some cranial regions, particularly rhombomeres 3 and 5, express inhibitory molecules to repel neural crest cells to ensure proper development of the craniofacial structures (Golding et al., 2004). Non-cranial neural crest cells, however, follow either a ventrolateral pathway through the anterior sclerotome to give rise to the dorsal root ganglia, sympathetic ganglia, adrenal medulla and aortic nerve clusters, or a dorsolateral pathway between the ectoderm and somites, where they give rise to melanocytes (Bronner-Fraser, 1993; Mort et al., 2015a) (Figure 1.1 C).

Each step of neural crest formation occurs in distinct areas of the embryo and at different times during development, spanning all of embryogenesis. Specification occurs in the blastoderm during gastrulation and early neurulation, delamination from the dorsal neural tube occurs at the end of neurulation, and migration and differentiation occur throughout the embryo over the course of organogenesis and late embryogenesis (Duband et al., 2015). Therefore, time and space are both important parameters underlying the process of neural crest development.

Canonical Wnt signaling is involved in many aspects of neural crest formation, from induction to delamination and migration. Canonical Wnt signaling involves the Wnt ligand binding to the seven-transmembrane Frizzled receptor and low-density lipoprotein-related receptor-5/6 (LRP5/6) coreceptors. These receptors recruit Dishevelled to the cell surface, which causes dissociation of the destruction complex, composed of Dishevelled, Axin, APC and GSK3. In the absence of the destruction complex, β-catenin is stabilized, accumulates in the cytoplasm and is transduced into the nucleus, where it interacts with the transcription factors TCF/Lef to activate transcription (Clevers, 2006; Clevers and Nusse, 2012). Overexpression of Wnt1, Wnt3a, Wnt7b or Wnt8 results in an expansion of the neural crest region, while Wnt inhibition results in reduction of the neural crest region (Stuhlmiller and García-Castro, 2012).

In addition to canonical Wnt signaling, a gradient of Bone Morphogenetic Protein (BMP) signaling along the dorsoventral axis is crucial for neural crest formation. This gradient helps to define the region from which the neural crest will form, and is established by secretion of BMPs in the ventral part of the embryo and BMP antagonists, such as Chordin and Noggin, from the dorsal mesoderm (Dale and Wardle, 1999). High levels of BMP signaling in the ventral ectoderm drive differentiation into epidermal fates while low levels of BMP signaling in the dorsal midline allow the neural plate to form. Intermediate levels of BMP signaling at the neural border zone are permissive for neural crest induction (Marchant et al., 1998).

Neurocristopathies arise from defects in development of neural crest-derived cells and tissues. Due to the widespread derivatives, these neurocristopathies include Hirschspring disease and congenital heart defects, which arise from defects in the migration of neural crest cells, Di George syndrome, which is in part due to apoptosis of neural crest cells, as well as melanoma and cleft lip and palate. Understanding the specification and differentiation of neural crest cells will shed light on the pathways involved in these neurocristophathies.

1.2 NEURAL CREST GENE REGULATORY NETWORK

The gene regulatory network (GRN) that underlies the formation of early neural crest cells is highly conserved across all vertebrates. This network is composed of transcription factors that, together with chromatin modifiers, regulatory RNAs and epigenetic factors, establish individual cell types within the neural crest lineage. The GRN is comprised of different sets of genes that are responsible for distinct features of the cell population, as well as transitioning cells to the next stage. During gastrulation, a gradient of BMP activity defines the regions of the ectoderm: the medial ectoderm with low BMP activity will become the neural plate, the lateral ectoderm with high BMP activity becomes epidermis, and the region in between with intermediate BMP activity will become the neural plate border (Marchant et al., 1998). This neural plate border will be further defined along the anteroposterior axis by Wnt and FGF signaling (Hong et al., 2008). The signaling pathways that define the neural plate border make up the first signaling module in which Wnt, BMP, Notch and FGF signaling pathways induce the expression of neural plate border specifier genes, which include *msx*, *dlx5/6*, *ap2α, pax3/7, zic* and *c-myc*. The first four genes, *msx*, *dlx5/6* and *tfap2α* are among the first activated in the ectoderm that is fated to become neural crest. Their expression pattern correlates with the dorsoventral gradient of BMP activity, and therefore, they are likely to be direct targets of BMP (Steventon et al., 2005). *pax3/7, zic* and *c-myc* are not expressed in the entire epidermis at the early stages, but have broader expression patterns than just premigratory neural crest cells (Steventon et al., 2005). These transcription factors then activate the neural crest specification module in which bona fide neural crest markers are expressed including *foxd3, snail1/2, twist1, ets1, tfap2α, pax3/7* and *soxE* family members *sox8/9/10* (Meulemans and Bronner-Fraser, 2004). *snail1/2* are required for the expression of the other neural crest genes, and therefore, specification of the neural crest (LaBonne and Bronner-Fraser, 2000). Additionally, *snail1/2* control cell cycle progression and inhibit neural crest apoptosis (Vega et al., 2004). *SoxE* family members are necessary for multiple steps of neural crest formation, including conferring competence for the cells at the neural plate border to become neural crest cells, maintaining the stem-like state and promoting survival (Haldin and LaBonne, 2010). In particular, *sox9* and *sox10* are expressed in the neural crest at different times of development and are thought to be survival factors (Hong and Saint-Jeannet, 2005). *foxd3* is one of the earliest neural crest genes to be expressed and its overexpression leads to ectopic expression of other neural crest genes including *snail2, tfap2α, foxd3, ets1* and *twist* (Sasai et al., 2001). Once the neural crest is specified, the genes responsible for EMT and migration from the neural tube to diverse positions throughout the body, such as *foxd3, tfap2, lmo4, rxrG, sox10* and *sox5/6*, are activated. Finally, the genes responsible for differentiation into the final derivatives are activated. These include *phox2b* for neurons and glia, *sox9* for chondrocytes and osteoblasts and *mitf* for melanocytes (Green et al., 2015).

It is important to note that the signaling pathways that set up the neural plate border are reused throughout development. Therefore, the development into specific cell types depends not only on the expression of extracellular ligands, but also on the presence of the receptors and secreted inhibitors. Therefore, the ability of a cell to become fate-restricted depends greatly on its ability to respond to, and interpret, the signals. To further complicate things, the impact of the secreted ligand depends on the duration of exposure, the concentration of the ligand and the interactions with other signaling molecules and the surrounding environment (Patthey and Gunhaga, 2014). Experiments in the next chapter set out to determine how two signaling pathways, Wnt and BMP, interact to establish the neural crest cells.

Although the regulatory program described here is shared among all developing neural crest cells, the neural crest is not a homogeneous population of cells and therefore, the specification of the neural crest subpopulations is probably due to differences in the underlying GRN. Neural crest cells that arise from different positions along the anteroposterior axis have distinct developmental potentials. Transplant studies show that when non-cranial neural crest cells are transplanted into the head, they fail to become bone or cartilage and instead become melanoctyes, dorsal root and sympathetic ganglia. In contrast, transplant studies show that cranial neural crest cells transplanted into the trunk can give rise to all trunk derivatives as well as ectopic cranial derivatives (Le Lievre et al., 1980). This indicates that trunk neural crest cells have a restricted developmental potential compared to cranial neural crest cells. The GRN regulating these differences remain unknown. In-depth studies of the GRN will be crucial to further our understanding of the differences in differentiation potential and migratory pathways of non-cranial neural crest cells at different axial levels. Furthermore, as neural crest cells migrate and differentiate, multiple extrinsic and intrinsic signals are integrated to elicit the proper response, and our understanding of that process is limited. It is therefore important to understand the pathways and signals involved, and advances in sequencing technologies will help these efforts. Experiments in Chapter 3 will begin to look into these differences in GRN.

1.3 WNT SIGNALING IN DEVELOPMENT AND DISEASE

Wnt genes encode a large evolutionarily conserved family of lipid-modified extracellular signaling molecules. The mammalian genome contains 19 Wnt genes, which fall into 12 conserved Wnt subfamilies, emphasizing the important role Wnt signaling plays in a wide range of organisms. Unicellular organisms do not contain Wnt proteins, which suggests Wnt signaling was involved in the evolution of multicellular organisms. Wnt signaling governs many processes during embryonic development such as cell proliferation, cell fate determination, differentiation, stem cell maintenance and adult homeostasis (Van Amerongen and Nusse, 2009). Wnt proteins function in two types of signaling determined by distinct sets of receptors as well as cellular context: canonical and non-canonical. Wnt proteins themselves are not canonical or non-canonical; instead, the pathways they initiate are determined by separate sets of receptors.

In canonical Wnt signaling, the Wnt ligand binds to the heterodimeric receptor complex consisting of the Frizzled transmembrane protein and LRP5/6 protein. The ten mammalian Frizzled receptors are seven-transmembrane proteins that contain a large extracellular N-terminal cysteine-rich domain (CRD) that Wnt proteins bind. A hydrophobic groove of the CRD interacts with a lipid on the Wnt protein. The binding between Wnt and Fzd is promiscuous; a single Fzd protein can bind to many Wnt proteins, and vice versa (Janda et al., 2012).

These receptors recruit Dishevelled (Dvl/Dsh) to the cell surface, which causes dissociation of the destruction complex, composed of Dishevelled, Axin, APC, CK-1 and GSK3. This leads to β-catenin stabilization and accumulation in the cytoplasm and translocation to the nucleus where it interacts with the transcription factor TCF/Lef to activate transcription of Wnt target genes (Behrens et al., 1996). Once β-catenin is transduced to the nucleus, it switches the TCF repressor complex into a transcriptional activator complex by displacing Groucho and/or recruiting the histone acetylase CBP/p300 (Logan and Nusse, 2004). In the absence of the Wnt

ligand, the destruction complex (Dvl, Axin, APC, CK-1 and GSK3) phosphorylates β-catenin at a series of N-terminal Ser/Thr residues, which marks it for ubiquitination and degradation, and ultimately prevents activation of Wnt target genes (Clevers and Nusse, 2012).

Non-canonical Wnt signaling is transduced via regulation of intracellular calcium, or small G-proteins Rho/Rac which control planar cell polarity (PCP) via actin cytoskeleton remodeling (Mayor and Theveneau, 2014). The PCP pathway controls the polarization of epithelial cells and regulates cell movements including convergent extension movements, in which cells move between one another to form a longer, narrower tissue (Keller 2002). Consequently, the PCP pathway has been found to be involved in axis elongation, neural tube closure, ciliary beating and directional cell migration in vertebrates (Vladar et al., 2009; Wallingford, 2012). The core PCP components include the four-transmembrane protein Vangl, the seven-transmembrane protein Frizzled, the cadherin Celsr, and the cytoplasmic proteins Prickle, Dishevelled and Diversin (Simons and Mlodzik, 2008).

Wntless (Wls) has been identified as the exclusive chaperone protein required for the secretion of all mammalian Wnts (Bänziger et al., 2006). The seven-transmembrane Wls protein binds Wnt ligands in the Golgi and sends Wnts to the membrane surface for release in Wnt-producing cells (Bartscherer et al., 2006). Wls is involved in diverse developmental process such as body axis formation, skeletal development and hair follicle growth. However, it is still unclear if these roles are solely through the action of the Wnt ligands, or other roles of the Wls protein itself (Fu et al., 2009; Huang et al., 2012; Myung et al., 2013).

Wnt signaling is tightly regulated at multiple levels, including by secreted Wnt antagonists such as Cerberus, Dickkopf (Dkk), Wnt inhibitory factors (WIF) and secreted Frizzled-related proteins (sFRPs), Frzb and Crescent. Cerberus, sFRPs and Dkks are highly expressed in the anterior part of the head organizer and prevent posteriorization of all germ layers by Wnt signaling. Dkk proteins are membrane bound and bind LRP co-receptors to inhibit Wnt signaling. Frzb is a secreted protein that contains a cysteine rich domain (CRD) found in Frizzled proteins. sFRPs and WIFs bind Wnts in the extracellular space and prevent them from binding Wnt receptors. Therefore, Frzb binds Wnt proteins and prevents the activation via Frizzled. Additionally, it has been proposed that sFRPs increase the signaling range of Wnt proteins by facilitating diffusion in the extracellular space (Mii and Taira, 2009, 2011).

Dysregulated activation of Wnt signaling has been implicated in many cancers, especially colon cancer (Reya and Clevers, 2005). In colorectal cancers, truncations in APC upregulate the LEF1 transcription factor which may lead to misregulation of Wnt target genes, and thus increased cell proliferation (Hovanes et al., 2001). Likewise, individuals with Axin2 mutations exhibit a predisposition to colon cancer (Lammi et al., 2004). In addition to excessive Wnt/β-catenin signaling leading to tumorigenesis, perturbations in *sfrp* genes are also associated with tumorigenesis. Downregulation of *sfrps* increases tumorigenesis due to their role in the inhibition of Wnt signaling; while upregulation has tumorigenic properties due to the increase in Wnt ligand diffusion and availability. In addition to their role in cancer, Wnt ligands have been attractive candidates for regenerative medicine since they are involved in so many aspects of developmental biology. Due to the importance of the Wnt signaling pathway in both cancer and regenerative medicine, manipulation of the pathway through small molecule targeting has been

extensively studied. However, even though the Wnt pathway is one of the best-studied signaling pathways, pharmacological inhibition of Wnt signaling has been difficult to achieve.

Wnt signaling is involved in many aspects of neural crest formation, from induction to delamination and migration. Overexpression of Wnt1, Wnt3a, Wnt7b or Wnt8 results in an expansion of the neural crest region, while Wnt inhibition results in its reduction (Barembaum and Bronner-Fraser, 2005). Therefore, it is well established that Wnt signaling is necessary for the initial phase of neural crest induction (Stuhlmiller and García-Castro, 2012).

1.4 BMP SIGNALING IN DEVELOPMENT AND DISEASE

Bone Morphogenetic Proteins (BMPs), named for their ability to induce ectopic bone formation (Urist and Strates, 1971), belong to the Transforming Growth Factor (TGF-β) superfamily of proteins, which is the most numerous group of growth factors in humans. In addition to their roles in bone formation, BMP ligands act as a morphogen gradient to pattern the dorsoventral (DV) tissues in the developing embryo. Through precise levels of signaling, BMPs specify distinct cell fates at specific positions along the DV axis. Additionally, BMP signaling is involved in numerous processes including cell fate decisions, proliferation, apoptosis, organogenesis, differentiation and adult homeostasis (Wang et al., 2014).

The BMP signaling cascade begins when the BMPs bind to type I and type II receptors, which are single-pass transmembrane proteins with intracellular Ser/Thr kinase domains. Once bound, the type I and type II receptors form a complex and the type 1 receptors are trans-phosphorylated by the type II receptors. In turn, the type I receptors recruit and phosphorylate the Smad1/5/8 transcription factors. Phosphorylated Smads form a complex with Smad4 and this complex is translocated to the nucleus, and together with transcriptional co-activators, bind to DNA and activates transcription of target genes (Kishigami and Mishina, 2005).

The actions of BMPs are tightly regulated by a family of soluble, extracellular secreted BMP antagonists, which function by directly binding BMPs in the extracellular space and therefore preventing receptor activation by BMPs. These antagonists are secreted dorsally and bind BMPs to prevent ligand-receptor binding and pathway activation. These antagonists include Noggin, Gremlin, Follistatin, Chordin, Cerberus, Twisted gastrulation and Crossveinless 2. Noggin, Follistatin and Chordin are all expressed in the Spemann organizer, a region that is important for determining dorsoventral patterning. If all three of these are knocked down in a developing embryo, the embryo will lack all dorsal structures (Khokha et al., 2005). Chordin is abundantly secreted by the organizer and acts in both the dorsal and ventral poles of the embryo (De Robertis and Moriyama, 2016). Ectopic Gremlin activity induces a secondary axis, and the endogenous gene is expressed primarily in the neural crest regions (Hsu et al., 1998). The timing and concentration of both the BMPs and their antagonists are crucial to normal development, as changes in either lead to defects in development. BMPs and their antagonists also regulate stem cell pluripotency and differentiation along defined lineages. Additionally, the reactivation of previously silent expression can contribute to human diseases such as cancer and fibrosis.

6

BMP signaling plays a critical role in stem cell biology, regulating the balance between differentiation and proliferation. Deletion of components of the BMP signaling pathway results in embryonic lethality or severe malformations. The BMP antagonists Follistatin and Gremlin facilitate self-renewal and proliferation in cancer cells (Sneddon et al., 2006). In melanoma, BMP7 is inhibited by Noggin, which promotes tumor progression (Hsu et al., 2008). In addition to its role in cancer progression, misregulation of BMP signaling is involved in kidney diseases (McMahon et al., 2000) and liver disorders (Yang et al., 2012). Due to the role of the BMP signaling pathway in disease pathogenesis, manipulation of the pathway through small molecule targeting has recently begun to be addressed.

A gradient of BMP signaling determines cell differentiation in the ectoderm, mesoderm and endoderm germ layers (De Robertis and Kuroda, 2004). In the mesoderm, low levels give rise to notochord, slightly higher levels to skeletal muscles and highest levels to blood. Low levels of BMP cause the ectoderm to differentiate into neural tissues, and high levels cause the differentiation into epidermis. Importantly, intermediate levels of this pathway define the ectodermal region from which the neural crest will form. Additionally, BMP signaling promotes neural crest migration, differentiation and apoptosis.

1.5 SUMMARY OF THESIS

Positional information has long been suggested to play an important role in pattern formation during development (Wolpert, 1971). A simple model for this is that each cell has "coordinates" for their position within the developing tissue or embryo, and the cells interpret this positional information by differentiating in a specific way (Wolpert, 1989). Therefore, positional information allows cells and tissues to determine their location relative to each other and in complex 3D environments, and to respond accordingly (Levin, 2012).

A central question in developmental biology is how these positional cues are imparted to cells, and how the cells interpret them for the appropriate response. The work in this thesis sets out to determine 1) how Wnt and BMP gradients define cells as neural crest, 2) how the position along the AP axis determines neural crest fate and 3) how abolishing one positional cue results in a craniofacial phenotype.

Historically, positional information has been thought to come in the form of morphogen gradients (Gurdon et al., 1999). In the frog embryo, Wnt and BMP proteins form perpendicular gradients that define the anteroposterior and dorsoventral axes (Niehrs, 2010). It is well accepted that neural crest induction requires initial BMP inhibition in combination with Wnt activity; however, it is not clear how the cells interpret and respond to these signals. The canonical Wnt signaling pathway has been extensively studied for its role in embryonic development, but its role in reiterative signaling during neural crest formation is still not well understood. Knowing the importance of these pathways in setting up the embryo axes, I wanted to further our understanding of the precise way these pathways initiate the neural crest program. The first step was to develop a method to rapidly and uniformly manipulate the signaling pathways in *Xenopus* embryos. I was able to validate that small molecules can replace the use of mRNA injections in order to manipulate signaling pathways. This is an important first step toward determining how

the intersection of the Wnt and BMP signaling pathways set up the neural crest cell program in space and time. The proposed future experiments will provide insight into how neural crest cells respond to Wnt signaling, if Wnt signaling confers axial identity, and if Wnt signaling is sustained or pulsed.

The next question I set out to answer was how neural crest cells are specified at different axial levels. The derivatives and migratory paths of neural crest cells in the cranial and non-cranial regions are very distinct, so the gene regulatory networks are likely to differ as well. Previous work has focused on the cranial neural crest cells, and therefore, regulation of the non-cranial neural crest program remains poorly understood. By taking advantage of transgenic zebrafish lines, I show that a neural crest cell's position along the anteroposterior (AP) axis during early development determines its fate.

In the final chapter of my thesis, I examine how abolishing one cue (Wnt signaling) affects patterning of neural crest-derived cells without affecting earlier aspects of neural crest formation, such as proliferation and differentiation. Analysis of the craniofacial structures in mutants for multiple components of non-canonical Wnt signaling provides evidence that each component is required for proper formation in different axes.
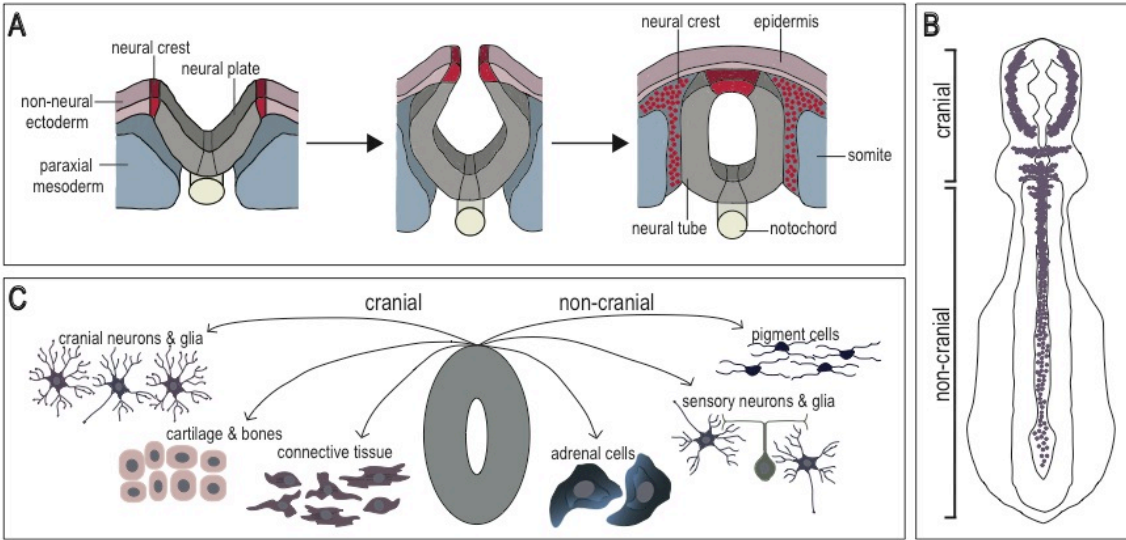
Figure 1.1. Overview of neural crest development.
(A) Neural crest cells (red) arise at the border of the non-neural ectoderm (pink) and the neural plate (grey) (left panel). After the neural plate folds during neurulation, the neural crest cells lie at the dorsal tip of the neural tube (middle panel). From here, the cells undergo EMT, delaminate from the neural tube and migrate throughout the embryo to give rise to a wide variety of derivatives (right panel). (B) Diagram of a flat mount of a chick embryo depicting the two subcategories of neural crest (purple): cranial and non-cranial. (C) The neural crest gives rise to a plethora of derivatives in the cranial and non-cranial subcategories. The cranial neural crest gives rise to the cranial neurons, glia, cartilage, bones, and connective tissues. The non-cranial neural crest gives rise to pigment cells throughout the body, sensory neurons and glia, adrenal cells, and smooth muscle cells of the heart. Adapted from figures by (Huang and Saint-Jeannet, 2004) and (Knecht and Bronner-Fraser, 2002).

Chapter 2: Elucidating the role of Wnt signaling in *Xenopus* neural crest induction and patterning

Positional cues are important for the development of neural crest cells. A significant question is how cells interpret and respond to these positional cues. In this chapter, I will address how the major signaling pathways, Wnt and BMP, set up the embryonic axes necessary for neural crest formation. I demonstrate that small molecules can replace the use of mRNA injections in order to manipulate these signaling pathways. This is an important first step in determining how the intersection of the Wnt and BMP signaling pathways set up the neural crest cell program in space and time. The proposed future experiments will help to elucidate the interaction between the two signaling pathways.

2.1 INTRODUCTION

Xenopus as a model organism

During the early twentieth century, the South African clawed frogs *Xenopus laevis* was widely used as a clinical pregnancy test to detect gonadotropin in the urine of pregnant women. Frogs were injected with the urine from a potentially pregnant woman, and evaluated 8-12 hours later for the presence of mature eggs, which indicated pregnancy (Gurdon and Hopwood, 2000). The use of frogs as a pregnancy test proved that the frog was robust, available year round and able to produce large numbers of embryos, and therefore, they became firmly established in biological research.

X. laevis has many advantages as a model organism for developmental biology. *X. laevis* can ovulate year round in response to injected hormones, producing hundreds of large (>1mm) eggs at a time. The large size of the eggs allows for easy microinjection and manipulations such as tissue transplantations and dissections. Additionally, the embryos develop quickly, which enables studies of development and differentiation to be done in a relatively short amount of time.

Among the many manipulations the large embryo size permits, the use of animal cap assays is especially useful for studies of induction. Animal caps serve as a useful substrate to test the activity of inducing factors because they can be induced to form endodermal, mesodermal or ectodermal cells. The animal cap is a region of the upper half of the *Xenopus* blastula and gastrula stage embryo (6-12 hours post fertilization), which is normally destined to become epidermal and neural derivatives, whereas the isolated animal cap develops solely into epidermal tissues. The animal cap assay has become popular because of the variety experiments that can be done. The animal cap can be forced to become tissues other than epidermis by contact with other tissues, exposure to growth factors and other molecules, or by injection of the embryo with RNA or DNA prior to cap excision (Green, 1999). Animal caps with decreased BMP will adopt an anterior neural fate, those exposed to high levels of Wnt will adopt a posterior neural fate and

those with activated Nodal signaling will become a variety of mesodermal cell types (Okabayashi and Asashima, 2003).

Wnt and BMP signaling

Wnt and BMP signaling act perpendicularly to each other, Wnt signaling acting along the anteroposterior (primary) axis while BMP acts along the dorsoventral (secondary) axis. Wnt signaling is high posteriorly and low anteriorly, while BMP signaling is high in the ventral region and low in the dorsal region of the developing embryo. These gradients are formed by the expression patterns of the ligands and their antagonists, as described in the previous chapter. The primary and secondary axes are not completely independent and instead cross-regulate each other to ensure proper growth and body axis patterning during development (Niehrs, 2010). Interestingly, both the embryonic DV and AP tissues are temporally patterned from anterior to posterior, allowing cells to acquire positional and temporal information simultaneously during gastrulation (Hashiguchi and Mullins, 2013).

In addition to their roles in body axis patterning, Wnt and BMP signaling pathways play an integral role in the formation of the neural crest. Temporal and spatial fine-tuning of BMP and Wnt signaling is necessary for proper neural crest induction, during which a combination of Wnt activation and BMP inhibition must occur. Therefore, Wnt and BMP signaling are thought to act concurrently and synergistically to mediate neural crest development. While this is a well-studied process (Steventon et al., 2009), the role of Wnt signaling alone has not been teased out; in particular, the dose-response relationship between Wnt signaling and neural crest induction has not been evaluated. In this work, I utilized neuralized animal cap explants of *Xenopus laevis* embryos in order to test how different levels of Wnt signaling affect NC induction. I sought to determine if Wnt signaling acts by a threshold-dependent or by a dose-dependent manner in the induction of neural crest.

2.2 RESEARCH METHODOLOGY

Xenopus embryo culture and microinjection
X. laevis embryos were obtained, cultured and microinjected (Sive 2000), and staged (Nieuwkoop and Faber 2004) as previously described. Ectodermal explants (animal caps) were cut using fine watchmaker's forceps from stage 9 embryos and cultured in ¾ NAM. Animal caps were left in ¾ NAM until control (whole embryos) reached the desired stage. *noggin* mRNA was microinjected into both blastomeres of two-cell staged *Xenopus laevis* embryos along with *mCherry* RNA, whose fluorescent product served to track successfully injected embryos. Embryos orient themselves animal side up, so injections were into the animal hemisphere, and mRNAs were injected near the center of the blastomere. All experiments were performed at least in duplicate.

Chemical treatment
Embryos were cultured until stage 9 when animal caps were excised and cultured with or without the small molecules LDN193189 or BIO (6-bromoindirubin-3'-oxime) to inhibit BMP signaling

or activate Wnt signaling, respectively. Animal caps were cultured until the stage 17 equivalent and collected for *in situ* hybridization or total RNA harvest using Trizol (see below). The vitelline membrane of whole embryos were removed using a pair of sharp watchmaker's forceps, and then the embryos were incubated the same way as the animal caps.

RNA isolation and quantitative PCR (qPCR)
RNA was isolated from whole embryos or animal caps using Trizol (Invitrogen), isopropanol precipitation, two phenol chloroform extractions and a final precipitation. 1ug total RNA was reverse transcribed with iScript (Bio-Rad) for quantitative PCR (qPCR). qPCR reactions were amplified on a CFX96 light cycler (Bio-Rad). Expression levels were normalized to the housekeeping genes elongation factor 1a1 (*ef1a1*) and glyceraldehyde-3-phosphate dehydrogenase (*gapdh*). All primers annealed at 60º and are listed in Appendix I.

Whole mount RNA *in situ* hybridization
Embryos were fixed in MEMFA for 1–2 h and processed following standard protocols (Harland 1991). In situ hybridization was performed as described (Sive 2000), with the alkaline phosphatase substrate BM purple (Roche). For each probe in a given experiment, all color reactions were developed for the same amount of time.

2.3 RESULTS

Precise control of BMP and Wnt signaling in both space and time is necessary for proper neural crest induction, during which a combination of Wnt activation and BMP inhibition must occur. While the distinct roles of Wnt and BMP signaling are well studied, the precise dose-response relationship between Wnt signaling and neural crest induction has not been elucidated. In this work, I aim to better understand the role of canonical Wnt signaling in neural crest formation. I utilized a small molecule activator of Wnt signaling (BIO) and a small molecule inhibitor of BMP signaling (LDN) to systematically alter signaling in *Xenopus laevis* embryo. Using neuralized animal cap explants of *Xenopus laevis* embryos, I tested how different levels of Wnt signaling affect neural crest induction.

Treatment with BIO activates Wnt signaling in whole embryos

As a first step to elucidate the reiterative role of Wnt signaling during neural crest induction, the tools to manipulate the signaling pathways had to first be assembled and validated. Previous work with Wnt signaling used injected *wnt* mRNA in order to activate Wnt signaling. While this method was reliable and reproducible, it lacked robustness and was hard to carry out with large numbers of embryos. Therefore, with discovery of new small molecules, we sought to determine if the small molecules for Wnt and BMP signaling would recapitulate the mRNA injections. In order to activate the canonical Wnt pathway, we utilized 6-bromoindirubin-3'-oxime (BIO) (Meijer et al., 2003), which specifically inhibits glycogen synthase kincase-3 (GSK3) and consequently leads to the stabilization of β-catenin. Previously, LiCl was used to activate Wnt signaling due to its ability to inhibit GSK3, and subsequently lead to the accumulation of β-

catenin. Embryos treated with LiCl become radially dorsalized, meaning that the dorsal blastophore lip forms around the entire embryo at the same time, with a dorso-anterior index (DAI) of 9-10 (Kao and Elinson, 1988). This occurs because LiCl transforms the entire mesoderm into Spemann's organizer. To confirm that BIO was indeed activating Wnt signaling, whole embryos were incubated with BIO and radial dorsalization was confirmed. Untreated whole embryos develop normally (Figure 2.1 A, top) while two representative embryos treated with 50mM BIO were severely radially dorsalized with a DAI index of 8-9 (Figure 2.1 A, bottom). BIO-treated embryos exhibited enhanced dorsoanterior structures and the tissues developed into a large proboscis extending outward at the end of gastrulation.

In addition to the gross whole embryo phenotype, quantitative PCR (qPCR) confirmed the activation of the Wnt pathway after BIO treatment. Axin is a multidomain scaffold protein that interacts with GSK-3β and APC in the β-catenin destruction complex to down-regulate Wnt signaling. There are two Axin genes, *Axin1* and *Axin2*, and both act as negative regulators. *Axin1* is constitutively expressed while *Axin2* is a direct target of Wnt signaling and acts in a negative feedback loop. qPCR of these genes showed that *Axin1* is unaffected with the addition of increasing concentrations of BIO or LiCl. *Axin2* expression on the other hand, was greatly increased following treatment with BIO or LiCl (Figure 2.1 B). Taken together, we conclude that the small molecule BIO is a suitable substitute for LiCl to activate Wnt signaling.

Treatment with LDN neuralizes whole embryos

Similar to Wnt signaling, previous studies examining the effects of BMP inhibition used injected mRNA encoding the BMP antagonists, Chordin, Follistatin or Noggin (Glavic et al., 2004). Chordin and Noggin bind BMP directly in the extracellular space and prevent their binding to BMP receptors. Follistatin also binds to BMPs; unlike the others, the Follistatin-BMP complex can bind to the BMP receptor, however, it is unable to signal. Recently, the use of mRNA injections of BMP antagonist has been replaced by the use of small molecules to specifically modulate BMP signaling. One small molecule inhibitor of BMP, Dorsomorphin, was discovered in a zebrafish screen in which embryos displayed a dorsalized axis similar to that seen in BMP pathway mutants. Dorsomorphin functions by inhibiting Smad1/5/8 phosphorylation (Yu et al., 2008a). A derivative of Dorsomorphin, LDN193189 (LDN), exhibits higher specificity for BMP receptors and can be used at lower concentrations (Boergermann et al., 2010; Cuny et al., 2008; Yu et al., 2008b). LDN is a cell permeable, highly potent and selective inhibitor of BMP signaling. This small molecule inhibits BMP signaling specifically preventing the phosphorylation of Smad1/5/8 by inhibiting BMP type-I receptors ALK2 and ALK3 (Boergermann et al., 2010; Cuny et al., 2008).

To test the BMP inhibitory effects of LDN, its neural-inducing ability was examined. Whole embryos were incubated in the indicated concentrations of the small molecule. Whole embryos were treated starting at stage 9, prior to neural crest induction, and incubated in the drug until stage 17, which is prior to neural crest migration (Figure 2.2). The vitelline membrane was manually removed to ensure the drug could enter the embryo. By stage 17 (18 hours post fertilization (hfp)), embryos are undergoing neurulation and express the pan neural marker *sox2* (Figure 2.2 A), forebrain/midbrain marker *otx2* (Figure 2.2 B) and hindbrain/midbrain marker

en-2 (Figure 2.2 C), neural crest marker *snail2* (Figure 2.2 D) and epidermal marker *cytoK* (Figure 2.2 E). Treatment with 10μM LDN, a moderate concentration, caused a modest expansion of the expression of neural markers *sox2* (Figure 2.2 F) and *otx-2* (Figure 2.2 G), as well as the neural crest marker *snail2* (Figure 2.2 I). However, the hindbrain/midbrain maker *en-2* and the epidermal marker cytoK were not affected (Figure 2.2 H, J). At a higher concentration of LDN, 20μM LDN, all of the neural and neural crest markers had an expanded expression domain (Figure 2.2 K-N), but interestingly, epidermal expression was also increased (Figure 2.2 O). Together, this data shows that the small molecule LDN is a moderately effective tool to induce neural tissue.

Whole embryos treated with both LDN and BIO

Wnt and BMP signaling act perpendicularly to pattern the body axis: Wnt signaling directs the primary/anteroposterior axis while BMP signaling directs the secondary or dorsoventral axis. Therefore, the next step to determine if these two small molecules could be harnessed to induce neural crest tissue was to treat whole embryos with the two small molecules. Knowing that each molecule alone affected the development of the neural and neural crest tissues, we expected to have a similar effect when the two drugs were combined.

Animal caps were excised and incubated in BIO and LDN until stage 17 as described above (Figure 2.3). With few exceptions, treatment with both BIO and LDN increased neural and neural crest marker expression while decreasing the expression of the epidermal marker. Upon treatment with 2.5 μM BIO and 10μM LDN, expression domains of neural and neural crest markers *sox2*, *otx-2*, *en-2* and *snail2* are expanded (Figure 2.3 F-I). No change is observed in the epidermal marker *cytoK* (Figure 2.3 J). Increasing the concentration of BIO, while keeping the concentration of LDN constant, 5 μM BIO and 10μM LDN, results in an expansion of neural makers *sox2*, *otx2* and *en-2* as well as the neural crest maker, *snail2* (Figure 2.3 K-N). No difference in expression was observed in the epidermal marker (Figure 2.3 O). Further increase in BIO concentration, 10 μM BIO and 10μM LDN, results in an expansion of expression domains of neural and neural crest makers *sox2*, *otx2* and *snail2*, with the exception of *en-2* (Figure 2.3 P-S). The expression of epidermal marker is slightly decreased (Figure 2.3 T). Using the lower dose of BIO, and increasing the concentration of LDN, 2.5 μM BIO and 20μM LDN, results in an expansion of neural and neural crest makers *sox2*, *otx2, en-2* and *snail2* (Figure 2.3 U-X), and a reduction of epidermal marker expression (Figure 2.3 Y). Finally, using an intermediate concentration of BIO and a high concentration of LDN, 5 μM BIO and 20μM LDN, results in an expansion of neural and neural crest markers *sox2*, *otx2*, *en-2* and *snail2* (Figure 2.3 Z-AC), and a complete reduction of the epidermal marker (Figure 2.3 AD).

Together, these data show that the small molecules for modulating BMP and Wnt signaling, LDN and BIO, respectively, are capable of altering their intended signaling pathways in whole embryos. Compared to mRNA injections, this method is much more robust, as every embryo is equally exposed to the solution and there is no limit as to how many embryos can be treated at once. For the following work, we use the small molecules rather than injections.

LDN neuralizes animal caps

The animal cap (AC) is a tissue located at the animal pole of the *Xenopus* embryo at the blastula stage. It is composed of multipotent cells that are normally specified to become epidermis; however, this population of cells is also competent to differentiate into neural, endodermal or mesodermal tissues upon exposure to the appropriate inducers. Animal caps with decreased levels of BMP, either by incubation with small molecule inhibitors or injection of an antagonist, such as Noggin, will adopt an anterior neural fate and express markers such as *sox2, otx2* and *bf1*. Animal caps exposed to high levels of Wnt, by injection of Wnt8, will adopt a posterior neural fate and express markers such as *krox20* and *hoxb9*. Animal caps exposed to intermediate levels of BMP and Wnt will become neural crest and express markers such as *snail2* and *foxd3*.

As a preliminary step to generate a homogeneous population of neural crest cells, the neural-inducing ability of LDN was examined. Animal caps were excised from early blastula embryos (stage 9), which is prior to neural crest induction, incubated with LDN, and collected prior to neural crest migration (stage 17). Neural-inducing ability was assessed by the increased expression, both qualitative (*in situ* hybridization) and quantitative (qPCR), of neural markers *sox2*, *otx2*, *en-2* and the decreased expression of epidermal marker *cytoK,* with the expression of *snail2* serving as a control (Figure 2.4). As expected, untreated animal caps do not form neural or neural crest tissue and instead only form epidermis (Figure 2.4 A-E). Upon animal cap treatment with intermediate levels of LDN (10μM), both neural tissues were induced at low levels, while still forming epidermis, with no neural crest induction (Figure 2.4 F-J). A higher concentration of LDN (20μM) was able to induce similar levels of neural tissues as seen at the intermediate levels of BMP inhibition, but without any neural crest or epidermis forming (Figure 2.4 K-O). Prior to the discovery of the BMP inhibitor LDN, the injection of the BMP antagonist Noggin was traditionally used for animal cap assays. Therefore, the neural inducing ability of LDN was compared to that of injection of 10pg of *noggin* mRNA. While *noggin* injection was able to induce neural tissue, there was still a significant amount of epidermis implying the neural induction was incomplete (Figure 2.4 P-T). To quantify the expression of the neural markers *sox2* and *otx2*, quantitative PCR analyses for expression were performed. The results demonstrate that while all treatments of LDN and *noggin* mRNA induce a neural fate, animal cap treatments with 5μM, 10μM and 20μM LDN are much more efficient than *noggin* mRNA injections (Figure 2.4 U). Together, the animal cap assays and the qPCR results demonstrate that the LDN drug is efficient at inducing neural tissue.

Treatment with both LDN and BIO induces posterior neural tissue

To attempt to generate a homogeneous population of neural crest, animal caps were again excised from early blastula embryos (stage 9) and treated with a small molecule activator of Wnt signaling and a small molecule inhibitor of BMP signaling. Since LDN was a better neural inducer than Noggin, LDN was used to inhibit BMP signaling. Animal caps were simultaneously treated with BIO and LDN, and analyzed prior to neural crest migration (stage 17). The expression of neural markers (*sox2*, *otx2*, *en-2, hoxB9* and *krox20)* was examined by *in situ* hybridization and qPCR. Untreated animal caps do not form neural tissue or neural crest tissue (Figure 2.5 A-D), and instead only form epidermis (Figure 2.5 E). Animal caps treated

with low levels of both BIO and LDN (2.5µM and 10µM, respectively) have increased expression of neural markers *sox2*, *otx2*, *en-2,* no neural crest markers, and small amounts of epidermal marker (Figure 2.5 F-J). If the concentrations of BIO is increased while keeping the LDN concentration constant, (5µM BIO and 10µM LDN), similar neural expression is seen with no induction of neural crest or epidermis (Figure 2.5 K-O). Further increase of BIO, 10µM BIO and 10µM LDN, shows similar expression of neural and neural crest expression, however, the epidermal marker, *cyto K*, begins to be expressed again (Figure 2.5 P-T). Treating the animal caps with either the low or intermediate concentration of BIO and the higher concentration of LDN, 2.5µM BIO and 20µM LDN, or 5µM BIO and 20µM LDN, results in an increase in neural marker expression, no neural crest and low amounts of epidermis (Figure 2.5 U-Y, Z-AD, respectively). Due to the higher level of LDN also inducing epidermis, we focused the rest of the studies on the lower (10µM) concentration of LDN.

In order to quantitatively establish that the drug treatments are indeed inducing neural and neural crest tissues, quantitative RT-PCR analyses for expression of *sox2, hoxB9, krox20, snail2* and *foxD3* was done. qPCR reveals that animal caps treated with all tested concentrations of LDN and BIO exhibit increased expression of neural maker *sox2* as well as posterior neural makers *hoxB9* and *krox20* (Figure 2.5 AE, left). In addition, neural crest markers, *foxd3* and *snail2* are also expressed in animal caps treated with all tested drug concentrations (Figure 2.5 AE, right). Expression of the posterior neural markers and neural crest markers in animal caps treated with LiCl and LDN was also examined (Figure 2.6). LiCl is a known activator of Wnt signaling, so this acted as a control for the BIO-treated animal caps. Compared to the BIO and LDN treatments, expression levels were not as drastically increased, and in some cases were actually decreased. This further confirms our findings that BIO and LDN are appropriate small molecules for the altering the Wnt and BMP signaling pathways.

Current studies aimed at understanding the signaling pathways in developmental processes depend on experimental methods to manipulate these signaling pathways. Manipulations are typically achieved via injections of mutant ligands or soluble receptors, or genetic approaches for gene silencing or protein overexpression. Due to the limitations of mRNA injections, both in terms of number of embryos successfully injected and the precise location of injections, a method to treat hundreds of embryos at the same time will be crucial to the studies of signaling pathways. The data presented here show that both BIO and LDN are efficient at modulating the Wnt and BMP signaling pathways, respectively. In both the whole embryos and animal cap assays, these small molecules effectively transformed the tissues into the expected tissue.

2.4 DISCUSSION

Wnt signaling is critical for neural crest formation, but crucial details about its contributions are unknown. From the work presented here, I demonstrate that the small molecule drugs for BMP and Wnt signaling are an alternative to mRNA injections for these pathways. Preliminary results confirm that the LDN drug induces neural tissue in animal caps, as evidenced by an increase in neural makers *otx2* and *sox2*. The final part of the work shown here was to determine at which

16

concentrations the LDN and BIO drugs would induce neural crest cells. Together, this work showed that neural crest was in fact induced at varying concentrations. Treatment with both LDN and BIO induced neural crest tissues as demonstrated by an increase in neural crest markers *snail2* and *foxd3*. Not only was the expression of RNA transcripts detectable by *in situ* hybridization, but it was also detected in qPCR. With this work, by regulating the degree of Wnt activation, we aim to describe the molecular mechanisms underlying the reiterative role of Wnt signaling in neural crest induction.

Signaling pathway manipulations via small molecules

Glycogen synthase kinase-3β (GSK3β) is a negative regulator of Wnt signaling, so efforts to inhibit Wnt signaling have focused on inhibition of GSK3β. Lithium chloride is the most commonly used small molecule inhibitor of GSK-3β, despite the high concentrations needed for an effect to be seen. Recently, it was discovered that indirubins, which are inhibitors of cyclin-dependent kinases, also inhibit GSK-3. One such indirubin is 6-bromoindirubin-3′-oxime (BIO), which was derived from Mollusks' Tyrian purple (Meijer et al., 2003). BIO inhibits GSK-3β with higher specificity than LiCl and efficiently activates Wnt signaling. From the experiments presented here, I found that BIO efficiently activates Wnt signaling as evidenced by the radially dorsalized embryos after treatment.

The chemical compound Dorsomorphin was first identified in a small molecule screen in Zebrafish where it was found to lead to a deformed dorsal-ventral axis in the embryos (Yu et al., 2008a). This body axis defect was similar to that seen in BMP pathway mutants indicating Dorsomorphin abrogated BMP signaling by blocking BMP induced Smad1/5/8 phosphorylation. Dorsomorphin binds to the ATP binding site of the kinase domain of the BMP type I receptors and inhibits their kinase activity, however, it also inhibits the receptor tyrosine kinases for PDGF and VEGF. These off-target effects led to the generation of the Dorsomorphin derivative LDN-193189, which has much higher specificity for BMP receptors and can be used at lower concentrations. This study confirmed that LDN was more efficient than *noggin* mRNA injections at inducing neural tissues in whole embryos and animal caps.

Differential regulation of *snail2* and *foxd3*

Animal caps treated with BIO and LDN have increased expression of the neural crest markers *snail2* and *foxd3*. Interestingly, although *snail2* and *foxd3* are both neural crest specifier genes and required for neural crest formation, they had very different levels of expression (484-fold increase of *snail2* versus 38-fold increase of *foxd3* in the 5μM BIO and 10 μM LDN treated caps). One possible explanation for this difference in expression is that, although both are specifier genes in the neural crest gene regulatory network, they are acting at different points during neural crest specification. *foxd3* is first expressed in the premigratory neural crest cells prior to *sox10* expression while *snail2* is expressed even before neural crest progenitors become apparent (Simões-Costa et al., 2012). Another possible explanation for this is that these genes have differential regulation that has not yet been elucidated in gene regulatory network analyses. Accordingly, loss of the antiphosphatase Paladin delays the expression of *snail2* but has no effect

on *foxd3* (Roffers-Agarwal et al., 2012). This could be due to Paladin modulating a protein that regulates *snail2* but not *foxd3*. Therefore, it will be necessary to do more thorough gene regulatory network analysis in order to distinguish between these two possibilities.

Animal cap assay considerations

Another interesting observation was that the *in situ* expression appeared as a spot on only one side of the embryo, instead of uniformly expressed all over the entire embryo. This, combined with the obersavtion that the neural crest induction varied from batch to batch of animal caps, and that there was never homogeneous neural crest induction, requires examination into the drawbacks of animal cap assays. One explanation for these results is that the embryos were not exposed to the drug in a uniform manner. In order to determine if the embryos were exposed uniformly to the drugs, and ensure that the drugs were able to fully penetrate the tissue, caps were bisected after drug treatment and *in situ* hybridization. Bisections showed the staining throughout the embryos, indicating the drug penetration was probably not the issue (data not shown). Another possibility is that the animal cap curled up too quickly for the drug to fully penetrate the cap. Low calcium magnesium Ringer's solution (LCMR) is commonly used in *Xenopus* studies to slow down the closing of animal caps, and therefore allow a more uniform exposure to small molecules. Animal caps in this solution during drug treatments did not appear any different than those in the normal buffer solution (data not shown). Therefore, the uniform exposure to the drugs while closing cannot explain the expression patterns seen from *in situ* hybridization. This leaves the possibility that the cells within the animal cap are not in fact a homogeneous population. There is no clear boundary between presumptive ectoderm and presumptive mesoderm, so there is always a possibility of presumptive mesodermal cell contamination in animal caps, though the lack of elongation of these caps argues against that possibility.

Even though there are some drawbacks to using animal cap assays, I believe it is still the best method to examine the effects of the sigaling pathways on neural crest behavior. Although not achieved in this study, animal cap assays have the potential to produce a homogenous population of cells, which is crucial for these studies.

2.5 FUTURE DIRECTIONS

Through these studies I was able to successfully show that the small molecule drugs LDN and BIO make suitable replacements for mRNA injections in order to induce neural and neural crest tissues. To fully answer the question of how reiterative Wnt signaling impacts neural crest induction, more studies need to be done. Some remaining questions about Wnt signaling and neural crest formation include: Is neural crest induction a dose-dependent or threshold effect of Wnt signaling? How does Wnt signaling affect neural crest specification at different axial levels? Are subsequent Wnt signals involved in other neural crest functions such as patterning? In order to address these remaining questions, I propose the following experiments.

Neural crest induction as a function of Wnt signaling

A study of the relationship between Wnt signaling, via BIO, and neural crest cell formation in animal caps by incubating the animal caps with a range of concentrations of BIO will provide insight into the dose-dependence of the relationship between neural crest formation and Wnt signaling. Immunohistochemistry for nuclear β-catenin will confirm Wnt activation by BIO. Plotting neural crest marker gene expression in the animal caps as a function of the concentration of BIO will quantitatively determine whether Wnt signaling induces NC formation in a threshold or dose-dependent manner. *In situ* hybridization and qPCR of neural crest marker *snail2,* anterior neural marker *otx2* and posterior neural maker *hoxb9,* will be utilized in order to determine at which point the animal cap has a decrease in anterior neural identity and an increase in neural crest identity. At this point, I will examine the slope of the neural crest line to determine the dependency of neural crest induction on Wnt signaling; a linear correlation would be indicative of a dose-dependent effect while a discrete increase in expression of *snail2* would be indicative of a threshold effect.

Wnt signaling at different axial levels

Once determing the manner in which Wnt signaling directs neural crest induction, it will be interesting to see how Wnt signaling influences neural crest differentiation at the different axial levels. The neural crest gene regulatory network (NC-GRN) responsible for the formation of the cranial neural crest cells has been well studied in a number of species since these cells' migration pattern is highly conserved across vertebrates (Meulemans and Bronner-Fraser, 2004; Prasad et al., 2012; Sauka-Spengler and Bronner-Fraser, 2006). However, due to the differences in migratory pathways and derivatives between trunk and cranial neural crest, the genes involved in regulation of the trunk neural crest are likely to be different than those involved in regulation of cranial neural crest. Cranial neural crest cells migrate dorsolaterally and into the pharyngeal arches where they give rise to neurons, glia, ossicles, and craniofacial cartilage, bone and connective tissue (Minoux and Rijli, 2010). Trunk neural crest cells follow two migratory routes (Collazo et al., 1993); early migration follows a ventrolateral route through the anterior half of each somite, and gives rise to dorsal root ganglia, sympathetic ganglia, adrenal medulla and aortic nerve clusters. Late migration follows a dorsolateral route and travels over the somites and into the epidermis where it gives rise to melanocytes (Knecht and Bronner-Fraser, 2002). To determine whether Wnt signaling is required for specification at different axial levels, transplantation assays (Borchers et al., 2000) will be executed, which will allow control of canonical Wnt signaling in a spatial and temporal manner.

Embryos will be co-injected at the two-cell stage with a Dexamethasone (Dex)-inducible dominant negative form of TCF (GR-dnTCF) (Molenaar et al., 1996) and GFP. The GR-dnTCF confers temporal control of Wnt signaling in the grafts, allowing Wnt signaling to be inhibited in the graft prior to migration of neural crest cells. Once the embryos reach mid-neurulation (stage 15/16), the neural crest region will be excised and transplanted into an uninjected embryo. The entire embryo can be incubated with Dex in order to inactivate Wnt signaling cell-autonomously

in the grafted tissue, leaving the surrounding uninjected host tissue unaffected. After the transplantations, the embryo will be examined after the neural crest cells have started migration (stage 18) and begun to differentiate and contribute to derivatives (stage 20, 22, 25), by fluorescence microscopy to track the fate of grafts and determine whether they formed cranial or trunk neural crest. Since the transplanted cells will be labeled with GFP, neural crest cell migration patterns and final fate can be easily tracked *in vivo*. Sectioning of the embryos followed by fluorescent immunohistochemistry using antibodies against GFP and Twist, a marker of cranial NC will provide further insight into the Wnt dependence at different axial levels. If transplants with dnTCF express the cranial NCC marker, *twist,* in an expanded region (a more posterior region) upon treatment with Dex, it can be concluded that Wnt signaling is necessary for posterior fate specification.

The transplantations can be repeated with activated Wnt signaling using TVGR, a Dex-inducible form of the Wnt pathway transcription cofactor TCF (Darken and Wilson, 2001) to determine if activated Wnt signaling affects the ability to adopt identity of a specific lineage. If Wnt is not required for and does not interfere with specification, I would not expect to see a difference in *twist* expression upon Wnt activation or inhibition. From these experiments, I will determine more precisely how Wnt signaling is involved in neural crest tissue specification at different axial levels.

Wnt signaling in other neural crest functions

It is understood that Wnt signaling is important for multiple aspects of NC formation, including induction, lineage decisions and differentiation. However, it is unclear if the initial signal is sufficient to activate the full developmental program or if subsequent Wnt signals are required after induction for the later neural crest events. To address this question, Wnt signaling will be inhibited at multiple time points after induction to determine if later events are affected.

Embryos will be co-injected with the Dex-inducible dominant-negative form of TCF (GR-dnTCF) and GFP at the eight-cell stage, and the neural crest region excised and transplanted into an uninjected embryo. Wnt signaling can be inhibited cell-autonomously in the neural crest region by incubating the entire embryo in Dex at various time points: immediately after induction (stage 12.5) before migration (stage 17), immediately after migration (stage 19), and once the cells have begun to differentiate (stage 20). The embryos can then be examined at various time points during epithelial-to-mesenchymal transition, migration and differentiation to determine if neural crest cell formation is occurring correctly.

By injecting the transplanted cells with GFP, the neural crest cells can be tracked to determine if they form correctly and localize to the appropriate sites. *In situ* hybridization, as well as qPCR, for markers of the different derivatives, such as, *mitf* for melanocytes and *tlx3* for sensory neurons will be useful to track lineage differentiation. Comparing these to embryos that have unaltered Wnt signaling will be crucial to determining if inhibition of Wnt signaling at different points during neural crest formation prevents normal neural crest cell migration or differentiation from occurring. These experiments will allow me to determine if one Wnt signal is enough to trigger neural crest formation, or if repeated signals are required.

If I discover the formation of neural crest is affected with late Wnt inhibition, more detailed analyses can be carried out, such as transplantations listed above. Combining these two approaches will allow for a high-throughput screen and also a more detailed approach to determine if Wnt signaling is sustained or pulsed.

Wnt signaling is critical for neural crest formation, but crucial details about its contributions are unknown. Through animal cap and transplantation assays, we hope to gain a better insight into the dependency of neural crest induction on Wnt signaling, as well as how Wnt signaling influences the different axial levels of neural crest. Finally, we hope to determine if multiple Wnt signals are involved in subsequent steps of neural crest formation, such as migration and specification of neural crest.
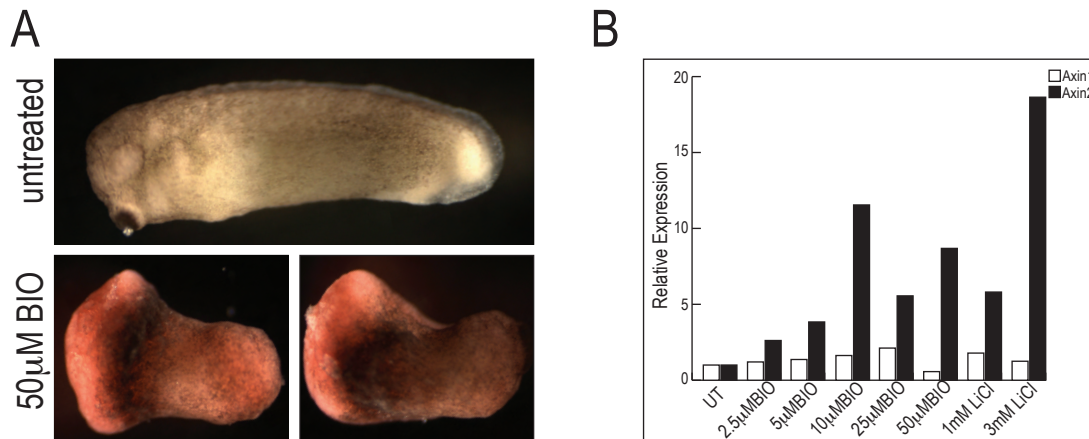
Figure 2.1. Whole embryos treated with BIO have increased Wnt signaling.
(A) Whole embryos treated with BIO are radially dorsalized with a DAI index of 8-9. (B) qPCR for *axin* genes demonstrates the constitutively active expressed *axin1* is unaffected by the treatment, while the direct Wnt target, *axin2*, is greatly increased following treatment.
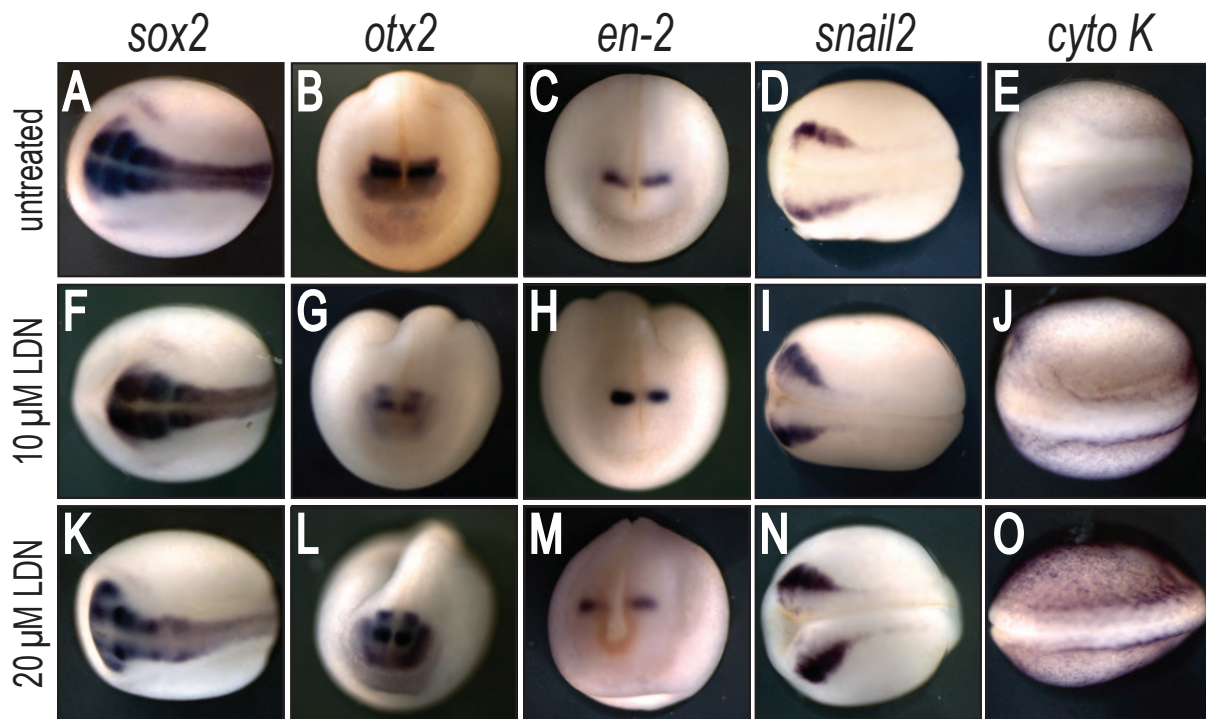
Figure 2.2. Whole embryos treated with LDN have an expansion of neural tissues.
Whole embryos were treated with the indicated concentrations of LDN from stage 9 until stage 17. (A-E) Untreated whole embryos express neural markers *sox2* (A), *otx2* (B) and *en-2* (C), neural crest marker *snail2* (D) and epidermal marker *cyto K* (E). (F-J) Upon treatment with 10μM LDN, expression of neural and neural crest markers *sox2* (F), *otx-2* (G) and *snail2* (I) are expanded with the exception of *en-2* (H). No change is observed in the epidermal marker *cyto K* (J). (K-O) Treatment of whole embryos with 20μM LDN results in an expansion of neural makers *sox2* (K), *otx2* (L) and *en-2* (M) as well as the neural crest maker, *snail2* (N). Additionally, an increase in epidermal marker is observed (O). Markers used: *sox2*- neural; *otx2*- forebrain/midbrain; *en-2* hindbrain/midbrain; *snail2*- neural crest; *cyto K*- epidermis.

	sox2	*otx2*	*en-2*	*snail2*	*cyto K*
untreated	A	B	C	D	E
2.5 µM BIO +10 µM LDN	F	G	H	I	J
5 µM BIO +10 µM LDN	K	L	M	N	O
10 µM BIO +10 µM LDN	P	Q	R	S	T
2.5 µM BIO +20 µM LDN	U	V	W	X	Y
5 µM BIO +20 µM LDN	Z	AA	AB	AC	AD

Figure 2.3. Whole embryos treated with LDN and BIO have an expansion of neural and neural crest markers.

Whole embryos were treated with the indicated concentrations of BIO and LDN from stage 9 until stage 17. (A-E) Untreated whole embryos express neural markers *sox2* (A), *otx2* (B) and *en-2* (C), neural crest marker *snail2* (D) and epidermal marker *cyto K* (E). (F-J) Upon treatment with 2.5 µM BIO and 10µM LDN, expression domains of neural and neural crest markers *sox2* (F), o*tx-2* (G), *en-2* (H) and *snail2* (I) are expanded. No change is observed in the epidermal marker *cyto K* (J). (K-O) Treatment of whole embryos with 5 µM BIO and 10µM LDN results in an expansion of neural markers *sox2* (K), *otx2* (L) and *en-2* (M) as well as the neural crest maker, *snail2* (N). No difference in expression was observed in the epidermal marker (O). (P-T) Treatment with 10 µM BIO and 10µM LDN results in an expansion of expression domains of neural and neural crest markers *sox2* (P), *otx2* (Q) and *snail2* (S), with the exception of *en-2* (R). The expression of epidermal marker is slightly decreased (T). (U-Y) Treatment with 2.5 µM BIO and 20µM LDN results in an expansion of neural and neural crest markers *sox2* (U), *otx2* (V), *en-2* (W) and *snail2* (X), and a reduction of epidermal marker expression (Y). (Z-AD) Treatment with 5 µM BIO and 20µM LDN results in an expansion of neural and neural crest markers *sox2* (Z), *otx2* (AA), *en-2* (AB) and *snail2* (AC), and a complete reduction of the epidermal marker (AD) Markers used: *sox2*- neural; *otx2*- forebrain/midbrain; *en-2* hindbrain/midbrain; *snail2*- neural crest; *cyto K*- epidermis.
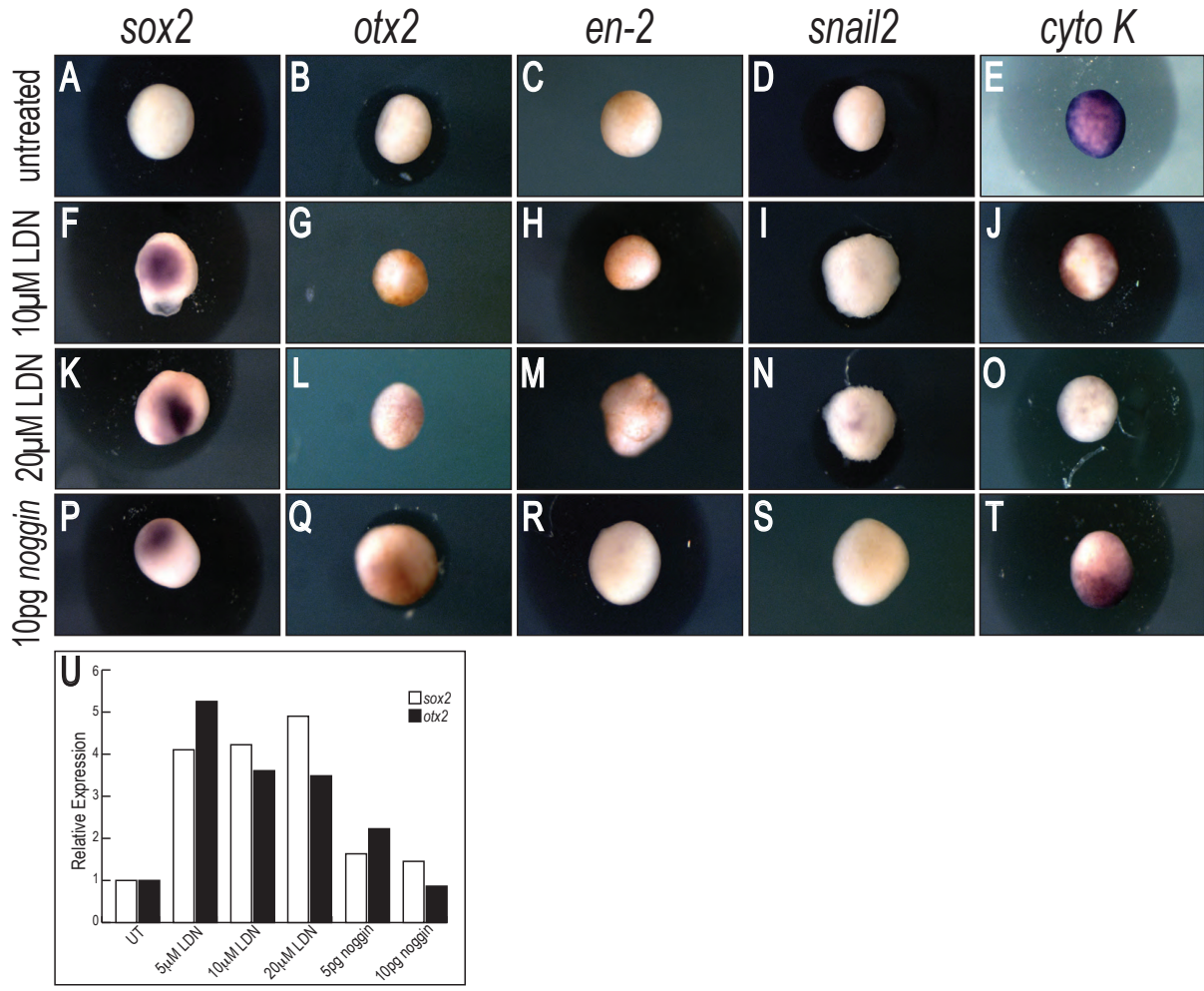
Figure 2.4. Treatment with LDN neuralizes animal caps.
Animal caps were excised at stage 9 and incubated with LDN until stage 17. (A-E) Untreated animal caps do not form neural tissue (A-C) or neural crest tissue (D), and instead form epidermis (E). (F-J) Animal caps created with 10μM LDN induce neural tissue (F-H), no neural crest (I) and minimal epidermis (J). (K-O) Increased concentration of LDN (20μM LDN) induces more neural tissues (K-M), and no neural crest (N) or epidermis (O). (P-T) Injection of 10pg of *noggin* mRNA induces neural tissue (P-R) as well as some epidermis (T), but no neural crest (S). (U) Quantitative RT-PCR analyses for expression of *sox2* (white bars) and *otx2* (black bars) demonstrate neural tissues are induced with treatment of LDN compared to *noggin* injections. Markers used: *sox2*- neural; *otx2*- forebrain/midbrain; *en-2*- hindbrain/midbrain; *snail2*- neural crest; *cyto K*- epidermis.

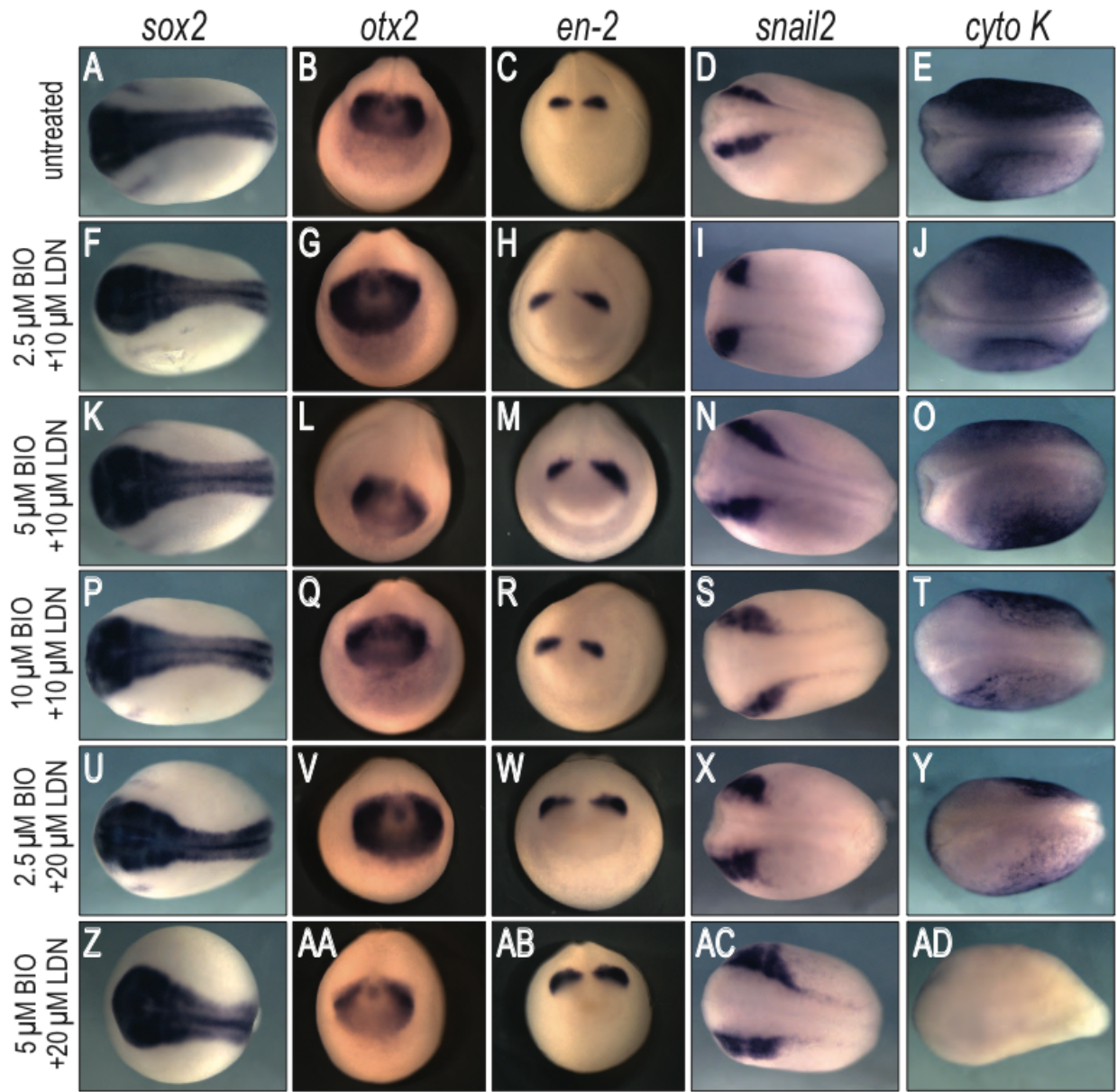|	*sox2*	*otx2*	*en-2*	*snail2*	*cyto K*
untreated	A	B	C	D	E
2.5 µM BIO +10 µM LDN	F	G	H	I	J
5 µM BIO +10 µM LDN	K	L	M	N	O
10 µM BIO +10 µM LDN	P	Q	R	S	T
2.5 µM BIO +20 µM LDN	U	V	W	X	Y
5 µM BIO +20 µM LDN	Z	AA	AB	AC	AD

AE
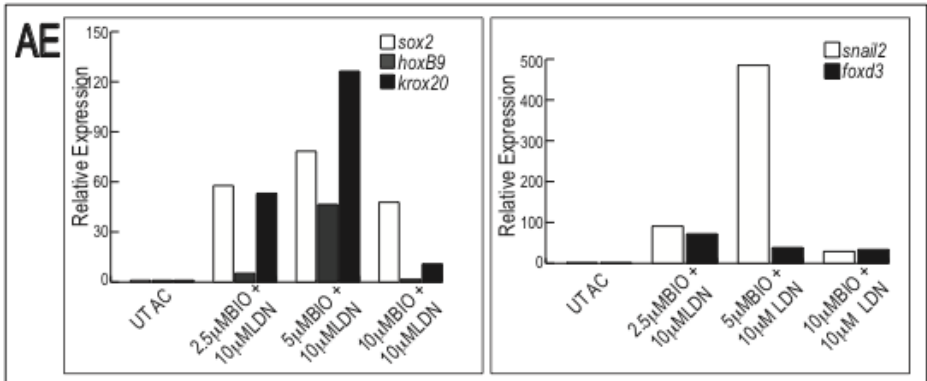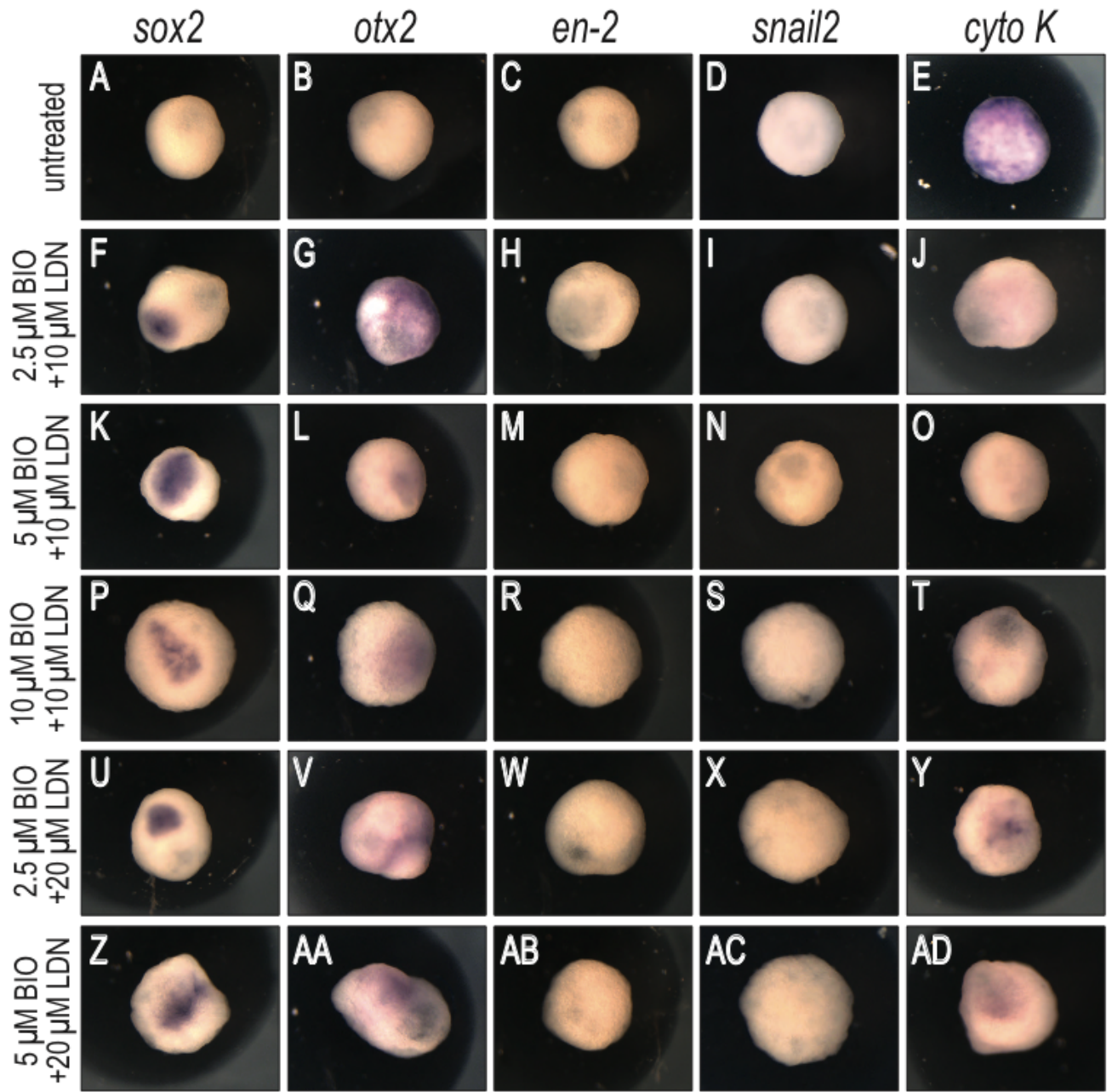
Figure 2.5. The combination of Wnt activation and BMP inhibition induces posterior neural tissue in animal caps.

(A-E) Untreated animal caps do not form neural tissue (A-C) or neural crest tissue (D), and instead form epidermis (E). (F-J) Treatment with 2.5µM BIO and 10µM LDN induces neural tissue (F-H), no neural crest (I) and small amounts of epidermis (J). (K-O) Treatment with 5µM BIO and 10µM LDN induces neural tissue (K-M) with no induction of neural crest (N) or epidermis (O). (P-T) Treatment with 10µM BIO and 10µM LDN induces neural tissue (P-R), no neural crest (S) and trace amounts of epidermis (T). (U-Y) Treatment with 2.5µM BIO and 20µM LDN induces neural tissue (U-W), no neural crest (X) and low amounts of epidermis (Y). (Z-AD) Treatment with 5µM BIO and 20µM LDN induces neural tissue (Z-AB), no neural crest (AC) and small amounts of epidermis (AD). (AE) Quantitative RT-PCR analyses for expression of *sox2*, *hoxB9, krox20, snail2* and *foxd3* demonstrate animal caps treated with LDN and BIO have increased expression of neural makers and neural crest markers. Left graph: Neural marker (*sox2*) as well as posterior neural makers (*hoxB9* and *krox20*) mRNA expressions are increased following incubation. Right graph: Neural crest marker (*snail2* and *foxd3*) expression is greatly increased following incubation. Markers used: *sox2*- neural; *otx2*- forebrain/midbrain; *en-2*- hindbrain/midbrain; *snail2*- neural crest; *cyto K*- epidermis; *hoxB9*- hindbrain; *krox20*- hindbrain; *foxd3*- neural crest.
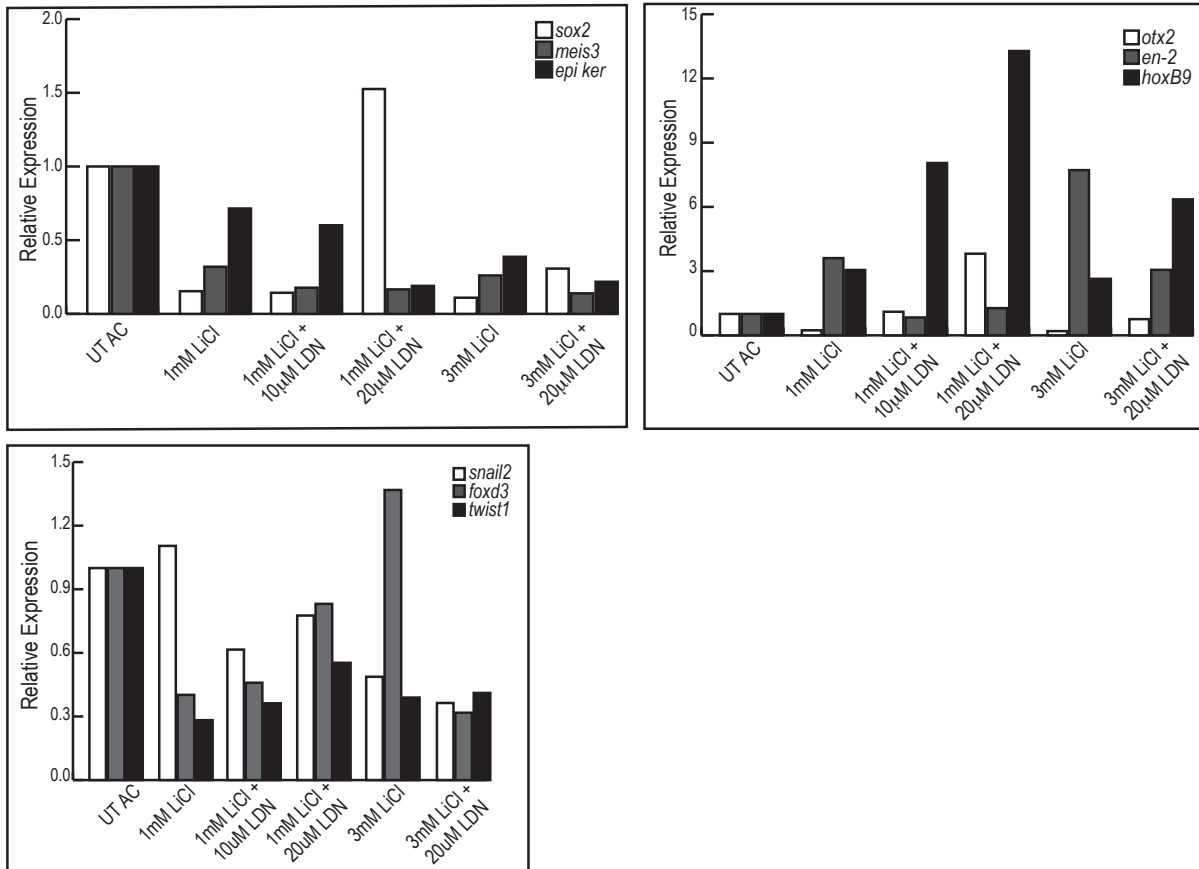
Figure 2.6. Comparison of small molecule drugs.
Gene expression of neural and neural crest markers in animal caps treated with LiCl and LDN. These treatments did not increase the expression to the same extent as treatment with BIO and LDN.

Chapter 3: Understanding melanoma pathogenesis by elucidating the gene regulatory network of melanocyte progenitors

3.1 INTRODUCTION

The previous chapter describes how the intersections of the Wnt and BMP signaling pathways set up the neural crest cell program in space and time. It is well accepted that positional cues are very important to set up the neural crest cell program, but the extent to how it regulates cell differentiation in the AP is less well understood. In this chapter, I demonstrate that transgenic zebrafish lines are the ideal models to determine how the position along the AP axis determines neural crest cell fate. Proposed experiments will begin to analyze the gene regulatory networks for the different cell fates, which will be useful for studying disease progression.

Zebrafish as a useful laboratory model

The Zebrafish, *Danio rerio,* has a relatively short relationship with science compared to the more commonly used mouse or frog; it has only been used in research since the late 1960s. The advantages, however, are abundant in that they are easy to maintain in tanks, one pair can produce up to 300 fertilized eggs a week, and they have a short generation time. The embryos develop outside of the body and are optically clear, allowing for easy observation and imaging of complex developmental events. Zebrafish are one of the most genetically tractable models since they can easily be injected with gene modifying constructs. Moreover, tissue-specific fluorescent transgenic fish have been generated in order to observe developmental, or disease, processes in real time using fluorescent microscopy. Transgenic fish also allow for fluorescence activated cell sorting (FACS) to be used to isolate specific cell populations which will allow for more detailed studies of small populations (Veldman and Lin, 2008).

A key issue with zebrafish, like any other model system, is establishing its relevance to human health. The zebrafish genome has been sequenced, providing genetic information for gene mapping studies and tools for studying novel genes. Furthermore, zebrafish are vertebrates, unlike the commonly used genetic models such as *Drosophila*, and over 80% of disease-causing genes in humans have zebrafish homologues, making them ideal for developmental and disease studies. For instance, they make an optimal model in which to study cancer biology since the oncogenes under cell-type specific promoters can be used to produce a variety of tumors, such as melanoma (Patton et al., 2005).

Non-cranial neural crest cells and melanoma

After the formation of the neural crest, the cells delaminate from the dorsal part of the neural tube and undergo EMT. The anteroposterior position at which the neural crest cells delaminate generally defines their fate, and there are remarkable differences between neural crest cells that originate from different axial levels. Roughly based on their position along the AP axis, the neural crest cells can be subdivided into two main groups: cranial and non-cranial. Non-cranial neural crest cells can be further divided into trunk, sacral, vagal and cardiac. The neural crest forms in a temporal manner, with the cranial neural crest being specified during gastrulation and the non-cranial crest later. One profound difference between the cranial and trunk neural crest is that cranial can form mesoderm-like tissues including skeletal, muscular and connective tissue while this skeletogenic potential of non-cranial neural crest cells is suppressed during normal development. This implies that while the different neural crest populations are exposed to a variety of unique regulatory interactions during their migration, the underlying gene network likely differ as well. Therefore, an important question in neural crest biology is when the neural crest cells segregate into distinct fates.

The gene regulatory network regulates the formation of the neural crest, and it involves complicated interactions between multiple signaling pathways and tissues. The GRN responsible for the formation of the cranial neural crest cells has been well studied in a number of species since its migration pattern is highly conserved across vertebrates (Meulemans and Bronner-Fraser, 2004; Prasad et al., 2012; Sauka-Spengler and Bronner-Fraser, 2006). However, due to the differences in migratory pathways and derivatives between trunk and cranial neural crest, the genes involved in regulation of the trunk neural crest are likely to be different than those involved in regulation of cranial neural crest. The cranial neural crest cells, which are the first neural crest population to form and initiate migration, migrate dorsolaterally and into the pharyngeal arches where they give rise to neurons, glia, ossicles, and craniofacial cartilage, bone and connective tissue (Minoux and Rijli, 2010). Trunk neural crest cells follow two migratory routes (Collazo et al., 1993); early migration follows a ventrolateral route through the anterior half of each somite, and gives rise to dorsal root ganglia, sympathetic ganglia, Schwann cells, adrenal medulla and aortic nerve clusters. Late migration follows a dorsolateral route and travels over the somites and into the epidermis where it gives rise to melanocytes (Knecht and Bronner-Fraser, 2002). In zebrafish, the melanocytes can also be formed from the ventrolateral route along nerves via a Schwann cell/melanoblast progenitor (Cramer, 1991). Some studies have begun to investigate the differences in the gene regulatory networks between cranial and non-cranial neural crest cells. Findings that cranial neural crest cells have a higher expression of mesenchymal genes is consistent with the fact that cranial neural crest cells differentiate into mesenchymal derivates, while non-cranial neural crest cells do not (Hagiwara et al., 2014).

The neural crest gives rise to three distinct pigment cell types in zebrafish: the black-brown melanocytes, the reflective iridophores and the yellow xanthophores, which together form the zebrafish stripes. Although these different pigment cells are closely related by lineage, different zebrafish mutants selectively affect only one cell type, indicating different genetic requirements for each type. Melanocytes arise from the trunk neural crest and migrate throughout the zebrafish body in two waves of migrating melanocytes. In the first wave, embryonic melanocytes, arise directly from the neural crest and contributes to four stripes of the body plan: the dorsal larval

stripe, lateral larval stripe, ventral larval stripe and yolk sac stripe. These cells follow either the dorsolateral migration pathway between the ectoderm and somites to contribute to the larval stripes or travel along nerves in a ventromedial pathway to contribute to lateral, ventral and yolk sac stripes (Dooley et al., 2013). While it was initially thought the stripe patterns are due to clones of migrating melanoblasts from a small number of precursors, studies have shown there is a large amount of mixing at axial levels, which makes studies of precise progenitors problematic (Wilkie et al., 2002). The second wave of migrating melanocytes occurs at later stages in development during metamorphosis to form the adult stripes of the zebrafish body (Hultman and Johnson, 2010).

The master regulator of melanocyte biology appears to be the transcription factor microphthalmia-associated transcription factor, MITF, which controls the differentiation of neural crest cells into melanocytes. Although it is not entirely clear how *mitf* is activated, studies have shown the traditional neural crest specifiers such as Foxd3, Sox2, Snail2 and Sox9 may be involved in *mitf* activation (Mort et al., 2015a). Zebrafish lacking *mitfa* lack all embryonic and adult melanocytes while ectopic expression produces ectopic melanocytes (Lister et al., 2014). Targets of this transcription factor include genes responsible for melanocyte-specific organelles as well as those in the melanin synthesis pathway.

Neural crest cells migrate throughout the developing embryo, interact with the environment during their migration to localize to specific positions in the embryo, and self-renew. These properties of neural crest are shared with the multipotent tumor cells and may be the reason melanoma, the cancer that arises from neural crest-derived melanocytes, is particularly aggressive and metastatic. Current understanding of melanoma pathogenesis suggests that melanoma arises from reinitiation of the embryonic developmental program in an aberrant fashion. The transformation of melanoctyes reinitiates an embryonic neural crest signature and activates a melanoma gene program that is frequently driven by mutations in BRAF or RAS, seen in 80% of cases (Mort et al., 2015b). Interestingly, aggressive melanoma cells upregulate a subset of neural crest cell guidance and differentiation genes compared to the non-aggressive melanoma cells (Kasemeier-Kulesa et al., 2008). The incidence of melanoma is rapidly growing owing to increased awareness, improved detection, and exposure to harmful UV radiation in the general population. Despite significant advances in the diagnosis and treatment of metastatic melanoma, melanoma is responsible for over 9,000 deaths and over 75,000 new cases in the United States each year (Siegel et al., 2013). Understanding the genetic and environmental elements of melanoma is necessary for reversing this deadly disease.

Isolation of single neural crest cells and allowing their differentiation *in vivo* shows some can give rise to mixed clones with neurons and glia, or glia and melanocytes, while others produce only a single cell type. This creates a complicated fate map, with glia arising from two different origins (Dupin and Le Douarin, 2003). Recently, it was found that iridophores and melanophores both originate from a shared dorsal root ganglia niche and follow the same migratory pathway along nerves. Melanoblasts continue on to the stripe where they eventually differentiate into melanocytes (Singh and Nüsslein-Volhard, 2015). The manner in which the multipotent neural crest cells become lineage restricted to the melanocyte fate has been well studied (Dupin et al., 2000). The neural crest cells become a multipotent glia-melanocyte progenitor and then become further restricted to committed pigmented melanoblasts. This commitment occurs either within

the neural tube or after migration has begun. In the case of zebrafish, this commitment occurs prior to migration.

One unanswered question in neural crest biology is the question of early neural crest commitment in relation to their time and position within the dorsal neural tube. Initial fate mapping studies have shown that subsets of neural crest cells have multiple fates, while other cells exhibit lineage restriction at pre-migratory stages (Raible and Eisen, 1994; Schilling and Kimmel, 1994). Therefore, this data argues for early neural crest fate restrictions. More recent studies using fluorescent dye microinjections have found that neural crest cells from any mediolateral position along the dorsal neural tube were able to follow both the dorsal and ventral migratory pathways, arguing against early fate determination of neural crest cells (McKinney et al., 2013). Discrepancies in results may be due to technical errors in injections or the timing at which injections were performed. Advances in genetic methods, such as the *sox10:kaede* transgenic line used here, will help to make sense of the mechanisms and timing of neural crest lineage restriction.

When the tightly regulated morphogenetic events of neural crest development are perturbed, either by genetic or environmental factors, malformations can occur ranging from congenital heart defects and Hirschsprung disease to melanoma and other cancers. Therefore, the inherent mobility and versatility of neural crest cells makes them capable of contributing to both normal development and severe developmental pathologies. A greater understanding of the genes that regulate neural crest migration and differentiation is necessary to inform our understanding of the etiology of neural crest diseases. Analysis of gene regulatory networks will provide insight into the program that contributes to tumor formation. One important question in developmental biology, and consequently cancer biology, is if non-cranial neural crest cells arise from the same progenitor population as the cranial neural crest cells. One way to address this question is to determine the gene regulatory networks of melanoma cells versus that of normal neural crest cells and determine which genes are expressed exclusively in melanoma cells. Understanding the biology of melanocytes is crucial to better understanding melanoma progression as well as to generating new therapeutics. While there are many parallels between neural crest cell biology and cancer metastasis, it is important to keep in mind there are likely to be profound differences between the two. Therefore, studies on neural crest biology can be considered one starting point for better understanding cancer progression.

3.2 RESEARCH METHODOLOGY

Zebrafish husbandry and strains
All embryos and fish were raised and cared for as described (Westerfield, 1993) and staged using established protocols (Kimmel et al., 1995). Zebrafish were maintained and bred at 28.5º on a 14-hour light and 10-hour dark cycle. Embryos were generated and collected by natural spawning. Tubingen fish were used as wild type.

Lineage analysis
Photoconversions of neural crest cells in the regions of interest of *sox10*:*kaede* embryos were carried out as follows: embryos were raised until the 10-somite stage, dechorionated, selected for

strong fluorescent expression, and mounted in 3% methylcellulose containing 0.013% tricaine. Embryos were photoconverted at the 10-somite stage using a Nixon Eclipse Ti AIR scanning confocal microscope. Photoconversion was performed using the full strength UV laser (404 nm) for 30 seconds, or until the green Kaede fluorescent signal disappeared completely. Embryos were raised until 72 hours post fertilization, and imaged on the confocal microscope every 24 hours by mounting in methylcellulose with tricaine. Photoconversions were performed unilaterally so the contralateral side served as an internal control. Green and red fluorescent signals were captured simultaneously by using the 488 nm and 563 nm laser wavelengths.

RNA *in situ* hybridization
In situ hybridization of mRNA transcripts was performed as described (Thisse and Thisse, 2008), with probes synthesized with T3 polymerase using the primers listed in Appendix II. Briefly, embryos are collected at the indicated stages and fixed overnight in 4% paraformaldehyde in 1X PBS at 4°. The next day, embryos are dehydrated in a series of methanol washes, and placed in 100% methanol for at least 2 hours at -20°. Embryos are rehydrated, placed in a formamide-containing prehybridization solution for 3-4 hours at 70°. Embryos are then incubated with the probe in hybridization buffer overnight at 70°. Next, they under go a series of stringent washes with SSC, blocked with 2mg/mL BSA in 2% sheep serum in PBST and incuated overnight with anti-DIG antibody at 1/10,000. Finally, the embryos are incubated with a labeling solution of NBT and BCIP until the color appears. For each probe in a given experiment, all color reactions were developed for the same amount of time

3.3 RESULTS AND DISCUSSION

Understanding aberrant reinitiation of embryonic signaling pathways in adult melanocytes is essential to elucidating the precise mechanisms behind the transition of melanocytes to melanoma (Libra, 2009). While a detailed embryonic lineage map of cranial neural crest cells has been described for craniofacial development (Dougherty et al., 2012), the non-cranial neural crest cells that give rise to melanocyte progenitors are understudied. To begin answering the question of how and when non-cranial neural crest cells segregate into distinct fates, I used the zebrafish model in order to construct the non-cranial neural crest cell lineage map and elucidate the gene regulatory network involved in melanocyte specification, migration and differentiation. The goal of this work is to better understand the molecular mechanisms that govern normal melanocyte development and migration in order to better understand the disease process of melanoma.

Expression patterns of neural crest genes in the developing embryo

Studies have indicated there are numerous genes important for the different stages of neural crest formation. SoxE family members, *sox8/9/10*, have been found to be among the earliest genes expressed in bona fide neural crest cells (McKeown et al., 2005) with *sox9* and *sox10* being

expressed earlier than *sox8*. *dlx2* belongs to the distal-less (Dll) family of genes that are important in craniofacial patterning, and highly expressed in migration neural crest cells (Akimenko et al., 1994; Yan et al., 2002). *Foxd3* is one of the earliest neural crest markers expressed and is required for expression of other neural crest specifier genes. An important first step of this study was to examine the gene expression patterns of *sox9*, *sox10, foxd3, dlx2* and *tfap2e* to determine how their expression changes over time, as the neural crest is developing. Zebrafish embryos were collected at various stages and mRNA transcripts were detected by *in situ* hybridization. By examining the expression at various time points from the earliest stages of neural crest formation (10-somite stage), to the stage at which melanocytes begin to form (24hpf) and after differentiation has begun (48hpf), I was able to get a temporal understanding of the dynamic changes the neural crest cells are undergoing at these stages.

Embryos were stained at the 10-somite stage, which is prior to neural crest migration, and 18-somite stage during which migration is occurring (Figure 3.1). As expected, the neural marker *sox2* was expressed through the entire head region (Figure 3.1. A, A'). The early neural crest markers *sox9* and *sox10* are expressed in the neural crest tissues, otic placode and somites (Figure 3.1 B-C'). *foxd3*, another early neural crest marker, is expressed throughout the neural crest tissue at the anterior-most part of the head (Figure 3.1 D, D'). The marker for migratory neural crest cells, *dlx2*, had no detectable expression at the 10-somite stage, confirming neural crest cells have not begun to migrate yet (Figure 3.1 E). At the 18-somite stage, *sox9* and *sox10* are still strongly expressed throughout the embryo's axis (Figure 3.1 F,F',G,G'). At this later stage, *dlx2* expression can be detected in the pharyngeal arches indicating the neural crest cells are migrating at this time.

These genes were also examined at later stages (24hpf, 28hpf, 38-48hpf) during which neural crest cells are migrating and differentiating (Figure 3.2). The neural marker *sox2* is strongly expressed in the head region but that expression diminishes over time and is undetectable by 38hpf (Figure 3.2 A,A', G, G', M,M'), which is a similar expression pattern to that seen for *foxd3* (Figure 3.2 E, E', K, K', Q, Q'). *sox9* and *sox10* are still strongly expressed in the neural crest tissues and otic placode, and also in the somites along the body axis. (Figure 3.2 B,B', H, H', N, N', C, C', I, I', O, O') . At all later stages examined, *dlx2* is expressed in branchial arches indicative of migrating neural crest cells (Figure 3.2D, D', J, J', P, P'). *tfap2e* is detected throughout the tissues at these stages, consistent with its role in neural crest development (Figure 3.2 F, F', L, L', R, R').

Together these *in situ* patterns show that every gene is expressed differently as neural crest development proceeds. Genes involved in early aspects of neural crest formation are highly expressed at earlier timepoints, and that expression is lost over time. Conversely, genes involved in later steps of neural crest formation, such as *dlx2* in migration, have an increase in expression as development proceeds.

Determination of cranial vs. non-cranial populations

In order to analyze the GRN regulating trunk neural crest cells, the cranial and trunk regions had to first be distinguished. *sox9* is biphasic with expression at the earliest stages of neural crest formation and again later in differentiated craniofacial cartilages (Cheung and Briscoe, 2003;

Spokony et al., 2002). *sox9* is an important mediator of the differentiation of neural crest cells into chondrocytes as it is a direct regulator of several genes that are crucial for chondrocyte development. The expression patterns combined with the biphasic functions of *sox9* made *sox10* the better marker for distinguishing the two populations. The expression of *sox10* remained constant over time, compared with the expression of *sox9*, and therefore the early expression patterns of *sox10* were re-examined (Figure 3.3*). sox10* is expressed from the earliest stages of neural crest formation and is required for early survival and migration of neural crest cells (McKeown et al., 2005), and therefore made a appropriate marker for neural crest cells. At both the 10-somite and 18-somite stages, two large populations of *sox10+* cells are separated by the otic vesicle (Figure 3.2 A, B, arrowhead in A). At the 10-somite stage, posterior to the otic vesicle, neural crest cells start as two distinct populations on either side of the midline and eventually combine into one single line of neural crest cells (Figure 3.2 A'). At the 18-somite stage, this single line has again been divided on either side of the midline (Figure 3.2 B'). From these expression patterns, we will consider the *sox10+* cells posterior to the otic vesicle as non-cranial neural crest cells.

sox10:kaede transgenic line as a tool for fate map construction

Previous studies have elucidated precise regions of neural crest cells along the A-P axis that give rise to craniofacial structures (Dougherty et al., 2012). Although the migration patterns of the trunk neural crest cells have been well described in zebrafish, it is still unknown where along the A-P axis they arise. The *sox10:kaede* transgenic fish (Dougherty et al., 2012) were utilized to construct a lineage map of the trunk neural crest. The 10-somite stage was selected as the time point for the construction of the fate map because this is a period in early embryogenesis during which *sox10* expression is robust and the neural crest cells can be visualized as a single sheet of cells just below the surface of the ectoderm. By using a *sox10:*kaede transgenic line, the *sox10* promoter confers lineage restriction of the photoconvertible protein Kaede to neural crest cells, beginning from the onset of neural crest delamination from the neural tube to subsequent derivatives. Upon UV-exposure, the Kaede protein undergoes irreversible photoconversion from green fluorescence to red, enabling us to precisely trace specific cells. In addition, this line ensures that only neural crest cells are photoconverted and, therefore, only their derivatives will be labeled at later stages, allowing for more specific imaging. Whole mount *in situ* hybridization to detect *sox10* was a control to be sure *kaede* expression was driven only where *sox10 is* endogenously expressed.

Photoconversions were carried out at the 10-somite stage by exposing a region of the green *sox10:kaede* cells to the UV light for 30-60 seconds until the green disappeared. Successful photoconversions were confirmed by examining the presence of red *sox10:kaede* cells. At this point, the *in situ* expression was compared to the photoconverted images to determine which regions were photoconverted (Figure 3.4 A-B). The embryos were then allowed to develop, in the dark, until they were collected for further imaging. At 96dpf, the photoconverted embryos were reexamined and it was confirmed that the photoconverted cells migrated throughout the trunk regions of the embryos (Figure 3.4 C-D). From these proof-of-concept experiments we conclude that this transgenic line will enables us to identify *in vivo* and isolate *in vitro* precise non-cranial neural crest populations that will give rise to specific derivatives.

Construction of a trunk neural crest fate map

The initial studies to determine the fate map of neural crest cells were performed by Nicole Le Douarin in the 1970s (Le Douarin, 1973; Le Douarin and Teillet, 1974; Le Lièvre and Le Douarin, 1975). By taking advantage of the differences in the quail and chick interphase nuclei, cells could readily be identified from either species. Quail cells contain a condensed mass of heterchromatin in their nucleus, while chick cells contain euchromatic DNA. Neural tubes from quail were transplanted into the same (or different) axial level of the chick embryo and the migration patterns and derivatives were followed. These quail-chick chimera experiments confirmed the migratory pathways of the trunk neural crest cells and made it possible to determine the full range of neural crest derivatives from different regions of the AP axis. Following these experiments, a quail-specific antibody was used to differentiate quail and duck cells in "quck" and "duail" chimeric experiments which replaced the need to examine the DNA (Schneider and Helms, 2003). More recently, a *sox10:kaede* transgenic line was developed and lineage analysis showed that at the 10-somite stage, cranial neural crest cells anterior to the eye contributed to the median palate, whereas cells medial to the eye formed the lateral palate and trabeculae and a posterior population formed the mandible (Dougherty et al., 2012). However, fate map studies using the transgenic line have not been carried out to verify the early fate maps obtained using chimeras. Therefore, once it was confirmed that the *sox10:kaede* line could be used to reliably photoconvert specific populations of non-cranial neural crest, we set out to construct the non-cranial neural crest fate map.

Photoconversions were performed prior to neural crest cell delamination and migration and analyzed after differentiation was complete. By 60hpf, red photoconverted cells can be seen in the iridophores between the melanocytes (Figure 3.5 B). This indicates that the small subset of non-cranial neural crest cells that were photoconverted selectively gave rise to iridophores and not melanocytes, even though they are both neural crest-derived. By 96hpf, the red photoconverted cells are still there but there are far fewer of them, either due to differentiation or remodeling of the zebrafish stripe. (Figure 3.5 C).

The photoconversions demonstrate that seemingly similar neural crest-derived tissues arise from very distinct positions along the anteroposterior axis of the developing vertebrate embryo. Iridophores and melanocytes are both neural crest-derived pigment cells known to follow the same migratory path, so we thought they would arise from the same positions along the AP axis. Interestingly, photoconversion of one portion of the 10-somite embryo showed only the iridophores were photoconveted, but not the melanocytes. The melanocytes are visible as dark and dendiritic in shape, without any red photoconversion.

Through these studies we hoped to gain insight into the molecular mechanisms that govern normal neural crest development and migration and how they are recapitulated in disease. The non-cranial neural crest lineage map is an invaluable tool for developmental biologists investigating development of cell types that originate from the non-cranial neural crest, such as dorsal root ganglia, enteric neurons, adrenal medulla, and aortic nerve clusters, in addition to the melanocytic progenitors. By creating a fate map of the non-cranial neural crest, we can determine how perturbations in signaling pathways known to be involved in early stages of neural crest formation can affect migration and differentiation, and ultimately the lineage map, of

the non-cranial neural crest cells. Zebrafish embryogenesis can easily and reliably be perturbed by incubations in small molecules, which are useful for studying the signaling pathways involved in later stages of neural crest formation such as Wnt and BMP signaling. Further, this work has the potential to elucidate the pathogenic nature of melanoma and therefore enable better molecular oncotyping and novel treatment modalities. This work, in conjunction with single cell RNA sequencing will elucidate the molecular program that directs non-cranial neural crest development and address broader questions in cellular specification and differentiation.

3.4 FUTURE DIRECTIONS

There are several unanswered questions in melanoma biology. How many melanoblast progenitors are there and how are they distributed? How much mixing is there between progeny from different progenitors? How large a region can one melanoblast progenitor populate? Zebrafish will be a great model to begin answering these questions. The ability to model cancer in zebrafish will help to advance cancer research due to the high-throughput and high-content screening approaches (Ceol et al., 2008; Patton et al., 2005; Tan and Zon, 2011). Small molecule screening in zebrafish has the potential to uncover novel and known molecules that affect melanoma and melanoma biology, such as melanocyte development, migration, pigmentation and survival.

The neural crest is a very heterogeneous population of cells. This is evident from the finding that neural crest cells give rise to a variety of derivatives from both the cranial and non-cranial subpopulations. Additionally, cells within one subpopulation will not always give rise to the same cells; for example, melanocytes form via a Schwann cell/melanoblast progenitor. Therefore, there are likely to be intrinsic differences in the GRN and differences in epigenetics, allowing cells to respond differently to the microenvironments they encounter during migration.

Defining the GRN of non-cranial neural crest cells

Studies have shown that the cranial and non-cranial neural crest populations are both capable of differentiating into glia, sensory neurons, and various other neurons. However, only the cranial neural crest cells are capable of giving rise to mesenchymal derivatives, cartilage and bone. Additionally, the surface properties of the cranial and non-cranial neural crest cells differ in many ways, notably they contain distinct integrins for interacting with the extracellular matrix during migration (Lallier et al., 1992). Together, these findings show that cranial and non-cranial neural crest populations share some properties, but they also have inherent differences.

For these reasons, studies on the gene regulatory network (GRN) of neural crest cells from different populations and axial levels are still necessary. In order to elucidate the GRN of non-cranial neural crest cells, I will utilize a new method for high-throughput single cell sequencing using a microfluidic approach to barcode individual cells, called inDrop (Klein et al., 2015). Microfluidics are an emerging technology leveraging miniature fluid-containing channels to allow for precise control of small volumes of reagent (Li et al., 2014). The key advantages to microfluidics include high throughput, low reagent usage, reproducibility, and automation.

Microfluidic chambers are commonly referred to as a "lab-on-a-chip" platform as they are often capable of automating laborious laboratory protocols in a single chip. This novel inDrop approach captures and barcodes cells in nanoliter droplets with high capture efficiency, allowing for sequencing of thousands of mRNAs. This highly reproducible and sensitive technique will allow for single cells from the cranial and non-cranial populations to be analyzed, and their GRNs compared. Cells from the *sox10:GFP* transgenic line will be FACs sorted from different positions along the A-P axis and subjected to the inDrop barcoding approach. Analysis of the sequencing data will reveal the GRN of both the cranial and non-cranial populations which will allow us to determine which genes differ between the two populations. Once I identify genes that are differentially expressed in the different populations, I will perform *in situ* hybridization to confirm the genes are differentially expressed along the A-P axis in embryos. In addition to comparing the GRN of cranial and non-cranial neural crest cells, I will repeat the sequencing at multiple time points of neural crest cell migration and differentiation. From this, I will be able to determine how the GRN changes as the cells undergo migration and differentiation, which will give further insight into the question of whether the cell identity is intrinsic or if it is acquired during migration when they are exposed to new microenvironments.

Epigenetic regulation in neural crest biology

The current understanding of the GRN has all been determined from interactions between transcription factors and signaling molecules, and does not include regulation imparted by epigenetic control. However, there is increasing data showing that epigenetic regulation is very important for neural crest formation and patterning. Like other progenitor cells, neural crest cells likely undergo global epigenetic modifications as they are specified and differentiate into various derivatives. For instance, miRNAs are known to modulate epigenetic landscapes in neural crest cells by regulating molecules that change histone marks during neural crest development. miR-140 regulates Pdgf signaling during palate development, and loss of miR-140 causes alterations in palate shape. Additionally, mutants of DGCR8, a RNA-binding protein that interacts with the RNase II enzyme, Drosha, display malformations in cardiac neural crest cell patterning (Chapnik et al., 2012).

There is also increasing evidence demonstrating that chromatin modifications are involved in the development of the neural crest (Strobl-Mazzulla and Bronner, 2012; Strobl-Mazzulla et al., 2010). A new way of gaining insight on cell fates is by looking at the cell-type specific open chromatin landmark (Stergachis et al., 2013), in which lineage differentiation is associated with loss of DNase-I hypersensitivity sites, implying that changes in DNA landscapes is an indicator of cell-fate transitions. Comparison of open chromatin landscapes in different cell types has revealed distinct patterns. There are many cell-type specific open chromatin regions that are likely to correspond to tissue-specific regulatory regions. Assay for transposase-accessible chromatin with sequencing (ATAC-seq) identifies regions of open chromatin. By taking advantage of advancements in ATAC-seq for single-cells (Buenrostro et al., 2015; Pott and Lieb, 2015), I will be able to study the DNA accessibility of the different neural crest populations and uncover hierarchies of the derivatives.

Another epigenetic regulator involved in neural crest formation is DNA methylation. During development, genetic repression by DNA methylation is a common way to turn off pathways

during specification and differentiation. In this way, DNA methylation at promoter regions of genes restricts cell fate choices during development. Global DNA demethylation is necessary for stem cells to acquire pluripotency (Mayer et al., 2000). The process of DNA methylation is mediated by the family of DNA methlytransferases, DNMT1, DNMT3A and 3B, which catalyze the transfer of a methyl group on cytosine. In the neural crest, DNMTs have been shown to be important for the development into specific lineages, and mutations in these genes have been associated with craniofacial defects. Each cell lineage is likely marked with different DNA methylation markers at a given developmental time, and revealing these epigenetic modifications be will be critical for understanding the differences in lineage.

Figure 3.1 Time-course expression patterns of *sox2, sox9, sox10, foxD3* and *dlx2*.

Early expression patterns show neural and neural crest markers at the 10-somite stage (A-D') and 18-somite stage (F-H'). (A,A') Neural marker *sox2* is expressed throughout the head region. (B-B') Early neural crest marker *sox9* is highly expressed in the otic placode and somites. (C-C') early neural crest marker *sox10* is expressed strongly in neural crest tissues and otic placode. (D-D') Neural crest marker *foxd3* is expressed in the anterior-most neural crest tissue, otic placode and somites. (E) At the 10-somite stage, no *dlx2* expression is detected. (F-F') At the 18-somite stage, *sox9* expression is decreased along the body axis. (G-G') At the 18-somite stage, *sox10* expression has decreased along the axis. (H-H') At the 18-somite stage, *dlx2* expression is detected in the pharyngeal arches, indicative of migratory neural crest cells. A-H Lateral views with anterior on the left. A'-H' dorsal views with anterior on the left.

sox2 *sox9* *sox10* *foxd3* *dlx2* *tfap2e*

| A | B | C | D | E | F |
| A' | B' | C' | D' | E' | F' |

24hpf

| G | H | I | J | K | L |
| G' | H' | I' | J' | K' | L' |

28hpf

42

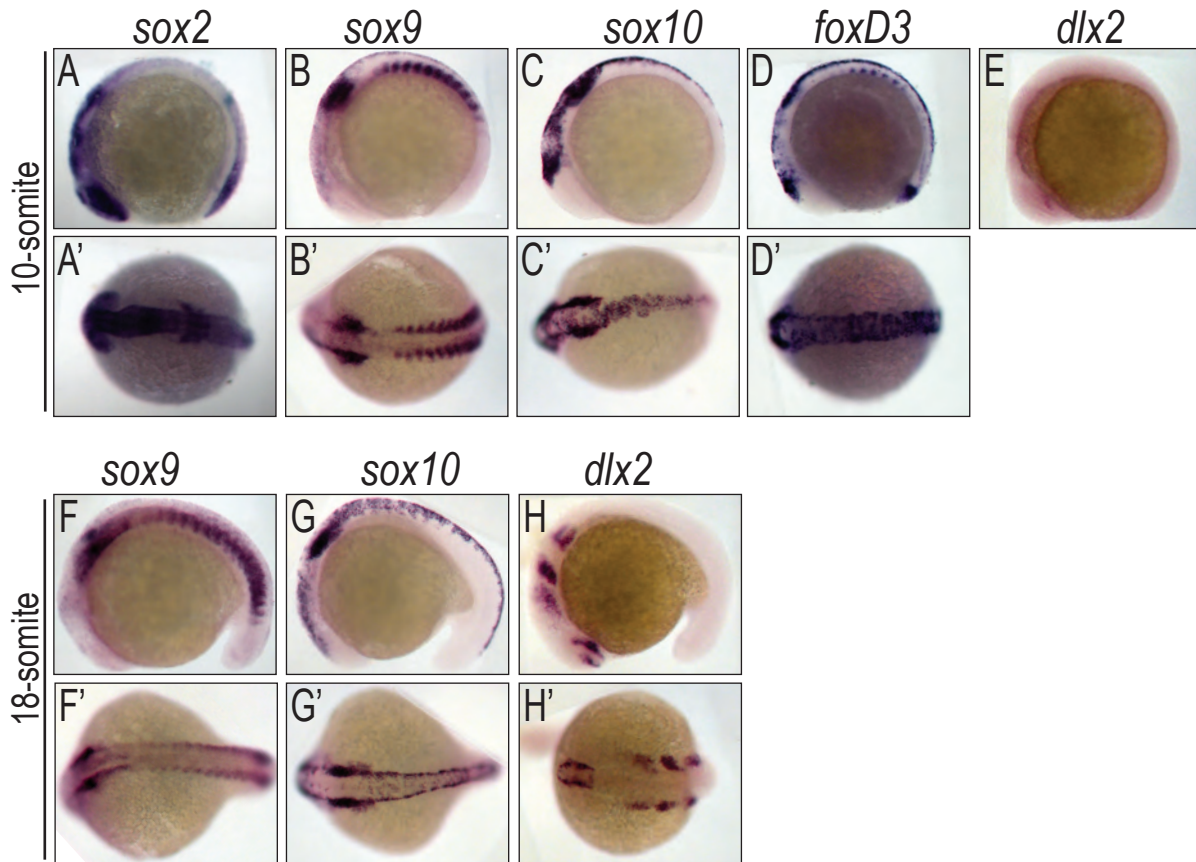| M | N | O | P | Q | R |
| M' | N' | O' | P' | Q' | R' |
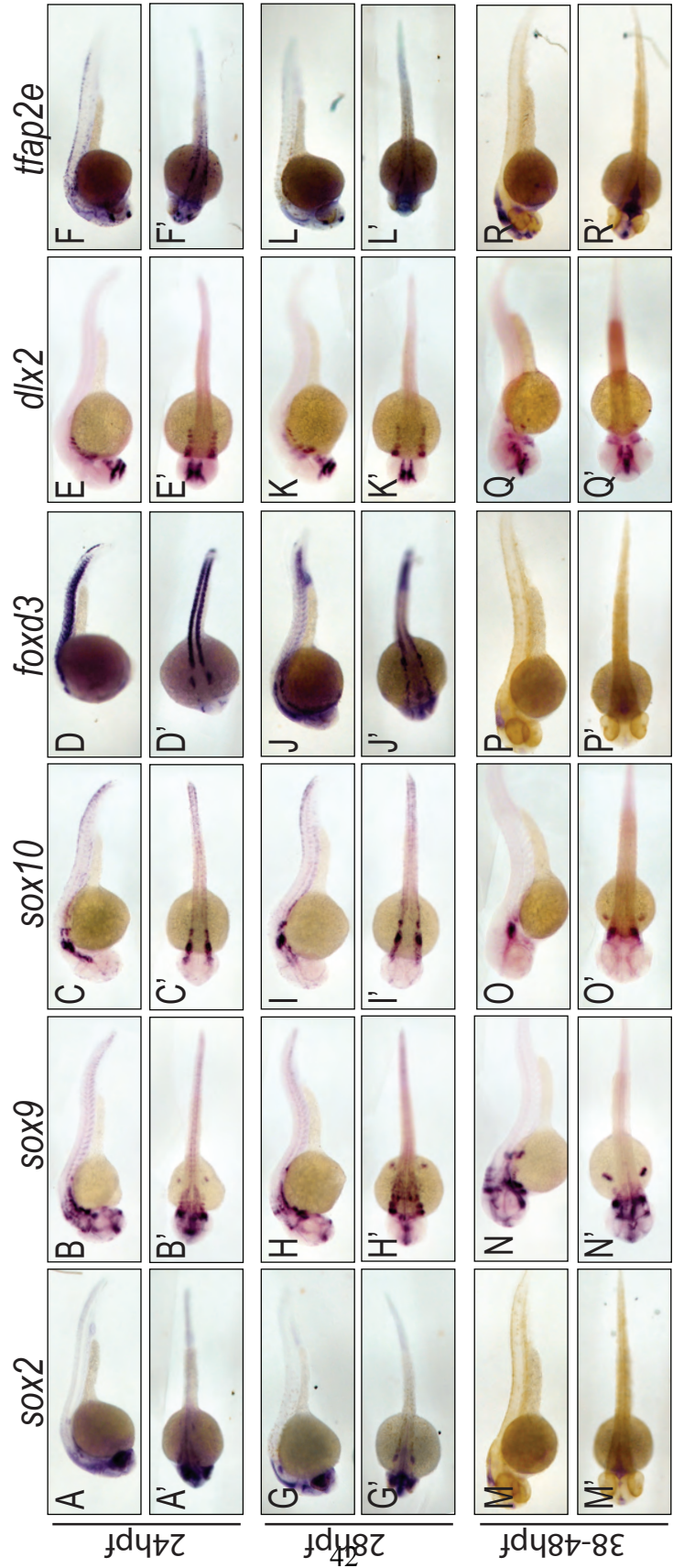
38-48hpf

Figure 3.2. Time-course expression patterns of *sox2, sox9, sox10, foxd3, dlx2 and tfap2e*.

Late expression patterns of neural and neural crest markers at 24 hpf (A-F'), 28hpf (G-L') and 38-48hpf (M-R'). (A,A', G, G', M,M') Neural marker *sox2* is strongly expressed in the head region but that expression diminishes over time. (B,B', H, H', N, N') Early neural crest marker *sox9* is highly expressed in the otic placode and somites. (C, C', I, I', O, O') early neural crest maker *sox10* is expressed strongly in neural crest tissues and otic placode. (D, D', J, J', P, P') Neural crest maker *foxd3* is expressed in the anterior-most neural crest tissue, otic placode and somites. (E, E', K, K', Q, Q') *dlx2* expression is detected in branchial arches. (F, F', L, L', R, R') *tfap2e* is expressed at all stages, with less expression in the trunk regions at the later stage. A-F, G-L, M-R Lateral views with anterior on the left. A'-F', G'-L', M'-R' dorsal views with anterior on the left.
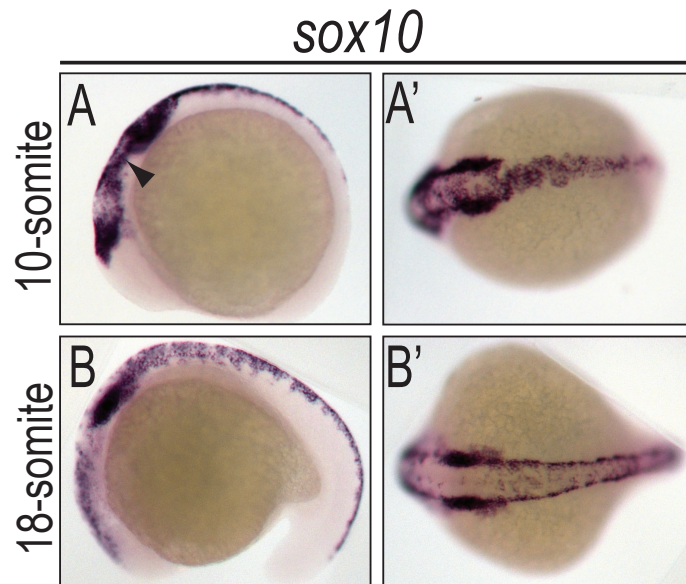
Figure 3.3. *sox10* expression defines cranial and trunk neural crest regions.
sox10 mRNA expression was detected by *in situ* hybridization in 10-somite (A, A') and 18-somite (B, B') wild-type embryos. Otic vesicle (arrowhead, A) appears to be separating the cranial and trunk regions. A, B Lateral views with anterior on the left. A', B' dorsal views with anterior on the left.

sox10 in situ

sox10:kaede

sox10:kaede

unconverted kaede converted kaede
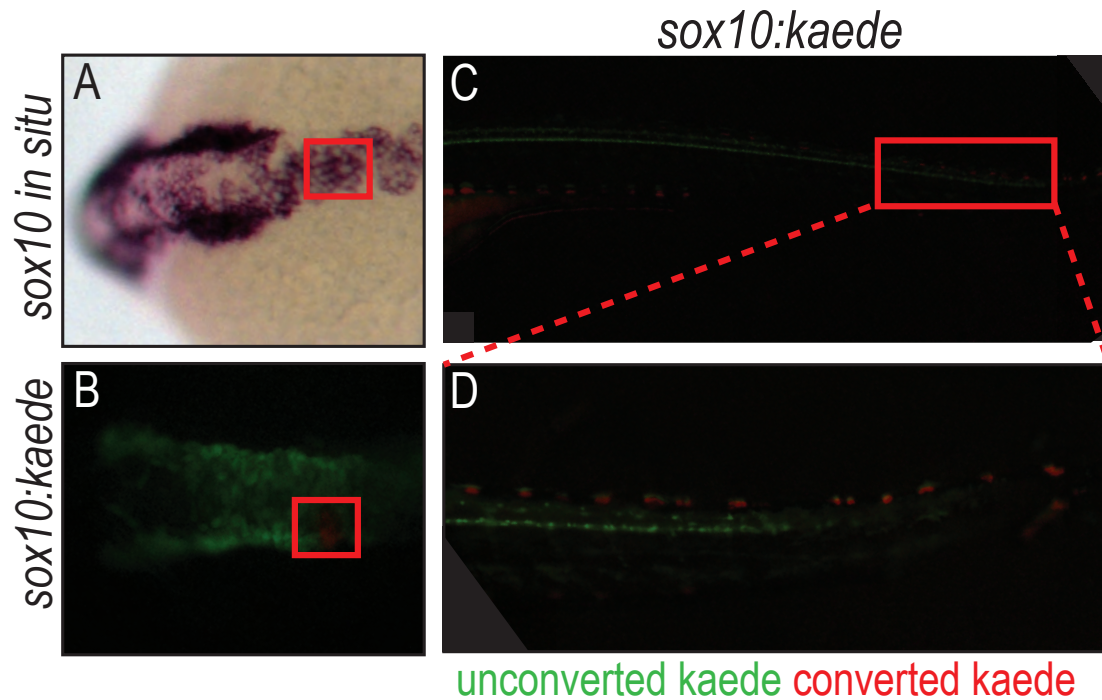
Figure 3.4. *sox10:keade* transgenic line to selectively label non-cranial neural crest cells.

Photoconverted non-cranial neural crest cells in *sox10:kaede* embryos**.** A) *In situ* hybridization image of a 10-somite wild type zebrafish embryo stained for *sox10*. B) Fluorescent microscopy image of photoconverted neural crest cells in a 10-somite *sox10:kaede* embryo depicted where photoconversion occurred. (C) Fluorescence microscopy image of photoconverted neural crest cells at 96hpf taken at 20X magnification. Green fluorescence depicts all *sox10*-expressing cells in the embryo and red fluorescence shows the photoconverted cells. (D) Magnified views of panel C, demonstrating successful photoconversion of neural crest cells in the trunk region.

Figure 3.5. Photoconverted cells in the tail region of the zebrafish embryo give rise to iridophores.

In situ hybridization shows *sox10* expression in 48hpf embryo (A). By 60hpf, red photoconverted cells can be seen in between the melanocytes (B). By 96hpf, red photoconverted cells are still present, but are less numerous (C).

Chapter 4: Analysis of the role of non-canonical Wnt signaling in craniofacial development

The previous chapter describes how the position along the A-P axis determines neural crest cell fate. Continuing along the studies of 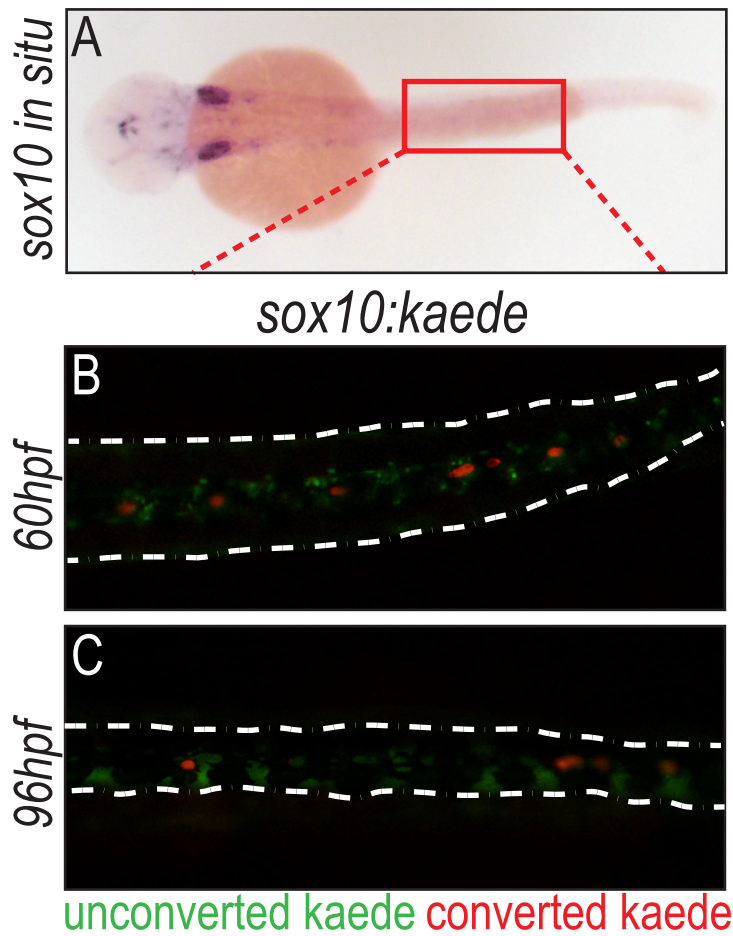positional cues in neural crest development, this chapter describes how abolishing one cue (Wnt signaling) results in developmental defects. Proposed experiments will provide further insight into the roles the Wnt receptors play in craniofacial development.

4.1 INTRODUCTION

Cranial malformations

Two central questions in developmental biology are how cells organize into higher ordered structures and which genes regulate these processes. In all vertebrates, the palate forms from segmented streams of neural crest cells migrating from the dorsal neural tube to the pharyngeal arches. One subset of the first stream of cranial neural crest cells resides below the eye and is referred to as frontonasal cranial neural crest. The second portion of the first stream populates the maxillary domain ventral to the eye and dorsal to the oral ectoderm, as well as the mandibular domain ventral to the oral ectoderm (Swartz et al., 2011). The orofacial region develops from the fusion of the frontonasal and maxillary facial prominences. Although there are species-specific differences during palatogenesis, there is a period in development of conserved embryonic face shape. This conserved shape is necessary to ensure the facial prominences will fuse at the correct time and place (Young et al., 2014). Multiple signaling pathways, transcription factors and epigenetic marks mediate the precise coordination of the complex processes needed for proper orofacial development. Cranial neural crest cells contribute to most of the craniofacial structures and therefore, most craniofacial malformations are due to defects in proliferation, migration or differentiation of the neural crest cells (Trainor and Krumlauf, 2001). Due in part to the large number of molecular and morphogenetic events occurring at this time, orofacial defects, such as cleft lip and palate, are the most common birth defect worldwide.

Extensive studies on the genetic basis of cleft lip with or without palate (CL/P) in human and animal models has led to the identification of genes and pathways involved in palate development and morphogenesis (Li and Dudley, 2009; Lidral and Murray, 2004; Moreno et al., 2004; Riley and Murray, 2007; Santiago et al., 2005). Among these, Wnt signaling has proved to be important for both normal and abnormal development of the palate (Carroll et al., 2005; Juriloff et al., 2006; Niemann et al., 2004; Woods et al., 2006). Both the canonical and non-canonical pathways have been shown to be essential for normal palate development, but play different roles (Chiquet et al., 2008; Clevers, 2006; He and Chen, 2012).

Wnt signaling in craniofacial development

Wnt signaling regulates tissue morphogenesis (Yin et al., 2009) and is required for convergent-extension (CE), a morphological process that operates in gastrulation, axis elongation, and organogenesis (Heisenberg and Tada, 2002; Heisenberg et al., 2000; Tudela et al., 2002; Wallingford et al., 2002; Westfall et al., 2003). For craniofacial structures such as the palate, form is intimately associated with function, and the molecular basis of craniofacial morphogenesis serves as a model for organogenesis in general. However, the details of Wnt signaling and CE events during craniofacial and palate development remain elusive.

The Wnt proteins are secreted signaling molecules required for induction, patterning and morphogenesis of cranial neural crest (Brugmann et al., 2007; García-Castro et al., 2002; Wodarz and Nusse, 1998). All Wnt molecules (19 in mammals) share common biosynthetic and secretion pathways, the latter being regulated by *wntless* (w*ls)* (Bänziger et al., 2006; Das et al., 2012). The highly conserved gene *wls* encodes a multi-pass transmembrane protein that shuttles Wnt molecules from the Golgi apparatus to the cell membrane(Bartscherer and Boutros, 2008; Bartscherer et al., 2006). Targeted disruption of *Wls* in the mouse results in a loss of anteroposterior (AP) patterning (Fu et al., 2009). Conditional inactivation of *Wls* demonstrated its requirement in bone homeostasis and craniofacial development (Fu et al., 2009).

After Wnt export into the extracellular space, it is thought that Frzb and Glypican proteins further facilitate Wnt diffusion to receiving cells in a long-range or short-range manner, respectively. Binding of Wnt proteins to the seven-transmembrane receptor Frizzled (Fzd) at the cell surface of the receiving cell activates the transduction of intracellular signals that can be β-catenin dependent, in the case of canonical Wnt signaling, or β-catenin independent, in the case of non-canonical signaling (Clevers, 2006; Clevers and Nusse, 2012; Veeman et al., 2003). Both canonical and non-canonical Wnt pathways play roles in the normal palatogenesis (Chiquet et al., 2008; Clevers, 2006; He and Chen, 2012).

A non-canonical pathway, Wnt/planar cell polarity (Wnt/PCP), has been implicated in craniofacial development through defects observed in several PCP mutant animal models (Szabo-Rogers et al., 2010; Yin et al., 2009; Yu et al., 2010). In the mouse, *Fz1*-/-; *Fz2*-/- compound mutants exhibit cleft palates and hypoplastic mandibles (Yu et al., 2010). Additionally, mutations in *Vangl2* (VANGL planar cell polarity protein 2) increases the penetrance of cleft palate in *Fz2 +/-; Fz7 -/-* mice, suggesting a role for these Wnt receptors in the PCP signaling pathway. Recently, the PCP core protein 1, Prickle1, was shown to be required for mammalian palate development, reinforcing the crucial role of this non-canonical Wnt pathway in craniofacial development (Yang et al., 2014).

It was previously shown that the zebrafish ethmoid plate (hereafter referred to as palate) forms by the convergence and the integration of the midline frontonasal prominence (FNP) and paired maxillary prominences (MXP) (Kamel et al., 2013; Szabo-Rogers et al., 2010; Topczewski et al., 2001). The embryonic palate constitutes a single sheet of chondrocytes; genetic or chemical perturbations of these cells result in morphological changes that can be readily measured by changes in palate and chondrocyte shape and size (Eberhart et al., 2008; Le Pabic et al., 2014; Topczewski et al., 2001).

Several mutants in zebrafish Wnt pathway genes are available, and CRISPR/Cas9 can be used to target additional genes of interest (Hwang et al., 2013). Mutations of the PCP components *gpc4*

(*knypek*) and *wnt5b* (*pipetail*) have been previously shown to cause craniofacial defects (Piotrowski et al., 1996; Rauch et al., 1997; Sisson and Topczewski, 2009; Topczewski et al., 2001). In the *gpc4* mutant, cells intercalate poorly, leading to defective cartilage morphogenesis in upper and lower jaw structures (LeClair et al., 2009; Topczewski et al., 2001).

Building on these important studies, we aimed to more clearly define the role of Wnt signaling in palate morphogenesis. By analyzing mutants for components of Wnt signaling, we are able to explore the role of Wnt/PCP signaling in cell-cell organization and arrangement during palate development. This work presents a model of Wnt signaling that correlates specific molecules to cellular behaviors and higher-order tissue morphogenesis, highlighting a mechanistic understanding of form and function relevant to organogenesis.

4.2 RESEARCH METHODOLOGY

Zebrafish husbandry and strains
All embryos and fish were raised and cared for as described (Westerfield, 1993) and staged using established protocols (Kimmel et al., 1995). Zebrafish were maintained and bred at 28.5° on a 14-hour light and 10-hour dark cycle. Embryos were generated and collected by natural spawning. Tubingen fish were used as wild type. Mutant lines ($gpc4^{hi1688Tg/+}$, $Wnt5b^{hi2735btg/+}$) were obtained from the Zebrafish International Resource Center and homozygous embryos were obtained by inbreeding of heterozygous adults. $wls^{c186/+}$ mutants were provided by the Halpern Laboratory, Baltimore, MD, USA (Kuan et al., 2015).

RNA isolation and quantitative PCR (qPCR)
RNA was isolated from whole embryos using Trizol and 1µg total RNA was reverse transcribed with iScript® (Bio-Rad) for quantitative PCR (qPCR). qPCR reactions were amplified on a Step One Plus Real-Time PCR System (Applied Biosystems). *Elongation factor 1a* (*ef1a*) was used for internal controls. All primers annealed at 60°C and are listed below.

Gene	Forward Primer	Reverse Primer
dvl2	5'-ATCACATCCAGCTCATCCGTCAC	5'-GTACAACCACTCCACCACATCTG
ef1a	5'-GACCAGCAAATACTACGTCAC	5'-GGTGAGTTTGAGGCTGGTAT
frzb	5'-CAAGACCCTGCGAAATGTAACC	5'-CTTTGACCTCCACAATGGCG
gpc4	5'-TGTTCGCCCTCCTGAGTCTTG	5'-CCTGAAGGAAATGACCAGCTG
vangl2	5'-CAAGTCTTCACACTCACGCAGC	5'-CATCCCGATCATCTCCGCGT
wnt9a	5'-GACCTCACAGCCAGACGAAAG	5'-GGTACATCGCTCCATTCGGC

RNA *in situ* hybridization
Whole embryos were stained by *in situ* hybridization as described (Thisse et al., 2004). Full-length probes were used for all experiments, made using the primers listed in Appendix II. Sections were prepared by OCT embedding and cryo-sectioning (10 μm) after RNA *in situ* hybridization.

Histological and morphological analysis

Cartilage was stained with alcian blue at 4 dpf as previously described(Walker and Kimmel, 2007). The palate was dissected in PBS plus 0.1% Tween and mounted in 95% glycerol for imaging. Length (μm) and surface area (μm) of cartilage elements were measured using ImageJ software. A minimum of 3 fish and 60 cells within the bounding box were used for analyses.

Statistical analysis

All data are represented as mean ± s.d. Significant differences between data sets were determined by one way ANOVA and Tukey post test. Significance was attained at $p < 0.05$, and all statistical analyses were performed using GraphPad Prism software.

4.3 RESULTS

Convergent extension cellular behaviors regulated by the Wnt pathway are critical for tissue morphogenesis. However, Wnt interactions between signaling and receiving cells in this contect are poorly understoodt. By focusing on two Wnt ligands (Wnt9a and Wnt5b) and three proteins responsible for their secretion (Wls) and diffusion (Frzb and Gpc4), this work aimed to determine the interactions between signal-producing ectodermal cells and Wnt-responsive chondrocytes. I have genetically dissected the interactions between Wnt signaling and receiving cells during palate development, sing morphogenetic analysis of *wls*, *gpc4*, *wnt5b*, *wnt9a* and *frzb* mutants. This study provides a mechanistic understanding of how different Wnt signaling components contribute to palate morphogenesis.

Co-expression of *wls*, *gpc4*, *wnt9a* and *wnt5b* in Wnt secreting epithelial cells and *gpc4* and *frzb* in neighboring palate chondrocytes

Previous works showed that expression of *wnt9a* in the oropharyngeal epithelium and *frzb* in the chondrocytes at the distal portion of the palate, are both required for palate extension (Dougherty et al., 2013; Kamel et al., 2013). In order to place the morphogenetic analysis of these genes in spatial and anatomical contexts, their gene expression patterns were compared with those of *wls*, *gpc4* and *wnt5b* (Figure 4.1). Whole mount RNA *in situ* hybridization was performed at 60 hours post fertilization (hpf), a critical point of palate morphogenesis, during which thefrontonasal prominence is integrating with maxillary prominences (Figure 4.1). Expression of *wls* was detected in pharyngeal arch derivatives, in the upper and lower jaws and more strongly in the midbrain (Figure 4.1 A, F, K), consistent with the previously described expression pattern (Jin et al., 2010; Kuan et al., 2015). Sagittal sections revealed that *wls* expression is restricted to the cell layer surrounding the palate and along the mouth opening (Figure 4.1 K). However, *wls* expression was not detected in the palate chondrocytes (Figure 4.1 K). Both *wnt9a* and *wnt5b* shared expression with *wls*; *wnt9a* and *wls* are co-expressed in the cell layer above and below the palate (Figure 4.1 A, F, K black arrow heads and D, I, N arrow heads), while *wls* and *wnt5b* are co-expressed in the epithelial cells lining the mouth opening (Figure 4.1 A, F, K open arrow head and E, J, O arrow head). These patterns of co-expression of *wls* and *wnt9a*/*wnt5b* are consistent with the requirement for Wls for secretion of these (Wnt) ligands from the epithelium.

In contrast, expression of *frzb* is restricted to the palate chondrocytes and excluded from the surrounding epithelial tissue (Figure 4. 1 C, H, M). *gpc4* (Figure 4.1 B, G, L) is more broadly expressed, in both the chondrocytes (Figure 4.1 L open arrow head) and the epithelium (Figure 4. 1 L black arrow head). Thus, epithelial cells expressing *wls/wnt9a/wnt5b* are juxtaposed to the chondrocytes expressing *frzb*, and both cell types express *gpc4* (Summary in Figure 4.1 P).

Notably, certain genes are regionally expressed along the AP axis, while others have a more uniformly distributed expression pattern. Transcripts of *frzb* are detected in the distal palate chondrocytes (Figure 4.1 C, H, M) and *wnt5b* expression was localized to the epithelium around the mouth opening (Figure 4.1 E, J, O). In contrast, *wls*, *gpc4* and *wnt9a* transcripts are more uniformly distributed along the AP axis (Figure 4.1, summarized in P).

CRISPR targeted mutagenesis of *wnt9a, wls, and frzb*

To test the necessity for each gene in palate development, mutants were collected, or generated if mutants were not available. Mutants for *wls* (*c186* allele) (Kuan et al., 2015), *gpc4* (*knypek*) (Topczewski et al., 2001) and *wnt5b* (*pipetail*) (Westfall et al., 2003) were previously described.

A postdoctoral fellow in the lab used CRISPR-Cas9 genome editing to introduce mutations in *wnt9a* and *frzb,* and to generate an additional *wls* allele (Hwang et al., 2013). She designed several small guide RNAs for *wnt9a* and *frzb* genes. Two guide RNAs were able to efficiently target *wnt9a*, while only one was able to target *frzb*. Since one *wls* mutant (c186) was already available (gift from Halpern laboratory (Kuan et al., 2015)), only one *wls* mutant was created by targeting one site on exon 2.

Founders bearing small mutations inducing frame shifts in the coding sequence of each gene were identified. Two small deletions in *wnt9a* genomic sequence, in exon 1 and 3 were identified. In exon 1, a 14 base-pair (bp) deletion was identified by sequencing and FAM-PCR (Figure 4.2, A and B). Simulated translation of this variant (c.73_86del) predicted a truncated protein of 29 amino acids compared to 327 amino acids for the WT protein. In exon 3, a 4 bp deletion was recovered (Figure 4.2 A and C), and simulated translation of this variant (c.115-118del) predicted a 41 amino acid protein. In both cases, the mutation induced a non-functional truncated protein. Reduction of wild type protein was confirmed by Western blot analysis (Figure 4.2 D). A 7bp deletion was recovered in exon 2 of *wls* (Figure 4.2 E and F). Western blot analysis validated major reduction of protein expression level in *wls* homozygote mutants (c.252_258del) (Figure 4.2 G). Exon 2 of *frzb* was targeted and two mutations were identified; one (-) 7bp deletion and a (+) 7bp insertion by sequencing and FAM-PCR (Figure 4.2 H-J). Transcripts appeared significantly reduced in *frzb* homozygote mutants (c.481_483delins) compared to wild-type embryos (Figure 4.2 K) as shown by quantitative RT-PCR (qPCR).

After validation of mutations, these founders and their descendents were out-crossed to generate stable mutant lines in order to investigate the role of these genes in craniofacial development.

Requirement of Wnt pathway genes in palate morphogenesis

To address the role of the Wnt signaling pathway in palate morphogenesis, larval craniofacial cartilage was examined in homozygous mutants of *wls*, *gpc4*, *frzb*, *wnt9a* and *wnt5b* (Figure 4.3). The palate dimensions of length (L, μm), width (W, μm) and length-width ratio (L/W) were measured to allow quantitative comparisons between wild type (WT) and mutant larvae (Figure 4.3 S). The measured typical L/W ratio for WT larvae is 1.15 ± 0.08 (n= 7) (Figure 4.3 S), illustrating that a normal palate is slightly longer in the AP axis than it is wide.

Both *wls* mutant alleles (c186 and c.252_258del) produced a craniofacial phenotype in which the craniofacial elements were formed but significantly hypoplastic (Figure 4.3 B, H, N and S) compared to WT. The palate is shorter in the AP axis and wider mediolaterally, illustrated in the measured L/W ratio (0.7 ± 0.06, n= 17) (Figure 4.3 N and S). The global craniofacial phenotype of *gpc4* mutants was similar to the *wls* mutant (Figure 4.3 B, H compared to C, I) with a L/W ratio of 0.38 ± 0.07 (n=6) (Figure 4.3 O and S).

Interestingly, *frzb* and *wnt9a* mutants did not exhibit severe shortened phenotypes as previously observed in morphants (Figure 4.3. 3 D-E, J-K, P-Q) (Dougherty et al., 2013; Kamel et al., 2013). One possible explanation for *frzb* and *wnt9a* mutants exhibiting less severe phenotypes than the previously published morphants is a gene compensation network. *frzb* mutants show a significant phenotypic difference from WT larvae (L/W ratio is 0.94 ± 0.12, n= 17). The distal tip of the palate where *frzb* expression is detected ((Kamel et al., 2013) and see also Figure 4.1 C, H)), which corresponds to the region of frontonasal prominence and maxillary prominence fusion, appeared less dense in chondrocytes or slightly delayed.

The *wnt9a* mutant palate appeared qualitatively longer and narrower compared to WT, but did not show significant variation in measurements (L/W ratio of 1.19 ± 0.15, n= 21) (Figure 4.3 E, K, Q and S). In contrast, the global shape of the *wnt5b* mutant palate resembled the *wls* mutant palate, with a shorter palate (Figure 4.3 F, L, R, S). However, quantitatively the width was not affected as illustrated in L/W ratio close to 1 (0.97 ± 0.19, n= 5) (Figure 4.3 R and S).

Chondrocyte stacking and polarity require Wnt signaling

The craniofacial cartilage elements are highly organized structures in which the chondrocytes are polarized in both their shape and orientation along the palate axis (LeClair et al., 2009; Sisson and Topczewski, 2009; Topczewski et al., 2001). To elucidate which chondrocyte defects underlie the palate phenotypes, chondrocyte stacking was quantified by measuring L/W ratio and orientation of chondrocytes. The L/W ratio was calculated with the longest cell axis measured as L (perpendicular to the AP axis of the palate), and the shorter axis as W (Figure 4.4).

The WT palate consists of a sheet of stacked and elongated chondrocytes with almost half of the chondrocytes (45%) oriented at 110° to 120° relative to the AP axis (Figure 4.4 S). In contrast, *wls* mutant chondrocytes are smaller in size, rounded (Figure 4.4 B, H compared to A, G) and lack stacking in linear columns reflected by the L/W ratio of 1.67 in *wls* compared to 1.95 in WT (Figure 4.4 N compared to M, quantified in Figure 4.4 AF). Cells were more randomly oriented, with 22% of them oriented from 131°-140°, and only 18% of them demonstrated an orientation similar to WT (110°-120°) (Figure 4.4 T compared to S). Furthermore, the *wls* mutant palate

exhibited excessive stacking in the DV axis with multiple cell layers instead of a single cell layer as in WT (Figure 4.4 Z).

Similar morphological defects were observed in *gpc4* mutants (Figure 4.4 C, I, O, U, AA) where chondrocytes showed defects in elongation (L/W ratio of 1.60, Figure 4.4 I and O), and orientation (17% of cells oriented 131°-140° Figure 4.4 U). The *gpc4* mutant palate also organized as a multi-layered structure, as observed in *wls* (Fig. 4 AA). Accordingly, these results correlate with the global palate shape of *wls* and *gpc4* mutants. The lack of chondrocyte stacking may explain the shorter and wider palate, which organized in several layers and failed to elongate (Figure 4.4 B, H, T and C, I and U).

Cell defects were less severe in *frzb*, *wnt9a* and *wnt5b* mutants (Figure 4.4 D-F, J-L). In the *wnt9a* mutant, chondrocytes exhibit a L/W ratio that is significantly increased from WT (2.23 ± 0.54 versus 1.95 ± 0.49, Figure 4.4 K and Q, quantified in Figure 4.4 AF). The range of cell orientation measurements was more broadly distributed than in WT (29% of cells are in the WT range) but more restricted than in the *wls* and *gpc4* mutants (18% and 10%, respectively) (Figure 4.4 W). Notably, even though the *wnt9a* mutant showed discrete chondrocyte stacking defects, the overall palate phenotype appeared normal (Figure 4.4 E, K and Q).

In contrast, *frzb* and *wnt5b* mutants did not show significant differences in L/W ratio (Figure 4.4 P and R, quantified in Figure 4.4 AF). However, in both mutants, cell orientation differed from WT. In the *frzb* mutants, 24% of cells oriented in 101°-110°, and in the *wnt5b* mutants 28% oriented 111°-120° (Figure 4.4 V and X). In *wnt5b* mutant, the global palate shape was shorter. Observation of chondrocytes revealed that the lack of elongation is not due to the aberrant DV stacking seen in *wls* or *gpc4*, but instead may be due to the reduced cell size compared to WT (Figure 4.4 R). The discrete cell orientation defects in *frzb* and *wnt5b* mutants may also contribute to the changes in palate shape compared to WT (Figure 4.3 P and R).

Taken together, these morphological analyses revealed that broad abrogation of Wnt signaling (*wls* and *gpc4* mutations) leads to loss of chondrocyte orientation and stacking along the AP, DV and mediolateral axes. Mutations of *wnt5b*, *wnt9a* or *frzb* did not phenocopy *wls* or *gpc4* mutants. The *wnt9a* palate did not exhibit significant differences compared to WT, even though chondrocytes have an increased L/W ratio. The *wnt5b* palate was short in the AP axis. In contrast, AP and mediolateral axes were preserved in *frzb* mutants even though cell orientation was defective. This suggests that each of these genes regulates an important but distinct component of palate morphogenesis and is required for distinct CE cell behaviors.

Genetic interactions between *wls*, *gpc4*, *frzb*, *wnt9a*, and *wnt5b* in the non-canonical Wnt pathway

A significant gap in the understanding of how Wnt signaling regulates tissue morphogenesis is the interaction of the different genes in the pathway, between the signaling and the recipient cell. The genes *wls*, *gpc4*, *frzb*, *wnt9a* and *wnt5b* are all components of the Wnt signaling pathway. *gpc4* has been described as a co-receptor of the PCP pathway (Ohkawara et al., 2003), and the Wnt5 protein was already described as a ligand in the PCP pathway in *Drosophila* (Shimizu et al., 2011) and in zebrafish (Westfall et al., 2003). Given that the palate and cellular morphology

of each single mutant exhibited different degrees of severity of the same chondrocyte stacking defects, we hypothesized that they may all have discrete and complementary functions in the same non-canonical Wnt pathway. To explore this hypothesis, we sought to test their genetic interactions by generating double mutants (Figure 4.5).

The *wls-/-; gpc4-/-* compound mutant exhibited a more severe palate malformation compared to thw *wls* single mutant, qualitatively shorter in the AP axis (Figure 4.5 C, I and O). Quantitative measurements revealed that there is no significant difference between the compound (*wls-/-; gpc4-/-*) and single (*gpc4-/-*) mutants (L/W ratio= 0.465 ± 0.019 compared to 0.38 ± 0.07) (Figure 4.5 S).

The *wnt9a-/-;wnt5b-/-* double mutant demonstrated a palate phenotype that appeared to be a combination of the respective single mutants; the palate shape is similar to that of the *wnt5b* single mutant and the lower jaw shows the same defect as in *wnt9a* single mutant (Figure 4.5 F, L and R). This is apparent in the quantification, where the palate L/W ratio of the double mutant (L/W ratio of 0.96 ± 0.022) (Figure 4.5 S) is similar to that of the *wnt5b* single mutant (L/W ratio of 0.97 ± 0.19, n=6). The *wnt9a-/-;wnt5b-/-* mutant phenotype did not recapitulate *wls* or *gpc4* mutant phenotypes.

The *wls-/-; frzb-/-* double mutant (L/W ratio of 0.72 ±0.04, n=22) exhibited a less severe palate phenotype compared to *wls* mutant (Figure 4.5 P and S compared to Figure 4.3 N and S). The *wls-/-; frzb-/-* palate was narrower than the *wls* palate, and closer to WT values (width of 310 µM compared to 322 µM in *wls* and 265 µM in WT) (Figure 4.5 S). Therefore, the addition of the *frzb* null allele to *wls* mutation partially rescued the *wls* palate phenotype (Figure 4.5 D, J and P).

A partial rescue of *wls* mutation consequence was also observed in the *wls-/-;wnt9a-/-* compound mutant. The palate of this double mutant was narrower (average width of 285 µM) compared to the *wls-/-* single mutant (Figure 4.5 E, K and Q). This implies an alleviating epistatic interaction between *wnt9a* and *wls*.

4.4 DISCUSSION

These results define the crucial role of the Wnt/PCP pathway in zebrafish palate development. We found that axial positional cues and mediolateral cell intercalation require *wls* and *gpc4* function. In addition, *wnt5b* is essential for anteroposterior extension, *wnt9a* for dorsoventral extension, and *frzb* for proper cell orientation. Our analysis delineates the Wnt pathway into the relative contributions of different components in palate morphogenesis.

While it is known that Wnt signaling regulates diverse developmental processes, assigning discrete gene functions in the Wnt pathway to particular morphogenetic events has been challenging, due to the large number of genes involved and their overlapping functions (Carroll et al., 2005; Das et al., 2012; Juriloff et al., 2006; Niemann et al., 2004; Woods et al., 2006). Our results begin to dissect how each studied component of the non-canonical Wnt pathway is involved in discrete aspects of zebrafish palate development. These studies revealed genetic interactions between *wls*, *gpc4*, *wnt9a*, *wnt5b* and *frzb* and their common function of regulating chondrocyte and palate morphology. In the broader context of developmental biology, this work

demonstrates a model useful for the study of CE, where functional assays are applied to delineate how these CE behaviors shape a relatively simple palate structure.

In addition to the simplicity of its palate morphology and developmental advantages where CE events can be directly visualized, the zebrafish model is increasingly versatile given its expanding genetic toolbox. Previous work has looked into the effects of *wnt9a* and *frzb* mutations on palate formation, however, they used morpholinos to knock down function. By utilizing CRISPR-Cas9 genome editing techniques, we were able to avoid off-target effects and misleading data.

Shaping the palate by the non-canonical Wnt pathway

In both animal models and human genetic studies, canonical and non-canonical Wnt pathways have been implicated in palate development (Carroll et al., 2005; Das et al., 2012; Juriloff et al., 2006; Niemann et al., 2004; Woods et al., 2006) but the specific function of each signaling pathway remained unclear. Phenotypes observed in *wnt5b* and *wnt9a* mutants suggest requirement in one axis (Fig. 4.6). In *wnt9a* mutants, chondrocytes are elongated compare to those in wild type, indicating that the cells acquired polarity and elongated. However, analysis of cell orientation showed that these cells did not properly orient and organize themselves. Similarly, *wnt5b* mutant cells do not orient properly along the AP axis. The roles played by *wnt5b* and *wnt9a* are consistent with their domains of expression, as *wnt5b* is expressed in the mouth opening epithelium located anterior to the distal front of the extending palate. Conversely, *wnt9a* expressed in the epithelium surrounding the palate appears to regulate cell extension in the mediolateral axis.

The palate of *wnt9a-/-; wnt5b-/-* double mutants remained a single cell layer in thickness, unlike in *wls* and *gpc4* mutants. This indicates that loss of *wnt9a* and *wnt5b* function did not affect DV axis morphology. This observation also suggests that additional Wnt ligand(s), such as Wnt11 or Wnt4 (He and Chen, 2012; Lee et al., 2008) may be involved in palate development and may play a role in defining this DV axis.

wls and *wnt9a* single mutants exhibited contrasting palate phenotypes; the *wls-/-* palate is shorter in the AP axis and wider in the mediolateral axis, while the *wnt9a-/-* palate is elongated along the AP axis and narrower mediolaterally. At the cellular level, *wnt9a-/-* chondrocytes are misshapen and do not orientate properly.

Insights about Wnt genetic interactions from compound mutants

Genetic interactions are revealed when mutations in one gene enhance or suppress the phenotype resulting from mutations in a second gene. In this study, we generated double mutants for members of the Wnt-PCP pathway to examine possible genetic interactions between these genes.

wls and *gpc4* mutants showed severe phenotypes with loss of axis cues, demonstrating requirement of non-canonical Wnt signaling in palate morphogenesis. Analysis of chondrocyte characteristics revealed a profound defect in morphology, polarity and stacking in the *wls* and

gpc4 mutants. However, *wls* mutation did not recapitulate the *gpc4* mutant phenotype, showing less severe phenotypes in AP and mediolateral shortening. The severe phenotype observed in *gpc4* mutants could simply be the consequence of earlier developmental defects, as they also showed anomalies in body extension. Another hypothesis could be that this severe *gpc4* palate dysmorphology could suggest that *gpc4* may integrate several signaling pathways. Thus, the *gpc4* mutant phenotype could be a consequence of the loss of several signaling pathways and not just Wnt alone. Another possible explanation is that Gpc4 integrates all Wnt signals in the receiving cell, while Wls is only necessary for the secretion of some Wnt proteins, as it has been suggested in literature. Accordingly, non-lipid-modified Wnt ligands, which are able to traffic without Wls activity, have been described in *Drosophila* (Ching et al., 2008). This opens the possibility of Wls-independent Wnt secretion in the palate. This suggests that secreted proteins can potentially reach their receptor even without an active co-receptor.

Notably, the double mutant *wls-/-;wnt9a-/-* generated a palate in which the AP and mediolateral axes are not as severely shortened as the *wls* mutant; hence, loss of *wnt9a* partially rescued *wls* deficiency. One explanation may be that *wls*-independent mechanisms of Wnt secretion are operating, so that aberrant localization of Wnt9a in the *wls* mutant using an alternative pathway caused the severe *wls* mutant phenotype. Likewise, when Wnt ligand spatial localization is disrupted in the *gpc4* mutant, a severe axis derangement phenotype resulted. Therefore when the Wnt ligand is also absent in the *wls-/-;wnt9a-/-* double mutant, the palate dysmorphology is less severe, as the aberrantly localized morphogen may be removed.

In addition to *wls* and *gpc*, Frzb is also responsible for trafficking of Wnt ligands. The *frzb* mutant showed no overt phenotype and larvae are able to survive to adulthood. This was consistent with previous mouse work, where knockout mice are viable and do not show craniofacial malformations (Lories et al., 2007). However, detailed examination of chondrocyte morphology and orientation revealed that *frzb* mutants do have defects in chondrocyte orientation, compatible with a role of the non-canonical Wnt pathway. Interestingly, analysis of the *frzb-/-;wls-/-* double mutant showed that loss of *frzb* partially rescued the *wls* phenotype, where the palate appeared more elongated in the AP axis than the *wls-/-* mutant. This observation indicates that Frzb may function in the absence of Wls. For example, the Wls-independent Wnt trafficking previously reported in *Drosophila* could also be present in zebrafish (Ching et al., 2008).

Wnt signaling in palate development and cleft pathogenesis

The role of the Wnt signaling has been investigated extensively in craniofacial development (Carroll et al., 2005; Chiquet et al., 2008; LeClair et al., 2009; Piotrowski et al., 1996; Rauch et al., 1997; Topczewski et al., 2001; Yang et al., 2014). Mutations in glycoproteins and other Wnt/Planar Cell Polarity (PCP) genes revealed a role for the non-canonical Wnt pathway in craniofacial skeleton development (Carroll et al., 2005; Chiquet et al., 2008; LeClair et al., 2009; Piotrowski et al., 1996; Rauch et al., 1997; Sisson et al., 2015; Topczewski et al., 2001, 2011; Yang et al., 2014). In mouse models, there is also an important role for the PCP pathway in palate development. For example, *prickle1* (Yang et al., 2014) or *vangl2* (Yu et al., 2010) mutations combined with *frizzled* receptor mutant backgrounds (*fz2 +/-; fz7 -/-*) induce cleft palatogenesis. In humans, the non-canonical Wnt factor *WNT9B* has been associated with cleft

lip and palate CL/P (Jin et al., 2012) suggesting a specific and important role of non-canonical Wnt signaling in normal palate morphogenesis. These studies demonstrated the crucial role of the non-canonical pathway in palate development, but did not resolve the cellular mechanism.

The zebrafish palate, which we suggest is developmentally similar to the human primary palate, further illustrates the function of Wnt/PCP signaling in palate morphogenesis. Our results indicate that the Wnt signaling pathway is involved in palate morphogenesis through the Wnt/PCP pathway. Wnt signaling is active in the epithelium surrounding the palate in a non-cell autonomous manner and triggers polarity in receiving chondrocytes. The initiation of polarity allows chondrocytes to organize and undergo a CE mechanism, which permits the elongation of palate.

4.5 FUTURE DIRECTIONS

Frizzled proteins are seven-transmembrane receptors that bind to the Wnt ligands. All Frizzled (Fz) proteins contain a conserved extracellular cysteine-rich domain (CRD) followed by seven transmembrane domains (Hsieh et al., 1999). Frizzleds act in canonical Wnt signaling, through the inhibition of β−catenin phosphorylation and subsequent translocation into the nucleus, and in PCP signaling through a small set of asymmetrically localized plasma membrane proteins and membrane-associated cytosolic proteins (Goodrich and Strutt, 2011; Nusse, 2012). Cellular communication mediated by Wnts and Fzds is necessary for proper embryogenesis and development. While the exact mechanism by which Wnts and Fzds signal is still unknown, it is clear that binding of the phosphoprotein Dvl and its membrane recruitment by Fzd is a critical step in the Fzd-mediated signal transduction in all pathways.

Wnt proteins cannot be specified as canonical versus non-canonical, and instead the outcome of signaling is regulated by the combination of Wnt proteins binding the different classes of receptors. The 19 mammalian Wnts are very promiscuous, and can each bind to more than one of the 10 Frizzled family members.

Based on the intron-exon structures of the 10 mammalian Frizzled family members, they can be subdivided into 5 branches: Fz1, Fz2 and Fz7 (subfamily 1), Fz5 and Fz8 (subfamily 2), Fz9 and Fz10 (subfamily 3), Fz4 (subfamily 4) and Fz3 and Fz 6 (subfamily 5) (Wang et al., 2016). Genetic redundancy studies have shown there is not a lot of redundancy between *frizzled* genes in different subfamilies; however, this data is incomplete and so needs to be taken with caution.

When members of subfamily 1 are knocked out in embryos containing one copy of a semidominant Vanlg2, there was an increased frequency of cleft palate defects (Yu et al., 2010, 2012). Therefore, it would be interesting to re-examine our single mutants in combination with mutants in Frizzled subfamily 1, in order to determine if there are any genetic interactions between these genes.
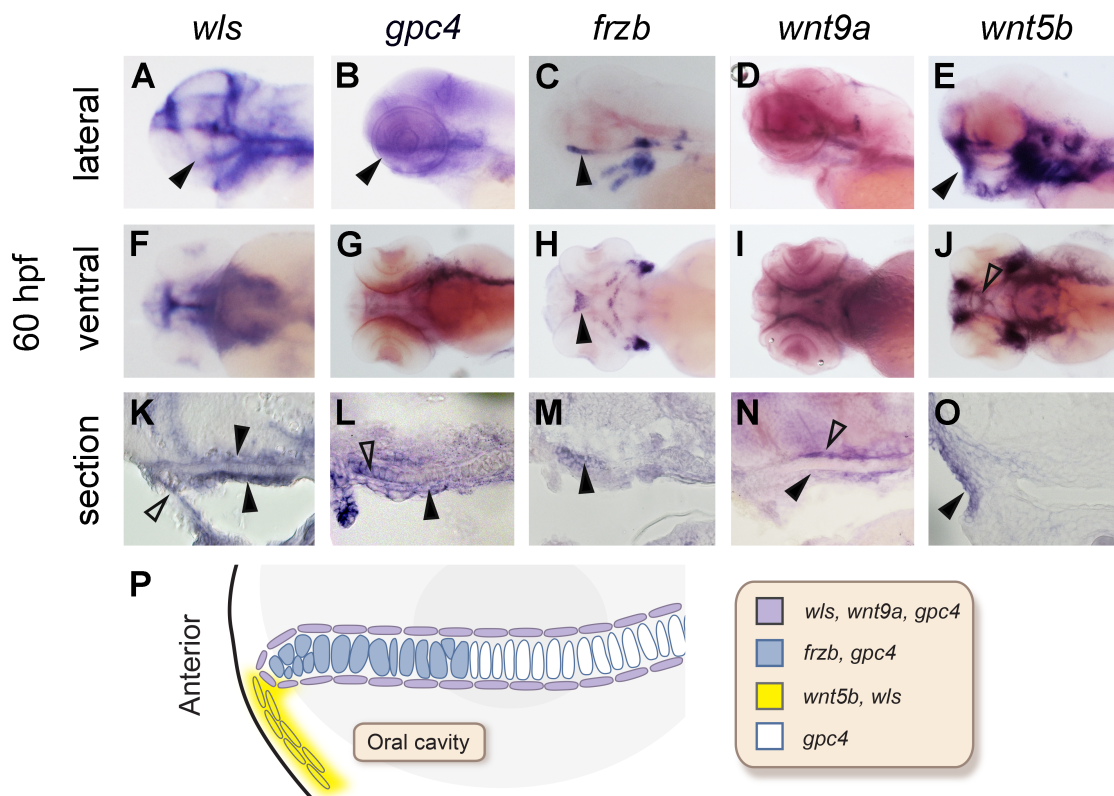
Figure 4.1. Expression pattern of non-canonical Wnt genes during craniofacial development.
Whole mount *in situ* hybridization with head to the left in lateral view (A-E), ventral view (F-J) and sagittal section (K-O). At 60hpf, during palate morphogenesis, *wls* (A, F and K) is co-expressed with *wnt9a* (D, I, N) and *gpc4* (B, G, L) in the oral epithelium surrounding chondrocytes and tissue above the palate. *frzb* (C, H, M) transcripts are detected in the chondrocytes at the distal tip of the palate. *wnt5b* (E, J and O) expression is detected in the oral epithelium at the mouth opening region. P: Summary of gene expression domains and their spatial relationships.
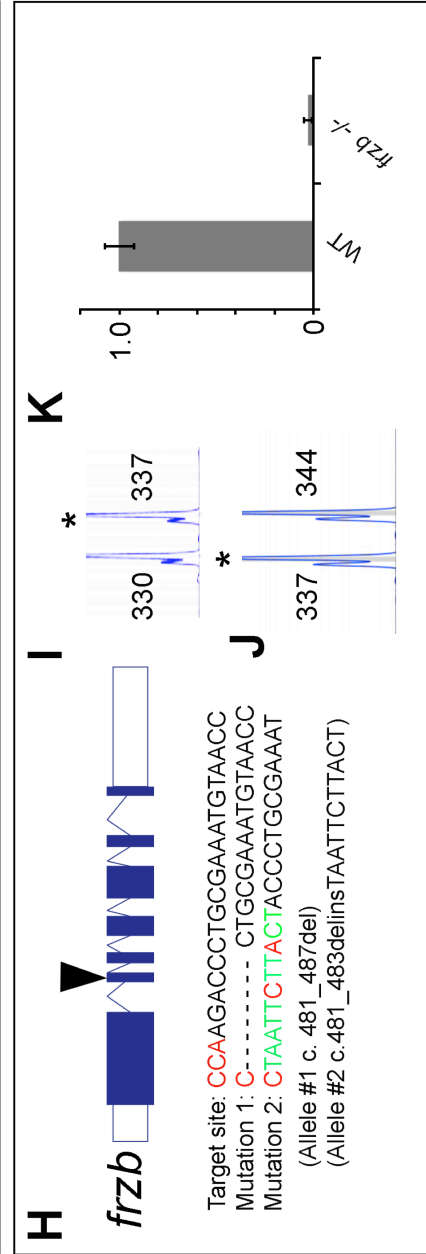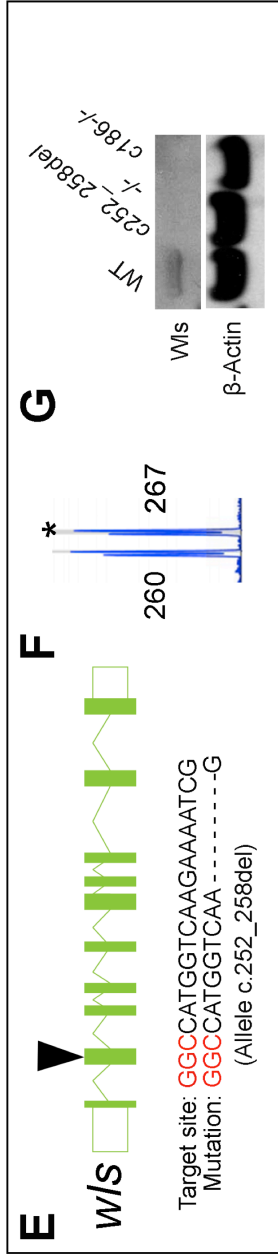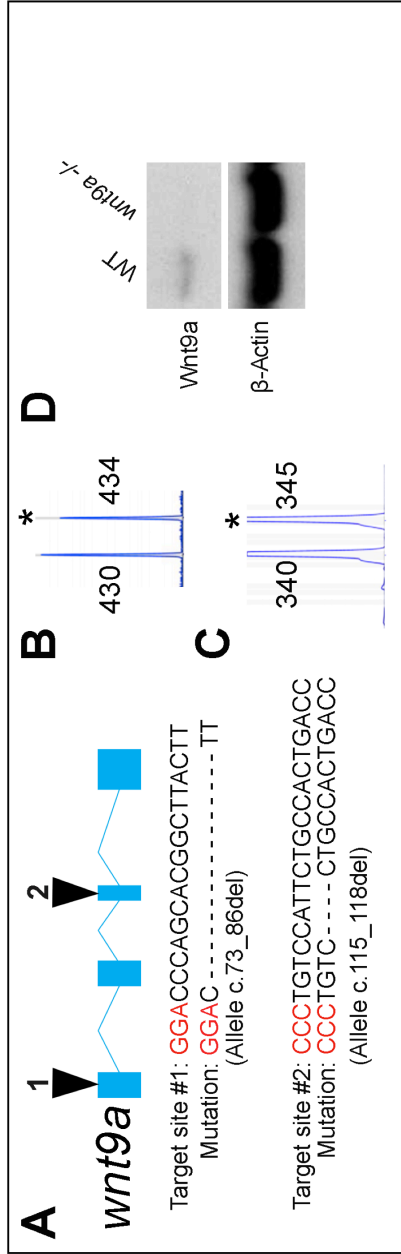
Figure 4.2. Targeted mutagenesis of *wnt9a*, *wls* and *frzb* using CRISPR/Cas9 genome editing.

Schematic representation of *wnt9a* exons, position of target sites #1 and #2, and sequences of induced mutations (A). Mutations were recovered in F1 and F2 generations and fish were genotyped using FAM-labeled PCR (B-C). Western blot analysis of Wnt9a protein in wild type and *wnt9a* homozygote mutants (D). Schematic representation of the *wls* gene. SgRNA was designed in the second coding exon. The sequence of the 7 bp deletion compared to the wild type sequence is presented beneath (E).   Example of FAM profile obtained for genotyping, showing the wild type allele (right peak, 267bp) and mutant allele (left peak, 260bp) (F). Western blot analysis of Wls protein in wild type and *wls* (CRISPR and C186) homozygote mutants (G). Schematic representation of *frzb* gene. SgRNA has been designed against the second exon. Two mutations have been obtained for this same target site, a 7 bp deletion and a 7 bp deletion-insertion (H). FAM-PCR genotyping of both alleles, -7 bp on the left and +7 bp on the right. K. qPCR analysis on 60hpf embryos shows the dramatic decrease of *frzb* expression in *frzb* homozygote mutants (+7 bp) compared to wild-type embryos (I-J).
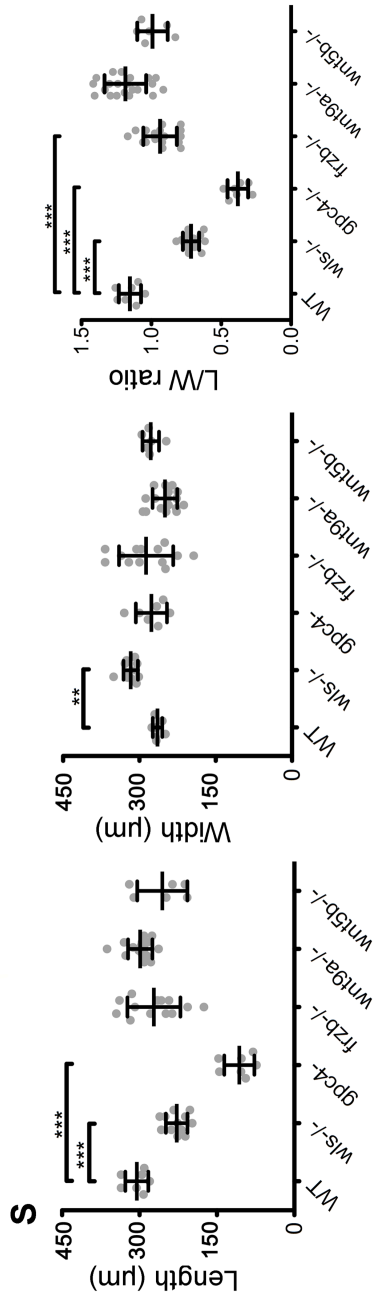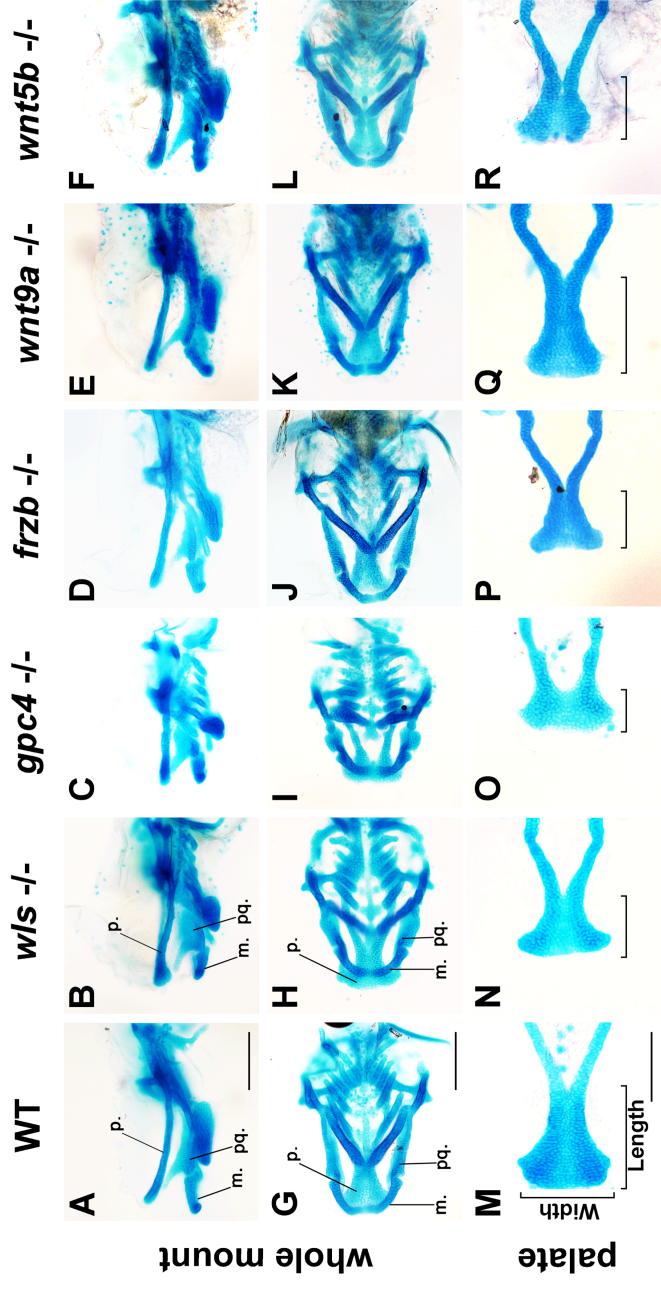
Figure 4.3. Wnt signaling is required for palate morphogenesis.
Whole mount 4.5 dpf Wnt signaling mutant embryos stained with Alcian blue to detect chondrocytes (A-F) lateral view; G-L ventral view).   For detailed view of structures, neurocranium (M-R) was dissected and flat-mounted.   Images were captured at 10X magnification. Y. Length (μm), width (μm) and average length / width (L/W) ratio measured in wild-type and mutants embryos as presented in diagram on the left (*p<0.05, **p<0.01, and ***p<0.0001). Scale bar= 200μm.

WT

50μm

15 μm

wls-/-

gpc4-/-

frzb-/-

wnt9a-/-

wnt5b-/-

40X dissected palate

representative cells

L/W ratio & cell orientation

M 1.95 ± 0.49
N 1.67 ± 0.41
O 1.60 ± 0.44
P 2.00 ± 0.54
Q 2.22 ± 0.54
R 1.85 ± 0.38

S 45%
T 22%
U 17%
V 24%
W 29%
X 28%

sections

AE

AF

L/W ratio

63
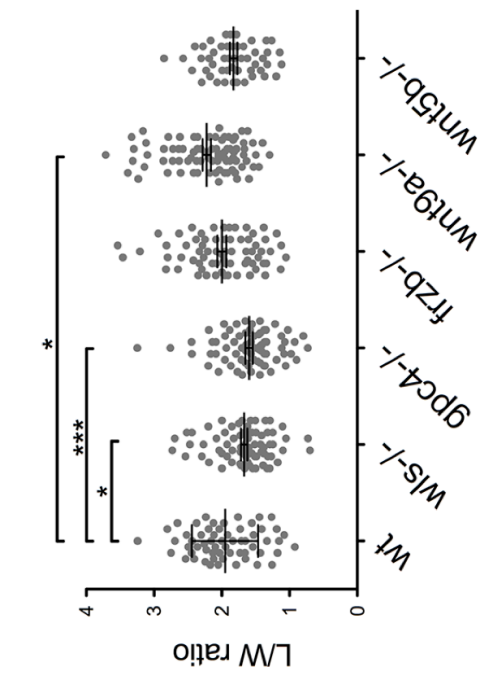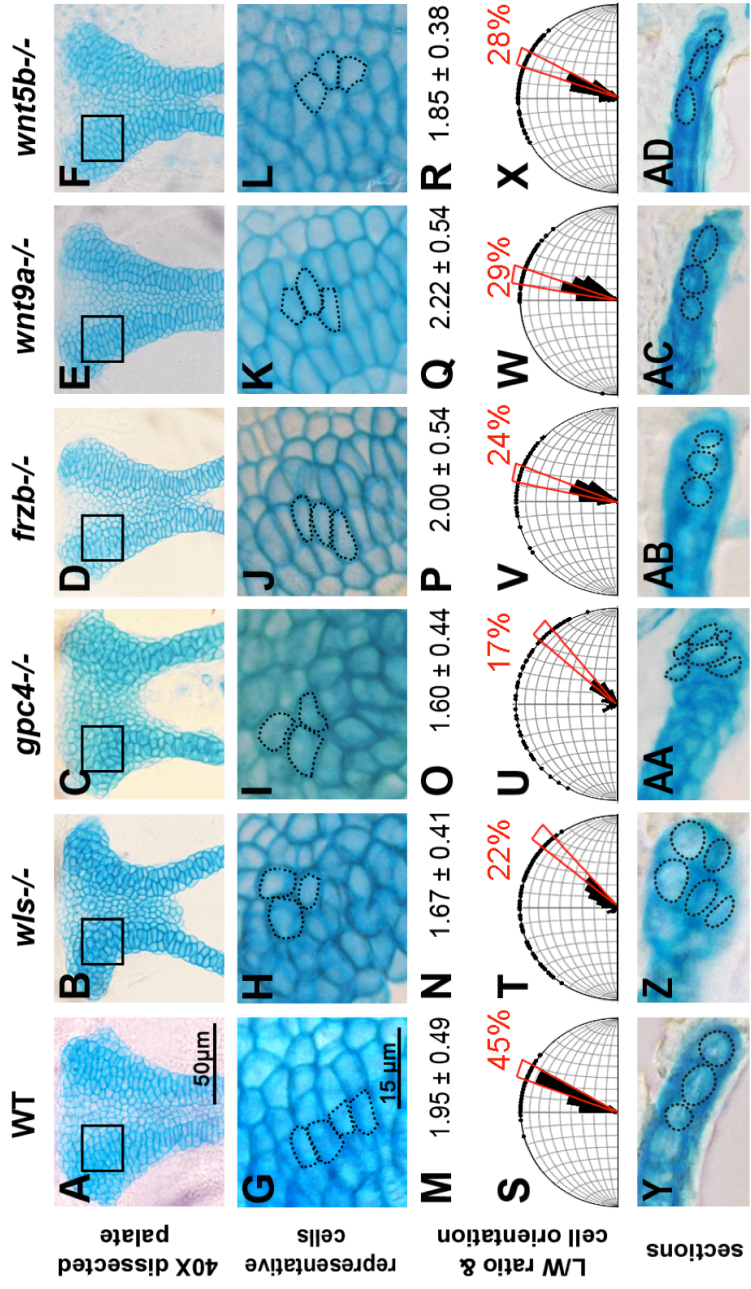
Figure 4.4. Cell shape and orientation are defective in Wnt signaling mutants.
Ventral view of dissected palate of wild-type and each mutant (magnification 40X) (A-F) .
Representative region of each palate has been magnified to illustrate cell shape and organization
Three cells were delineated in each mutant to illustrate the shape and orientation of cells (G-L).
Cell length-width (L/W) ratio measured values (M-R). Orientation of longest cell axis relative to
anteroposterior axis measured in palates (S-X). Transversal sections of 4 dpf embryos Alcian
blue stained illustrate cell organization of palate in wild type and mutants (Y-AD). Schematic
plane of section in Y-AD (AE). Graphic representation of cells L/W ratio values (AF). (*p<0.05,
**p<0.01, and ***p<0.0001).
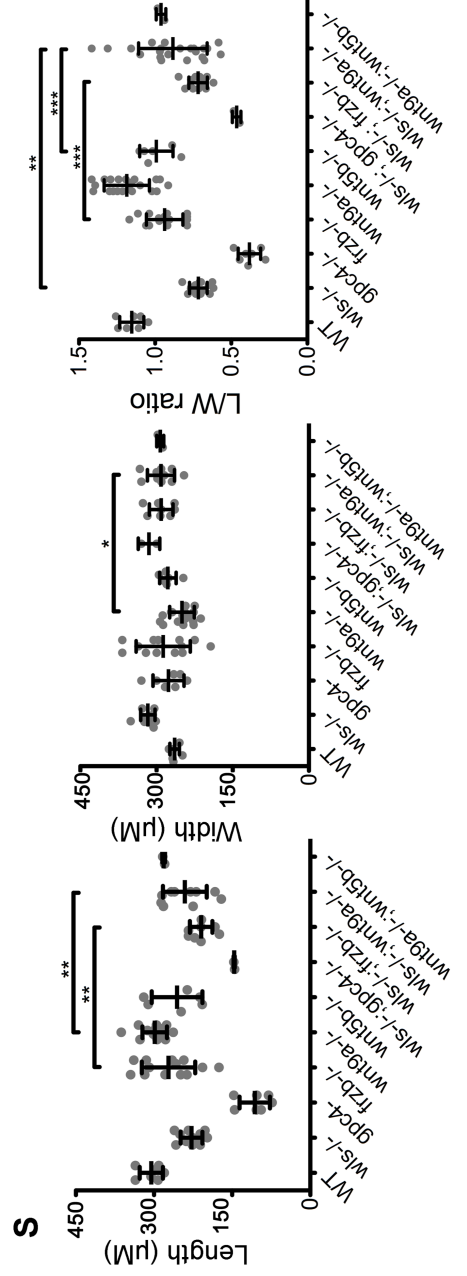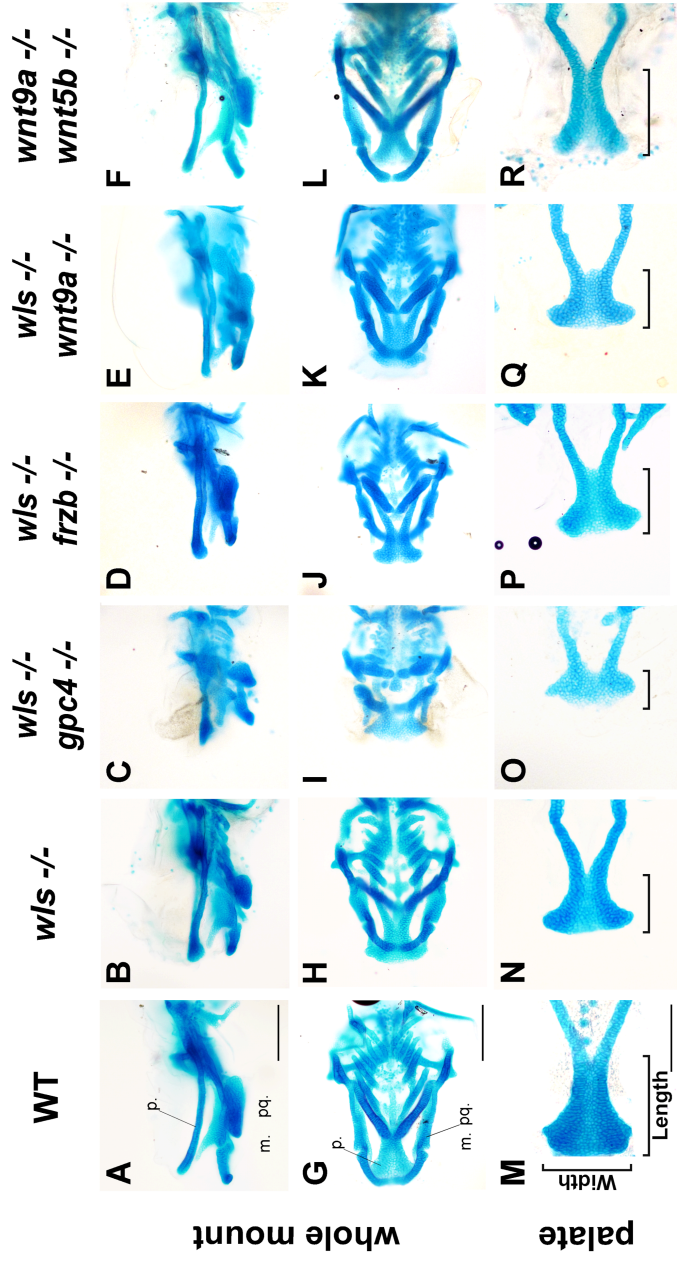
Figure 4.5. Genetic interactions between *wls*, *gpc4*, *wnt9a*, *wnt5b* and *frzb* regulate palate morphogenesis.
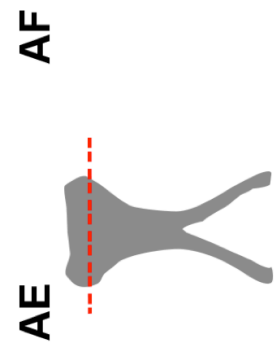Anterior head of embryos is toward the left in all views. (A-L) Whole mount 4.5 dpf Wnt signaling double mutant embryos stained with Alcian blue to detect cartilage. (A-F) Lateral view. (G-L) Ventral view. (M-R) Dissected and flat mounted palate in ventral view. (S) Length (μm), width (μm) and average length / width (L/W) ratio measured in each and compound mutants compared to wild-type. (*p<0.05, **p<0.01, and ***p<0.0001) Scale bar= 200μm.

genes cell behavior	wls	gpc4	wnt5b	wnt9a	frzb
A-P	●	●	●	○	○
D-V	●	●	○	○	○
Transverse	●	●	○	●	○
Proliferation	○	○	○	○	○
Intercalation	●	●	○	○	○
Orientation	●	●	●	●	●

Required ●
Not required ○

Figure 4.6. Summary of relative contributions of *wls*, *gpc4*, *frzb*, *wnt9a* and *wnt5b* to palate morphogenesis.
The zebrafish palate consists of a single sheet of chondrocytes formed from the union of the frontonasal-derived median element and paired maxillary-derived lateral elements. Wnt signaling originates in the surrounding epithelium, ligands (Wnt9a and Wnt5b) are chaperoned by Wls for export into the extracellular matrix, where Frzb and Gpc4 are important to target the ligands to the recipient chondrocyte. The principle axes of the palate are diagramed: anteroposterior (AP), transverse, and dorsoventral (DV). The chart summarizes the morphogenetic processes during palate development and the genetic requirement for *wls*, *gpc4*, *wnt5b*, *wnt9a*, and *frzb*.

REFERENCES

Akimenko, M.A., Ekker, M., Wegner, J., Lin, W., and Westerfield, M. (1994). Combinatorial expression of three zebrafish genes related to distal-less: part of a homeobox gene code for the head. J. Neurosci. *14*, 3475–3486.

Van Amerongen, R., and Nusse, R. (2009). Towards an integrated view of Wnt signaling in development. Development *136*, 3205 –3214.

Bänziger, C., Soldini, D., Schütt, C., Zipperlen, P., Hausmann, G., and Basler, K. (2006). Wntless, a conserved membrane protein dedicated to the secretion of Wnt proteins from signaling cells. Cell *125*, 509–522.

Barembaum, M., and Bronner-Fraser, M. (2005). Early steps in neural crest specification. Semin. Cell Dev. Biol. *16*, 642–646.

Bartscherer, K., and Boutros, M. (2008). Regulation of Wnt protein secretion and its role in gradient formation. EMBO Rep. *9*, 977–982.

Bartscherer, K., Pelte, N., Ingelfinger, D., and Boutros, M. (2006). Secretion of Wnt Ligands Requires Evi, a Conserved Transmembrane Protein. Cell *125*, 523–533.

Behrens, J., Von Kries, J.P., Kühl, M., Bruhn, L., Wedlich, D., Grosschedl, R., and Birchmeier, W. (1996). Functional interaction of beta-catenin with the transcription factor LEF-1. Nature *382*, 638–642.

Boergermann, J.H., Kopf, J., Yu, P.B., and Knaus, P. (2010). Dorsomorphin and LDN-193189 inhibit BMP-mediated Smad, p38 and Akt signalling in C2C12 cells. Int. J. Biochem. Cell Biol. *42*, 1802–1807.

Borchers, A., Epperlein, H.H., and Wedlich, D. (2000). An assay system to study migratory behavior of cranial neural crest cells in Xenopus. Dev. Genes Evol. *210*, 217–222.

Bronner-Fraser, M. (1993). Mechanisms of neural crest cell migration. Bioessays *15*, 221–230.

Brugmann, S.A., Goodnough, L.H., Gregorieff, A., Leucht, P., Ten Berge, D., Fuerer, C., Clevers, H., Nusse, R., and Helms, J.A. (2007). Wnt signaling mediates regional specification in the vertebrate face. Development *134*, 3283–3295.

Buenrostro, J.D., Wu, B., Litzenburger, U.M., Ruff, D., Gonzales, M.L., Snyder, M.P., Chang, H.Y., and Greenleaf, W.J. (2015). Single-cell chromatin accessibility reveals principles of regulatory variation. Nature *523*, 486–490.

Carroll, T.J., Park, J.-S., Hayashi, S., Majumdar, A., and McMahon, A.P. (2005). Wnt9b plays a central role in the regulation of mesenchymal to epithelial transitions underlying organogenesis of the mammalian urogenital system. Dev. Cell *9*, 283–292.

Ceol, C.J., Houvras, Y., White, R.M., and Zon, L.I. (2008). Melanoma Biology and the Promise of Zebrafish. Zebrafish *5*, 247–255.

Chapnik, E., Sasson, V., Blelloch, R., and Hornstein, E. (2012). Dgcr8 controls neural crest cells survival in cardiovascular development. Developmental Biology *362*, 50–56.

Cheung, M., and Briscoe, J. (2003). Neural crest development is regulated by the transcription factor Sox9. Development *130*, 5681–5693.

Chiquet, B.T., Blanton, S.H., Burt, A., Ma, D., Stal, S., Mulliken, J.B., and Hecht, J.T. (2008). Variation in WNT genes is associated with non-syndromic cleft lip with or without cleft palate. Hum. Mol. Genet. *17*, 2212–2218.

Clevers, H. (2006). Wnt/beta-catenin signaling in development and disease. Cell *127*, 469–480.

Clevers, H., and Nusse, R. (2012). Wnt/β-Catenin Signaling and Disease. Cell *149*, 1192–1205.

Collazo, A., Bronner-Fraser, M., and Fraser, S.E. (1993). Vital dye labelling of Xenopus laevis trunk neural crest reveals multipotency and novel pathways of migration. Development *118*, 363–376.

Cramer, S.F. (1991). The origin of epidermal melanocytes. Implications for the histogenesis of nevi and melanomas. Arch. Pathol. Lab. Med. *115*, 115–119.

Cuny, G.D., Yu, P.B., Laha, J.K., Xing, X., Liu, J.-F., Lai, C.S., Deng, D.Y., Sachidanandan, C., Bloch, K.D., and Peterson, R.T. (2008). Structure-activity relationship study of bone morphogenetic protein (BMP) signaling inhibitors. Bioorg. Med. Chem. Lett. *18*, 4388–4392.

Dale, L., and Wardle, F.C. (1999). A gradient of BMP activity specifies dorsal-ventral fates in early Xenopus embryos. Semin. Cell Dev. Biol. *10*, 319–326.

Darken, R.S., and Wilson, P.A. (2001). Axis induction by wnt signaling: Target promoter responsiveness regulates competence. Dev. Biol. *234*, 42–54.

Das, S., Yu, S., Sakamori, R., Stypulkowski, E., and Gao, N. (2012). Wntless in Wnt secretion: molecular, cellular and genetic aspects. Front Biol (Beijing) *7*, 587–593.

Dooley, C.M., Mongera, A., Walderich, B., and Nusslein-Volhard, C. (2013). On the embryonic origin of adult melanophores: the role of ErbB and Kit signalling in establishing melanophore stem cells in zebrafish. Development *140*, 1003–1013.

Le Douarin, N. (1973). A biological cell labeling technique and its use in expermental embryology. Dev. Biol. *30*, 217–222.

Le Douarin, N.M., and Teillet, M.A. (1974). Experimental analysis of the migration and differentiation of neuroblasts of the autonomic nervous system and of neurectodermal mesenchymal derivatives, using a biological cell marking technique. Dev. Biol. *41*, 162–184.

Dougherty, M., Kamel, G., Shubinets, V., Hickey, G., Grimaldi, M., and Liao, E.C. (2012). Embryonic fate map of first pharyngeal arch structures in the sox10: kaede zebrafish transgenic model. J Craniofac Surg *23*, 1333–1337.

Dougherty, M., Kamel, G., Grimaldi, M., Gfrerer, L., Shubinets, V., Ethier, R., Hickey, G., Cornell, R.A., and Liao, E.C. (2013). Distinct requirements for wnt9a and irf6 in extension and integration mechanisms during zebrafish palate morphogenesis. Development *140*, 76–81.

Duband, J.-L., Dady, A., and Fleury, V. (2015). Resolving Time and Space Constraints During Neural Crest Formation and Delamination. In Current Topics in Developmental Biology, (Elsevier), pp. 27–67.

Dupin, E., and Le Douarin, N.M. (2003). Development of melanocyte precursors from the vertebrate neural crest. Oncogene *22*, 3016–3023.

Dupin, E., Glavieux, C., Vaigot, P., and Le Douarin, N.M. (2000). Endothelin 3 induces the reversion of melanocytes to glia through a neural crest-derived glial-melanocytic progenitor. Proc. Natl. Acad. Sci. U.S.A. *97*, 7882–7887.

Dupin, E., Creuzet, S., and Le Douarin, N.M. (2006). The contribution of the neural crest to the vertebrate body. Adv. Exp. Med. Biol. *589*, 96–119.

Eberhart, J.K., He, X., Swartz, M.E., Yan, Y.-L., Song, H., Boling, T.C., Kunerth, A.K., Walker, M.B., Kimmel, C.B., and Postlethwait, J.H. (2008). MicroRNA Mirn140 modulates Pdgf signaling during palatogenesis. Nature Genetics *40*, 290–298.

Fu, J., Jiang, M., Mirando, A.J., Yu, H.-M.I., and Hsu, W. (2009). Reciprocal regulation of Wnt and Gpr177/mouse Wntless is required for embryonic axis formation. Proceedings of the National Academy of Sciences *106*, 18598–18603.

García-Castro, M.I., Marcelle, C., and Bronner-Fraser, M. (2002). Ectodermal Wnt function as a neural crest inducer. Science *297*, 848–851.

Glavic, A., Maris Honoré, S., Gloria Feijóo, C., Bastidas, F., Allende, M.L., and Mayor, R. (2004). Role of BMP signaling and the homeoprotein iroquois in the specification of the cranial placodal field. Developmental Biology *272*, 89–103.

Golding, J.P., Sobieszczuk, D., Dixon, M., Coles, E., Christiansen, J., Wilkinson, D., and Gassmann, M. (2004). Roles of erbB4, rhombomere-specific, and rhombomere-independent cues in maintaining neural crest-free zones in the embryonic head. Dev. Biol. *266*, 361–372.

Goodrich, L.V., and Strutt, D. (2011). Principles of planar polarity in animal development. Development *138*, 1877–1892.

Green, J. (1999). The animal cap assay. Methods Mol. Biol. *127*, 1–13.

Green, S.A., Simoes-Costa, M., and Bronner, M.E. (2015). Evolution of vertebrates as viewed from the crest. Nature *520*, 474–482.

Gurdon, J.B. (1987). Embryonic induction--molecular prospects. Development *99*, 285–306.

Gurdon, J.B., and Hopwood, N. (2000). The introduction of Xenopus laevis into developmental biology: of empire, pregnancy testing and ribosomal genes. Int. J. Dev. Biol. *44*, 43–50.

Gurdon, J.B., Standley, H., Dyson, S., Butler, K., Langon, T., Ryan, K., Stennard, F., Shimizu, K., and Zorn, A. (1999). Single cells can sense their position in a morphogen gradient. Development *126*, 5309–5317.

Hagiwara, K., Obayashi, T., Sakayori, N., Yamanishi, E., Hayashi, R., Osumi, N., Nakazawa, T., and Nishida, K. (2014). Molecular and Cellular Features of Murine Craniofacial and Trunk Neural Crest Cells as Stem Cell-Like Cells. PLoS ONE *9*, e84072.

Haldin, C.E., and LaBonne, C. (2010). SoxE factors as multifunctional neural crest regulatory factors. The International Journal of Biochemistry & Cell Biology *42*, 441–444.

Hall, B.K. (2000). The neural crest as a fourth germ layer and vertebrates as quadroblastic not triploblastic. Evol. Dev. *2*, 3–5.

Hashiguchi, M., and Mullins, M.C. (2013). Anteroposterior and dorsoventral patterning are coordinated by an identical patterning clock. Development *140*, 1970–1980.

He, F., and Chen, Y. (2012). Wnt signaling in lip and palate development. Front Oral Biol *16*, 81–90.

Heisenberg, C.P., and Tada, M. (2002). Zebrafish gastrulation movements: bridging cell and developmental biology. Semin. Cell Dev. Biol. *13*, 471–479.

Heisenberg, C.P., Tada, M., Rauch, G.J., Saúde, L., Concha, M.L., Geisler, R., Stemple, D.L., Smith, J.C., and Wilson, S.W. (2000). Silberblick/Wnt11 mediates convergent extension movements during zebrafish gastrulation. Nature *405*, 76–81.

Hong, C.-S., and Saint-Jeannet, J.-P. (2005). Sox proteins and neural crest development. Semin. Cell Dev. Biol. *16*, 694–703.

Hong, C.-S., Park, B.-Y., and Saint-Jeannet, J.-P. (2008). Fgf8a induces neural crest indirectly through the activation of Wnt8 in the paraxial mesoderm. Development *135*, 3903–3910.

Hovanes, K., Li, T.W., Munguia, J.E., Truong, T., Milovanovic, T., Lawrence Marsh, J., Holcombe, R.F., and Waterman, M.L. (2001). Beta-catenin-sensitive isoforms of lymphoid enhancer factor-1 are selectively expressed in colon cancer. Nat. Genet. *28*, 53–57.

Hsieh, J.C., Rattner, A., Smallwood, P.M., and Nathans, J. (1999). Biochemical characterization of Wnt-frizzled interactions using a soluble, biologically active vertebrate Wnt protein. Proc. Natl. Acad. Sci. U.S.A. *96*, 3546–3551.

Hsu, D.R., Economides, A.N., Wang, X., Eimon, P.M., and Harland, R.M. (1998). The Xenopus Dorsalizing Factor Gremlin Identifies a Novel Family of Secreted Proteins that Antagonize BMP Activities. Molecular Cell *1*, 673–683.

Hsu, M.-Y., Rovinsky, S.A., Lai, C.-Y., Qasem, S., Liu, X., How, J., Engelhardt, J.F., and Murphy, G.F. (2008). Aggressive melanoma cells escape from BMP7-mediated autocrine growth inhibition through coordinated Noggin upregulation. Lab. Invest. *88*, 842–855.

Huang, X., and Saint-Jeannet, J.-P. (2004). Induction of the neural crest and the opportunities of life on the edge. Dev. Biol. *275*, 1–11.

Huang, S., Zhu, X., Liu, Y., Tao, Y., Feng, G., He, L., Guo, X., and Ma, G. (2012). Wls Is Expressed in the Epidermis and Regulates Embryonic Hair Follicle Induction in Mice. PLoS ONE *7*, e45904.

Hultman, K.A., and Johnson, S.L. (2010). Differential contribution of direct-developing and stem cell-derived melanocytes to the zebrafish larval pigment pattern. Developmental Biology *337*, 425–431.

Hwang, W.Y., Fu, Y., Reyon, D., Maeder, M.L., Tsai, S.Q., Sander, J.D., Peterson, R.T., Yeh, J.-R.J., and Joung, J.K. (2013). Efficient genome editing in zebrafish using a CRISPR-Cas system. Nat. Biotechnol. *31*, 227–229.

Janda, C.Y., Waghray, D., Levin, A.M., Thomas, C., and Garcia, K.C. (2012). Structural basis of Wnt recognition by Frizzled. Science *337*, 59–64.

Jin, J., Morse, M., Frey, C., Petko, J., and Levenson, R. (2010). Expression of GPR177 (Wntless/Evi/Sprinter), a highly conserved Wnt-transport protein, in rat tissues, zebrafish embryos, and cultured human cells. Dev. Dyn. *239*, 2426–2434.

Jin, Y.-R., Han, X.H., Taketo, M.M., and Yoon, J.K. (2012). Wnt9b-dependent FGF signaling is crucial for outgrowth of the nasal and maxillary processes during upper jaw and lip development. Development *139*, 1821–1830.

Juriloff, D.M., Harris, M.J., McMahon, A.P., Carroll, T.J., and Lidral, A.C. (2006). Wnt9b is the mutated gene involved in multifactorial nonsyndromic cleft lip with or without cleft palate in A/WySn mice, as confirmed by a genetic complementation test. Birth Defects Res. Part A Clin. Mol. Teratol. *76*, 574–579.

Kamel, G., Hoyos, T., Rochard, L., Dougherty, M., Tse, W., Shubinets, V., Grimaldi, M., and Liao, E.C. (2013). Requirement for frzb and fzd7a in cranial neural crest convergence and extension mechanisms during zebrafish palate and jaw morphogenesis. Dev. Biol.

Kao, K.R., and Elinson, R.P. (1988). The entire mesodermal mantle behaves as Spemann's organizer in dorsoanterior enhanced Xenopus laevis embryos. Dev. Biol. *127*, 64–77.

Kasemeier-Kulesa, J.C., Teddy, J.M., Postovit, L.-M., Seftor, E.A., Seftor, R.E.B., Hendrix, M.J.C., and Kulesa, P.M. (2008). Reprogramming multipotent tumor cells with the embryonic neural crest microenvironment. Developmental Dynamics *237*, 2657–2666.

Khokha, M.K., Yeh, J., Grammer, T.C., and Harland, R.M. (2005). Depletion of three BMP antagonists from Spemann's organizer leads to a catastrophic loss of dorsal structures. Dev. Cell *8*, 401–411.

Kimmel, C.B., Ballard, W.W., Kimmel, S.R., Ullmann, B., and Schilling, T.F. (1995). Stages of embryonic development of the zebrafish. Dev. Dyn. *203*, 253–310.

Kishigami, S., and Mishina, Y. (2005). BMP signaling and early embryonic patterning. Cytokine & Growth Factor Reviews *16*, 265–278.

Klein, A.M., Mazutis, L., Akartuna, I., Tallapragada, N., Veres, A., Li, V., Peshkin, L., Weitz, D.A., and Kirschner, M.W. (2015). Droplet barcoding for single-cell transcriptomics applied to embryonic stem cells. Cell *161*, 1187–1201.

Knecht, A.K., and Bronner-Fraser, M. (2002). Induction of the neural crest: a multigene process. Nature Reviews Genetics *3*, 453–461.

Kuan, Y.-S., Roberson, S., Akitake, C.M., Fortuno, L., Gamse, J., Moens, C., and Halpern, M.E. (2015). Distinct requirements for Wntless in habenular development. Developmental Biology *406*, 117–128.

LaBonne, C., and Bronner-Fraser, M. (2000). Snail-related transcriptional repressors are required in Xenopus for both the induction of the neural crest and its subsequent migration. Dev. Biol. *221*, 195–205.

Lallier, T., Leblanc, G., Artinger, K.B., and Bronner-Fraser, M. (1992). Cranial and trunk neural crest cells use different mechanisms for attachment to extracellular matrices. Development *116*, 531–541.

Lammi, L., Arte, S., Somer, M., Jarvinen, H., Lahermo, P., Thesleff, I., Pirinen, S., and Nieminen, P. (2004). Mutations in AXIN2 cause familial tooth agenesis and predispose to colorectal cancer. Am. J. Hum. Genet. *74*, 1043–1050.

LeClair, E.E., Mui, S.R., Huang, A., Topczewska, J.M., and Topczewski, J. (2009). Craniofacial skeletal defects of adult zebrafish Glypican 4 (knypek) mutants. Dev. Dyn. *238*, 2550–2563.

Lee, J.-M., Kim, J.-Y., Cho, K.-W., Lee, M.-J., Cho, S.-W., Kwak, S., Cai, J., and Jung, H.-S. (2008). Wnt11/Fgfr1b cross-talk modulates the fate of cells in palate development. Dev. Biol. *314*, 341–350.

Levin, M. (2012). Morphogenetic fields in embryogenesis, regeneration, and cancer: Non-local control of complex patterning. Biosystems *109*, 243–261.

Li, Y., and Dudley, A.T. (2009). Noncanonical frizzled signaling regulates cell polarity of growth plate chondrocytes. Development *136*, 1083–1092.

Li, Y., Yang, F., Chen, Z., Shi, L., Zhang, B., Pan, J., Li, X., Sun, D., and Yang, H. (2014). Zebrafish on a chip: a novel platform for real-time monitoring of drug-induced developmental toxicity. PLoS ONE *9*, e94792.

Libra (2009). Melanoma: Molecular pathogenesis and emerging target therapies (Review). International Journal of Oncology *34*.

Lidral, A.C., and Murray, J.C. (2004). Genetic approaches to identify disease genes for birth defects with cleft lip/palate as a model. Birth Defects Res. Part A Clin. Mol. Teratol. *70*, 893–901.

Le Lievre, C.S., Schweizer, G.G., Ziller, C.M., and Le Douarin, N.M. (1980). Restrictions of developmental capabilities in neural crest cell derivatives as tested by in vivo transplantation experiments. Dev. Biol. *77*, 362–378.

Le Lièvre, C.S., and Le Douarin, N.M. (1975). Mesenchymal derivatives of the neural crest: analysis of chimaeric quail and chick embryos. J Embryol Exp Morphol *34*, 125–154.

Lister, J.A., Capper, A., Zeng, Z., Mathers, M.E., Richardson, J., Paranthaman, K., Jackson, I.J., and Patton, E.E. (2014). A Conditional Zebrafish MITF Mutation Reveals MITF Levels Are Critical for Melanoma Promotion vs. Regression In Vivo. Journal of Investigative Dermatology *134*, 133–140.

Logan, C.Y., and Nusse, R. (2004). THE WNT SIGNALING PATHWAY IN DEVELOPMENT AND DISEASE. Annual Review of Cell and Developmental Biology *20*, 781–810.

Marchant, L., Linker, C., Ruiz, P., Guerrero, N., and Mayor, R. (1998). The inductive properties of mesoderm suggest that the neural crest cells are specified by a BMP gradient. Dev. Biol. *198*, 319–329.

Mayer, W., Niveleau, A., Walter, J., Fundele, R., and Haaf, T. (2000). Embryogenesis: Demethylation of the zygotic paternal genome. Nature *403*, 501–502.

Mayor, R., and Theveneau, E. (2014). The role of the non-canonical Wnt-planar cell polarity pathway in neural crest migration. Biochem. J. *457*, 19–26.

McKeown, S.J., Lee, V.M., Bronner-Fraser, M., Newgreen, D.F., and Farlie, P.G. (2005). Sox10 overexpression induces neural crest-like cells from all dorsoventral levels of the neural tube but inhibits differentiation. Developmental Dynamics *233*, 430–444.

McKinney, M.C., Fukatsu, K., Morrison, J., McLennan, R., Bronner, M.E., and Kulesa, P.M. (2013). Evidence for dynamic rearrangements but lack of fate or position restrictions in premigratory avian trunk neural crest. Development *140*, 820–830.

McMahon, R., Murphy, M., Clarkson, M., Taal, M., Mackenzie, H.S., Godson, C., Martin, F., and Brady, H.R. (2000). IHG-2, a mesangial cell gene induced by high glucose, is human gremlin. Regulation by extracellular glucose concentration, cyclic mechanical strain, and transforming growth factor-beta1. J. Biol. Chem. *275*, 9901–9904.

Meijer, L., Skaltsounis, A.-L., Magiatis, P., Polychronopoulos, P., Knockaert, M., Leost, M., Ryan, X.P., Vonica, C.A., Brivanlou, A., Dajani, R., et al. (2003). GSK-3-selective inhibitors derived from Tyrian purple indirubins. Chem. Biol. *10*, 1255–1266.

Meulemans, D., and Bronner-Fraser, M. (2004). Gene-regulatory interactions in neural crest evolution and development. Dev. Cell *7*, 291–299.

Mii, Y., and Taira, M. (2009). Secreted Frizzled-related proteins enhance the diffusion of Wnt ligands and expand their signalling range. Development *136*, 4083–4088.

Mii, Y., and Taira, M. (2011). Secreted Wnt "inhibitors" are not just inhibitors: Regulation of extracellular Wnt by secreted Frizzled-related proteins: Extracellular distribution of Wnt ligands. Development, Growth & Differentiation *53*, 911–923.

Minoux, M., and Rijli, F.M. (2010). Molecular mechanisms of cranial neural crest cell migration and patterning in craniofacial development. Development *137*, 2605–2621.

Molenaar, M., Van de Wetering, M., Oosterwegel, M., Peterson-Maduro, J., Godsave, S., Korinek, V., Roose, J., Destrée, O., and Clevers, H. (1996). XTcf-3 transcription factor mediates beta-catenin-induced axis formation in Xenopus embryos. Cell *86*, 391–399.

Moreno, L.M., Arcos-Burgos, M., Marazita, M.L., Krahn, K., Maher, B.S., Cooper, M.E., Valencia-Ramirez, C.R., and Lidral, A.C. (2004). Genetic analysis of candidate loci in non-syndromic cleft lip families from Antioquia-Colombia and Ohio. Am. J. Med. Genet. A *125A*, 135–144.

Mort, R.L., Jackson, I.J., and Patton, E.E. (2015a). The melanocyte lineage in development and disease. Development *142*, 620–632.

Mort, R.L., Jackson, I.J., and Patton, E.E. (2015b). The melanocyte lineage in development and disease. Development *142*, 620–632.

Myung, P.S., Takeo, M., Ito, M., and Atit, R.P. (2013). Epithelial Wnt Ligand Secretion Is Required for Adult Hair Follicle Growth and Regeneration. Journal of Investigative Dermatology *133*, 31–41.

Niehrs, C. (2010). On growth and form: a Cartesian coordinate system of Wnt and BMP signaling specifies bilaterian body axes. Development *137*, 845–857.

Niemann, S., Zhao, C., Pascu, F., Stahl, U., Aulepp, U., Niswander, L., Weber, J.L., and Müller, U. (2004). Homozygous WNT3 mutation causes tetra-amelia in a large consanguineous family. Am. J. Hum. Genet. *74*, 558–563.

Nusse, R. (2012). Wnt Signaling. Cold Spring Harbor Perspectives in Biology *4*, a011163–a011163.

Okabayashi, K., and Asashima, M. (2003). Tissue generation from amphibian animal caps. Curr. Opin. Genet. Dev. *13*, 502–507.

Le Pabic, P., Ng, C., and Schilling, T.F. (2014). Fat-Dachsous signaling coordinates cartilage differentiation and polarity during craniofacial development. PLoS Genet. *10*, e1004726.

Patthey, C., and Gunhaga, L. (2014). Signaling pathways regulating ectodermal cell fate choices. Exp. Cell Res. *321*, 11–16.

Patton, E.E., Widlund, H.R., Kutok, J.L., Kopani, K.R., Amatruda, J.F., Murphey, R.D., Berghmans, S., Mayhall, E.A., Traver, D., Fletcher, C.D.M., et al. (2005). BRAF Mutations Are Sufficient to Promote Nevi Formation and Cooperate with p53 in the Genesis of Melanoma. Current Biology *15*, 249–254.

Piotrowski, T., Schilling, T.F., Brand, M., Jiang, Y.J., Heisenberg, C.P., Beuchle, D., Grandel, H., Van Eeden, F.J., Furutani-Seiki, M., Granato, M., et al. (1996). Jaw and branchial arch mutants in zebrafish II: anterior arches and cartilage differentiation. Development *123*, 345–356.

Pott, S., and Lieb, J.D. (2015). Single-cell ATAC-seq: strength in numbers. Genome Biology *16*.

Prasad, M.S., Sauka-Spengler, T., and LaBonne, C. (2012). Induction of the neural crest state: control of stem cell attributes by gene regulatory, post-transcriptional and epigenetic interactions. Dev. Biol. *366*, 10–21.

Raible, D.W., and Eisen, J.S. (1994). Restriction of neural crest cell fate in the trunk of the embryonic zebrafish. Development *120*, 495–503.

Rauch, G.J., Hammerschmidt, M., Blader, P., Schauerte, H.E., Strähle, U., Ingham, P.W., McMahon, A.P., and Haffter, P. (1997). Wnt5 is required for tail formation in the zebrafish embryo. Cold Spring Harb. Symp. Quant. Biol. *62*, 227–234.

Reya, T., and Clevers, H. (2005). Wnt signalling in stem cells and cancer. Nature *434*, 843–850.

Riley, B.M., and Murray, J.C. (2007). Sequence evaluation of FGF and FGFR gene conserved non-coding elements in non-syndromic cleft lip and palate cases. Am. J. Med. Genet. A *143A*, 3228–3234.

De Robertis, E.M., and Kuroda, H. (2004). Dorsal-ventral patterning and neural induction in Xenopus embryos. Annu. Rev. Cell Dev. Biol. *20*, 285–308.

De Robertis, E.M., and Moriyama, Y. (2016). The Chordin Morphogenetic Pathway. In Current Topics in Developmental Biology, (Elsevier), pp. 231–245.

Roffers-Agarwal, J., Hutt, K.J., and Gammill, L.S. (2012). Paladin is an antiphosphatase that regulates neural crest cell formation and migration. Developmental Biology *371*, 180–190.

Saint-Jeannet, J.-P., and Moody, S.A. (2014). Establishing the pre-placodal region and breaking it into placodes with distinct identities. Developmental Biology *389*, 13–27.

Santiago, H.C., Feng, C.G., Bafica, A., Roffe, E., Arantes, R.M., Cheever, A., Taylor, G., Vieira, L.Q., Vierira, L.Q., Aliberti, J., et al. (2005). Mice deficient in LRG-47 display enhanced susceptibility to Trypanosoma cruzi infection associated with defective hemopoiesis and intracellular control of parasite growth. J. Immunol. *175*, 8165–8172.

Sasai, N., Mizuseki, K., and Sasai, Y. (2001). Requirement of FoxD3-class signaling for neural crest determination in Xenopus. Development *128*, 2525–2536.

Sauka-Spengler, T., and Bronner-Fraser, M. (2006). Development and evolution of the migratory neural crest: a gene regulatory perspective. Current Opinion in Genetics & Development *16*, 360–366.

Sauka-Spengler, T., and Bronner-Fraser, M. (2008). A gene regulatory network orchestrates neural crest formation. Nature Reviews Molecular Cell Biology *9*, 557–568.

Schilling, T.F., and Kimmel, C.B. (1994). Segment and cell type lineage restrictions during pharyngeal arch development in the zebrafish embryo. Development *120*, 483–494.

Schneider, R.A., and Helms, J.A. (2003). The cellular and molecular origins of beak morphology. Science *299*, 565–568.

Shimizu, K., Sato, M., and Tabata, T. (2011). The Wnt5/planar cell polarity pathway regulates axonal development of the Drosophila mushroom body neuron. J. Neurosci. *31*, 4944–4954.

Siegel, R., Naishadham, D., and Jemal, A. (2013). Cancer statistics, 2013. CA: A Cancer Journal for Clinicians *63*, 11–30.

Simões-Costa, M.S., McKeown, S.J., Tan-Cabugao, J., Sauka-Spengler, T., and Bronner, M.E. (2012). Dynamic and Differential Regulation of Stem Cell Factor FoxD3 in the Neural Crest Is Encrypted in the Genome. PLoS Genetics *8*, e1003142.

Simons, M., and Mlodzik, M. (2008). Planar cell polarity signaling: from fly development to human disease. Annu. Rev. Genet. *42*, 517–540.

Singh, A.P., and Nüsslein-Volhard, C. (2015). Zebrafish stripes as a model for vertebrate colour pattern formation. Curr. Biol. *25*, R81–92.

Sisson, B.E., and Topczewski, J. (2009). Expression of five frizzleds during zebrafish craniofacial development. Gene Expr. Patterns *9*, 520–527.

Sisson, B.E., Dale, R.M., Mui, S.R., Topczewska, J.M., and Topczewski, J. (2015). A role of glypican4 and wnt5b in chondrocyte stacking underlying craniofacial cartilage morphogenesis. Mech. Dev. *138 Pt 3*, 279–290.

Sneddon, J.B., Zhen, H.H., Montgomery, K., Van de Rijn, M., Tward, A.D., West, R., Gladstone, H., Chang, H.Y., Morganroth, G.S., Oro, A.E., et al. (2006). Bone morphogenetic protein antagonist gremlin 1 is widely expressed by cancer-associated stromal cells and can promote tumor cell proliferation. Proc. Natl. Acad. Sci. U.S.A. *103*, 14842–14847.

Spokony, R.F., Aoki, Y., Saint-Germain, N., Magner-Fink, E., and Saint-Jeannet, J.-P. (2002). The transcription factor Sox9 is required for cranial neural crest development in Xenopus. Development *129*, 421–432.

Stergachis, A.B., Neph, S., Reynolds, A., Humbert, R., Miller, B., Paige, S.L., Vernot, B., Cheng, J.B., Thurman, R.E., Sandstrom, R., et al. (2013). Developmental fate and cellular maturity encoded in human regulatory DNA landscapes. Cell *154*, 888–903.

Steventon, B., Carmona-Fontaine, C., and Mayor, R. (2005). Genetic network during neural crest induction: from cell specification to cell survival. Semin. Cell Dev. Biol. *16*, 647–654.

Steventon, B., Araya, C., Linker, C., Kuriyama, S., and Mayor, R. (2009). Differential requirements of BMP and Wnt signalling during gastrulation and neurulation define two steps in neural crest induction. Development *136*, 771–779.

Strobl-Mazzulla, P.H., and Bronner, M.E. (2012). A PHD12-Snail2 repressive complex epigenetically mediates neural crest epithelial-to-mesenchymal transition. J. Cell Biol. *198*, 999–1010.

Strobl-Mazzulla, P.H., Sauka-Spengler, T., and Bronner-Fraser, M. (2010). Histone demethylase JmjD2A regulates neural crest specification. Dev. Cell *19*, 460–468.

Stuhlmiller, T.J., and García-Castro, M.I. (2012). Current perspectives of the signaling pathways directing neural crest induction. Cellular and Molecular Life Sciences: CMLS.

Swartz, M.E., Sheehan-Rooney, K., Dixon, M.J., and Eberhart, J.K. (2011). Examination of a palatogenic gene program in zebrafish. Developmental Dynamics *240*, 2204–2220.

Szabo-Rogers, H.L., Smithers, L.E., Yakob, W., and Liu, K.J. (2010). New directions in craniofacial morphogenesis. Dev. Biol. *341*, 84–94.

Tan, J.L., and Zon, L.I. (2011). Chemical screening in zebrafish for novel biological and therapeutic discovery. Methods Cell Biol. *105*, 493–516.

Thisse, C., and Thisse, B. (2008). High-resolution in situ hybridization to whole-mount zebrafish embryos. Nature Protocols *3*, 59–69.

Topczewski, J., Sepich, D.S., Myers, D.C., Walker, C., Amores, A., Lele, Z., Hammerschmidt, M., Postlethwait, J., and Solnica-Krezel, L. (2001). The zebrafish glypican knypek controls cell polarity during gastrulation movements of convergent extension. Dev. Cell *1*, 251–264.

Topczewski, J., Dale, R.M., and Sisson, B.E. (2011). Planar cell polarity signaling in craniofacial development. Organogenesis *7*, 255–259.

Trainor, P.A., and Krumlauf, R. (2001). Hox genes, neural crest cells and branchial arch patterning. Curr. Opin. Cell Biol. *13*, 698–705.

Tudela, C., Formoso, M.-A., Martínez, T., Pérez, R., Aparicio, M., Maestro, C., Del Río, A., Martínez, E., Ferguson, M., and Martínez-Alvarez, C. (2002). TGF-beta3 is required for the adhesion and intercalation of medial edge epithelial cells during palate fusion. Int. J. Dev. Biol. *46*, 333–336.

Urist, M.R., and Strates, B.S. (1971). Bone morphogenetic protein. J. Dent. Res. *50*, 1392–1406.

Veeman, M.T., Axelrod, J.D., and Moon, R.T. (2003). A second canon. Functions and mechanisms of beta-catenin-independent Wnt signaling. Dev. Cell *5*, 367–377.

Vega, S., Morales, A.V., Ocaña, O.H., Valdés, F., Fabregat, I., and Nieto, M.A. (2004). Snail blocks the cell cycle and confers resistance to cell death. Genes Dev. *18*, 1131–1143.

Veldman, M.B., and Lin, S. (2008). Zebrafish as a Developmental Model Organism for Pediatric Research. Pediatric Research *64*, 470–476.

Vladar, E.K., Antic, D., and Axelrod, J.D. (2009). Planar cell polarity signaling: the developing cell's compass. Cold Spring Harb Perspect Biol *1*, a002964.

Walker, M.B., and Kimmel, C.B. (2007). A two-color acid-free cartilage and bone stain for zebrafish larvae. Biotech Histochem *82*, 23–28.

Wallingford, J.B. (2012). Planar cell polarity and the developmental control of cell behavior in vertebrate embryos. Annu. Rev. Cell Dev. Biol. *28*, 627–653.

Wallingford, J.B., Fraser, S.E., and Harland, R.M. (2002). Convergent extension: the molecular control of polarized cell movement during embryonic development. Dev. Cell *2*, 695–706.

Wang, R.N., Green, J., Wang, Z., Deng, Y., Qiao, M., Peabody, M., Zhang, Q., Ye, J., Yan, Z., Denduluri, S., et al. (2014). Bone Morphogenetic Protein (BMP) signaling in development and human diseases. Genes & Diseases *1*, 87–105.

Wang, Y., Chang, H., Rattner, A., and Nathans, J. (2016). Frizzled Receptors in Development and Disease. Curr. Top. Dev. Biol. *117*, 113–139.

Westerfield, M. (1993). The zebrafish book: a guide for the laboratory use of zebrafish (Danio rerio). (University of Oregon press).

Westfall, T.A., Brimeyer, R., Twedt, J., Gladon, J., Olberding, A., Furutani-Seiki, M., and Slusarski, D.C. (2003). Wnt-5/pipetail functions in vertebrate axis formation as a negative regulator of Wnt/beta-catenin activity. J. Cell Biol. *162*, 889–898.

Wilkie, A.L., Jordan, S.A., and Jackson, I.J. (2002). Neural crest progenitors of the melanocyte lineage: coat colour patterns revisited. Development *129*, 3349–3357.

Wodarz, A., and Nusse, R. (1998). Mechanisms of Wnt signaling in development. Annu. Rev. Cell Dev. Biol. *14*, 59–88.

Wolpert, L. (1971). Positional information and pattern formation. Curr. Top. Dev. Biol. *6*, 183–224.

Wolpert, L. (1989). Positional information revisited. Development *107 Suppl*, 3–12.

Woods, C.G., Stricker, S., Seemann, P., Stern, R., Cox, J., Sherridan, E., Roberts, E., Springell, K., Scott, S., Karbani, G., et al. (2006). Mutations in WNT7A cause a range of limb malformations, including Fuhrmann syndrome and Al-Awadi/Raas-Rothschild/Schinzel phocomelia syndrome. Am. J. Hum. Genet. *79*, 402–408.

Yan, Y.-L., Miller, C.T., Nissen, R.M., Singer, A., Liu, D., Kirn, A., Draper, B., Willoughby, J., Morcos, P.A., Amsterdam, A., et al. (2002). A zebrafish sox9 gene required for cartilage morphogenesis. Development *129*, 5065–5079.

Yang, T., Chen, S.L., Lu, X.J., Shen, C.Y., Liu, Y., and Chen, Y.P. (2012). Bone morphogenetic protein 7 suppresses the progression of hepatic fibrosis and regulates the expression of gremlin and transforming growth factor β1. Mol Med Rep *6*, 246–252.

Yang, T., Jia, Z., Bryant-Pike, W., Chandrasekhar, A., Murray, J.C., Fritzsch, B., and Bassuk, A.G. (2014). Analysis of PRICKLE1 in human cleft palate and mouse development demonstrates rare and common variants involved in human malformations. Mol Genet Genomic Med *2*, 138–151.

Yin, C., Ciruna, B., and Solnica-Krezel, L. (2009). Convergence and extension movements during vertebrate gastrulation. Curr. Top. Dev. Biol. *89*, 163–192.

Young, N.M., Hu, D., Lainoff, A.J., Smith, F.J., Diaz, R., Tucker, A.S., Trainor, P.A., Schneider, R.A., Hallgrimsson, B., and Marcucio, R.S. (2014). Embryonic bauplans and the developmental origins of facial diversity and constraint. Development *141*, 1059–1063.

Yu, H., Smallwood, P.M., Wang, Y., Vidaltamayo, R., Reed, R., and Nathans, J. (2010). Frizzled 1 and frizzled 2 genes function in palate, ventricular septum and neural tube closure: general implications for tissue fusion processes. Development *137*, 3707–3717.

Yu, H., Ye, X., Guo, N., and Nathans, J. (2012). Frizzled 2 and frizzled 7 function redundantly in convergent extension and closure of the ventricular septum and palate: evidence for a network of interacting genes. Development *139*, 4383–4394.

Yu, P.B., Hong, C.C., Sachidanandan, C., Babitt, J.L., Deng, D.Y., Hoyng, S.A., Lin, H.Y., Bloch, K.D., and Peterson, R.T. (2008a). Dorsomorphin inhibits BMP signals required for embryogenesis and iron metabolism. Nat. Chem. Biol. *4*, 33–41.

Yu, P.B., Deng, D.Y., Lai, C.S., Hong, C.C., Cuny, G.D., Bouxsein, M.L., Hong, D.W., McManus, P.M., Katagiri, T., Sachidanandan, C., et al. (2008b). BMP type I receptor inhibition reduces heterotopic [corrected] ossification. Nat. Med. *14*, 1363–1369.

APPENDICES

Appendix I: Primers used for *Xenopus* qPCR

Gene	Forward Primer	Reverse Primer
axin1	5'-ACGCCAGCAAAATGAGTGTC-3'	5'-GGTGGCTGTTGAGGTTTCGT-3'
axin2	5'-CTGGCAGCCATGAGTTCTG-3'	5'-TGGTGAACTTTTCGGGCTTGT-3'
ef1a	5'-AATCCACAATGGGAAAGGAAAAGAC-3'	5'-ATGGTTCTCTTGTCGATGCCA-3'
en-2	5'-AGGCAAGAAGAAGCTTTGGAA-3'	5'-ACTCCGGCCGTAGAATGTTG-3'
epi ker	5'-CTTCCTATAGGTCCAGCTCTGC-3'	5'-TGAAAAGCCAGAACCCACAC-3'
gapdh	5'-TGACCCGCGCTGCCTTTGAT-3'	5'-TAAAGCGGCCGTGGGTGGAG-3'
hoxb9	5'-ATTTCTGGGCCTCTCACCAA-3'	5'-GCTGATAGACTGGAGGGTGC-3'
krox20	5'-TCAGACCATGGCGGCTAAAG-3'	5'-CTCCTGTCACTCCGCTCATC-3'
meis3	5'-TCTTCCACAAGTCTCCCAGGC-3'	5'-TACTCGGTGACCTGCTCCTG-3'
otx2	5'-ACGAGCATGATGTCTTATCTCAA-3'	5'-AGTTGGGCCCTGGTAAAAGTG-3'
snail2	5'-TGTGTCTGTGCTTCCCCAGCC-3'	5'-TGGGGCTCTCCGAGCCACTAT-3'
sox2	5'-TCCCCACACGCCGCCTCGAT-3'	5'-CCTCTGGCCCCTGGACCATACC-3'
twist1	5'-ATTGTGCCGGGAGAAAATGATGC-3'	5'-TCGGGGCTTTTCCTAGCAGAT-3'

Appendix II: Primers used for *Danio rerio in situ* hybridization

Gene	Forward primer	Reverse Primer
foxd3	5'-ATGACCCTGTCTGGAGGCAC-3'	5'-GGATCCAATTAACCCTCACTAAAG GGAAGGCCATTTCGATACCGCT-3'
gpc4	5'-CACCCAGCGATGAAGATGAT CG-3'	5'-AGCAGAATCAGCCCAAGA-3'
sox2	5'-CTCCTCGGGAAACAACCAGA A-3'	5'-GGATCCAATTAACCCTCACTAAAG GG GTTAATCGTCGTACCGGGCA-3'
sox10	5'-CTAGTGGACCGATGTCG-3'	5'-GGATCCAATTAACCCTCACTAAAG GGTGTCACGGTCGAGACAGT-3'
tfap2e	5'-TGTCCAGCTCCTCTCCGGG-3'	5'-GGATCCAATTAACCCTCACTAAAG GG CTTTGTCCAGCAGTTTTAGGGC-3'
wls	5'-ATGGCTGGGGCAATTATTGA G-3'	5'-TGGGTGGAGGTTATTCTTGAGC-3'
wnt5b	5'-TAATACGACTCACTATAGGG AGAACACCTACTTCTGGCAGTG ACC-3'	5'-TCTCCCTTTAGTGAGGGTTAATTCT TGTTGCATAGGCGGCCTT-3'